University of Alberta

Role of the Wnt/PI3-K Pathway in the Regulation of Beta-catenin in Melanoma Progression

by

Jaskiran Sidhu

A thesis submitted to the Faculty of Graduate Studies and Research

in partial fulfillment of the requirements for the degree of

Master of Science

in

Medical Sciences-Paediatrics

Department of Paediatrics

Fall 2012

Edmonton, Alberta

Dedication

To My Parents

ABSTRACT

Melanoma has the most rapidly rising incidence of all cancers and once metastasized it is very difficult to treat. This makes the identification of molecular pathways that are deregulated in melanoma a novel area of study. β-catenin (β-cat) is a multifunctional protein of the Wnt signaling pathway that is key in driving metastasis. Understanding what regulates the high levels of active-β-cat expressed in metastatic melanomas was the goal of this study. We looked into the PI3K pathway as the possible mediator, as PTEN the negative regulator of the pathway, is lost in 30-60% of melanomas.

We found that there is an inverse relationship in β-cat and PTEN expression through melanoma progression. The inhibition of the PI3K pathway decreased expression of the active form of β-cat and downstream effector genes, independent of Wnt signaling. Therefore, the suppression of active-β-cat is a potential molecular target that may serve to limit metastatic progression.

Acknowledgments

Firstly, I would like to express my appreciation for all the guidance and support I received from Dr. Sujata Persad during my time period in her laboratory. Her words of wisdom, knowledge and support were a driving force in supporting me to completing my MSc degree. Thank you for taking me into your laboratory and allowing me to have this life changing journey.

Secondly, I would like to extend my gratitude to my supervisory committee, Drs Shairaz Baksh and Alan Underhill. I thank you for you sharing your knowledge and provoking me to completing this study and helping me over road bumps encountered in the way. I would also like to thank Dr. Mary Hitt, Dr. Kunimasa Suzuki (Molecular Biology and Biochemistry Core Facility University of Alberta, Alberta Diabetes Institute), Dr. Richard Fahlman, Jack Moore (Integrated DNA Technologies) and their laboratory staff for allowing me to use their facilities for my project. A thank you to Trish Kryzanowski and Dr. Po-Yin Cheung for their support, guidance and advice throughout my time in the Department of Pediatrics.

I would also like to thank my fellow graduate student Jacqueline Ha, for all her support and kindness throughout my time at the University of Alberta. I would like to extend my sincerest thank you to Dr. Li Hao for training me and supporting me throughout my entire laboratory training. I would also like to thank Susan Van Nispen for not only being an administrative assistant but also a great friend and the sarcastic, smiling, most clear headed individual that was willing to hear all the rambling and ranting I had through times of frustration.

Last but not least I could not have come this far without the love and support of my parents, family and friends. I would like to dedicate this thesis to my parents, without whom I would not be at this stage. They have been nothing but supportive in my life's ventures and have provided utmost wisdom throughout the way. Their belief in me during these times was the driving force behind my completion of this program. A special thank you to my best friend, who taught me to never quit and motivated me to move forward at times where I was at a complete breakdown. For always allowing me to vent, giving nothing but the best advice, being a shoulder to rest on and being the push that was needed at times, I could never thank you enough.

I could not have completed this MSc project without each and every one of you. I am very humble for the support I had throughout this journey.

Table of Contents

List of Figures

List of Abbreviations

ABC: active-β-catenin

APC: Adenomatous Polyposis Coli

AJCC: American Joint Committee on Cancer

AKT/PKB: Protein Kinase B

Arm: Armadillo

ATP: Adenosine triphosphate

β-catenin: Beta-catenin

β-Trcp: β-transducin repeat-containing protein

CD1: cyclin d1

CER: Cytoplasmic Extraction Reagent

CK-1: Casein Kinase-1

cMyc: c-myelocytomatosis oncogene

CRC: colorectal cancer

CTD: C-terminal Domain

DMEM: Dulbecco's Modified Eagle Medium

DKK-1: dickkopf homolog 1

Dvl: Dishellved

E.Coli: *Escherichia coli*

EMSA: electrophoretic mobility shift assay

EMT: Epithelial to Mesenchymal Transition

FBS: fetal bovine serum

Fz: Frizzled

GSK3β: Glycogen Synthase Kinase-3β

ICAT/ CTNNB1: catenin beta interacting protein 1

IDT: integrated DNA technologies

IF: immunofluorescence

IGF: insulin like growth factor

IR: infrared

LEF: Lymphoid Enhancer Factor

LB: lithium-borate

MITF: microphthalmia-associated transcription factor

MMP: matrix metalloprotease

NER: Nuclear Extraction Reagent

NLS: nuclear localization sequence

NRAS: Neuroblastoma RAS

NTD: N-terminal Domain

P-AKT: Phospho-AKT

PBS: Phosphate buffered saline

PDK-1: phosphoinositide-dependent kinase 1

p-EGFP: empty GFP plasmid vector

P16 (INK4A)/ CDKN2A:cyclin-dependent kinase inhibitor 2A

PH: pleckstrin-homology

PI3K: phosphoinositide-3-kinase

PIP2: Phosphatidylinositol 4,5-bisphosphate

PIP3: Phosphatidylinositol (3,4,5)-triphosphate

P/S: penicillin/streptomyosin

PTEN: phosphatase and tensin homolog

PVDF: Polyvinylidene fluoride

RGP: radial growth phase

Ser/S: Serine

sFRP-1: Secreted frizzled-related protein 1

TBE: Tris/Borate/EDTA

TBP: TATA-binding protein

TBS-T: Tris-Buffered Saline-Tween 20

TCF:T-cell factor

Thr/T:Threonine

Tyr: Tyrosine

VEGF: vascular endothelial growth factor A

VGP: vertical growth phase

WB: Western blot

$\Delta\Delta Ct = \Delta Ct$ sample – ΔCt Reference(control)

Chapter 1: Introduction

1.1 Melanoma

1.1.1 Malignant Melanoma

Worldwide, melanoma has the most rapidly rising incidence rate of any human cancer. It arises from the malignant transformation of the melanocyte cells of the skin. Due to the inefficacy of present chemotherapeutic regimens and the resistance of melanocyte cells to radiotherapy, 95% of stage IV metastatic melanoma patients die within five years of diagnosis (Grossman and Altieri, 2001; Helmbach et al., 2001; Soengas and Lowe, 2003). Metastasis, the spread of a cancer from the site of the primary tumour to distant sites of the body, makes melanoma very hard to treat. Risk factors associated with malignant melanoma include excessive sun exposure which can cause mutations in specific genes and deregulation of signal transduction pathways.

1.1.2 Stages of Melanoma

Malignant melanoma is characterized by the uncontrollable proliferation of melanocytes, cells originating from neural crest cells. The liver, brain, and lungs are the most common targets of melanoma metastasis, and patients with metastasized melanoma have a median survival of six months (Kim et al., 2010).

Melanocytes are located in the basal layer of the epidermis surrounded by keratinocytes. Keratinocytes maintain controlled growth of melanocytes through (1) extracellular communication via paracrine growth factors, (2) intracellular communication through second messengers and signal transduction, and (3) intercellular communication through cell–cell adhesion molecules, cell–matrix

adhesion, and gap junctional intercellular communication (Haass et al., 2004). Perturbations in the cellular environment can lead to alterations in molecules involved in cell-cell adhesion and cell communication, leading to melanoma development (Haass et al., 2005). Uncontrolled proliferation, homeostatic balance upset through deregulation of signal transduction, and loss in cell adhesion can all lead to metastasis. The American Joint Committee on Cancer (AJCC) has devised a system to categorize melanoma. This system incorporates tumour thickness, nodal status, and metastatic disease (Piris et al., 2011). Figure 1.1 summarizes the steps leading to metastasis.

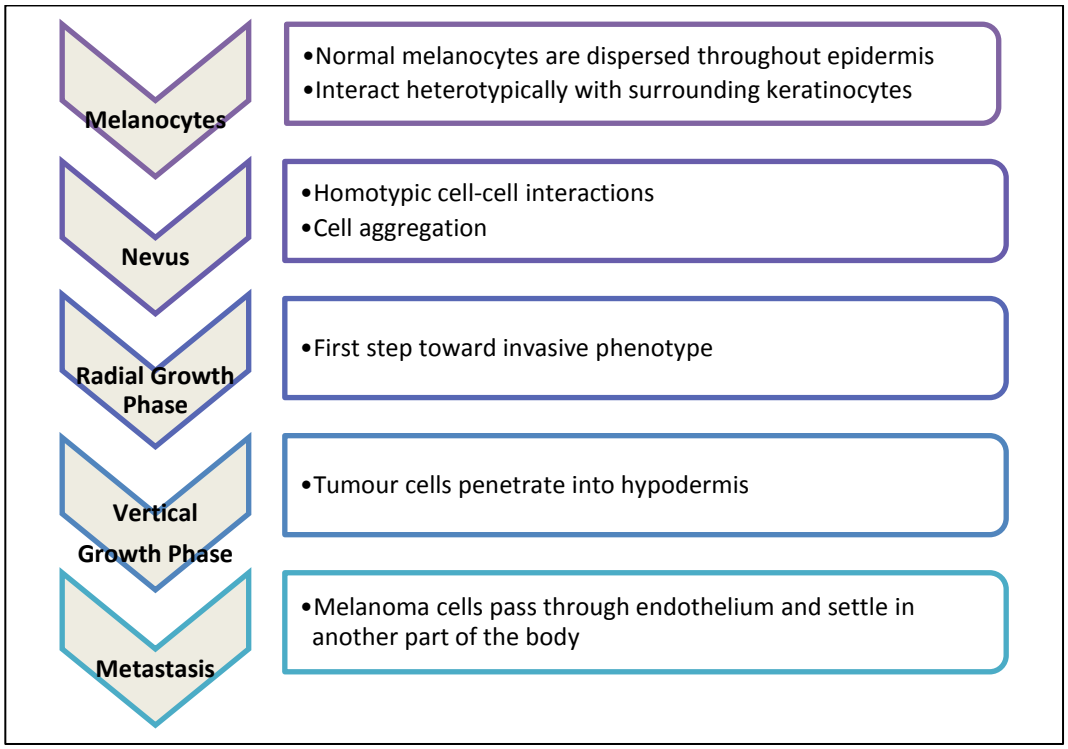

Figure 1.1: Summary of stages of melanoma from melanocytes to metastasis. Simplified depiction of changes that occur in the phenotype of the cell and cellular environment from melanocytes, nevus (e.g., birthmarks, moles), radial growth, vertical growth, to metastasis.

Normal melanocytes are transformed to malignant melanocytes through distinct

phenotypic changes, as they progress through an epithelial to mesenchymal transition (EMT). A disruption in adherens junctions of melanocytes, a result of the down regulation of E-cadherin and up regulation of N-cadherin (the "cadherin switch") (Hao et al., 2012), causes a loss of cell adhesion and an increase in cell mobility.

Loss of E-cadherin allows melanocytes to escape from keratinocyte growth control and allows malignant melanocytes to escape from the primary tumour focus (Hirohashi et al., 1998). EMT must take place for cells to progress to a metastatic stage, as cells must shed their epithelial phenotype and gain a mesenchymal phenotype. To gain metastatic potential, cells must invade the basement membrane and make their way into the bloodstream. Figure 1.2 shows healthy tissue progressing through distinct stages and reaching a metastatic state.

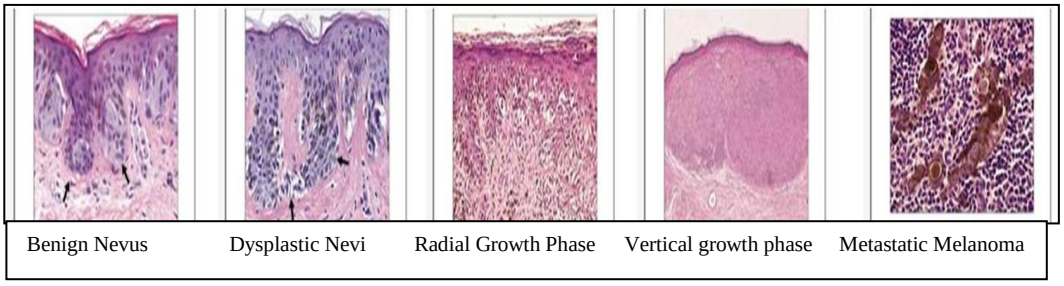

Figure 1.2: Stages of melanoma: Progression of benign nevus to metastasis. Changes in pathology depict stages of melanoma progression from benign nevus, to dysplastic nevi, to radial-growth phase, to vertical growth phase, to a metastatic melanoma.

1.1.3 Current Therapeutics

Currently there are five different types of therapies for melanoma, depending on the stage of the cancer. Surgery, chemotherapy, radiation therapy, targeted therapy and biologic therapy are the treatments presented by the National Cancer

Institute. Surgery is the form of primary treatment as it excises the tumour from its primary site, or the lymph nodes to which the tumour has reached may be removed. Chemotherapy and radiation therapy are two commonly used conventional cancer treatments. Biologic therapy, another form of cancer treatment, targets the patient's immune system to fight the cancer. This therapy boosts the body's immune system by restoring the body's natural defences. An example is Interleukin-2 (IL-2), which promotes the growth and activity of lymphocytes in the body, which are used by the immune system to fight off cancer cells. The negative effect of such treatment is that a higher dose results in severe side effects, so therefore lower doses are usually combined with another form of therapy. A more specific treatment is targeted therapy, which targets signal transduction components that are deregulated in melanoma. This form of treatment is very cancer specific in comparison to other conventional therapies mentioned above (http://www.cancer.gov/cancertopics/pdq/treatment/melanoma).

Drugs that target the mutations that are highly prevalent in melanoma, such as BRAF mutations are commonly used in targeted therapy. A commonly used BRAF inhibiting drug is Vemurafenib which targets specific BRAF substitution mutations. Sorafnib is a multikinase inhibitor that targets vascular endothelial-growth factor and Raf/MEK pathways at the level of RAF kinase. Monoclonal antibodies that target molecules to enhance anti-tumour immunity are a major breakthrough in melanoma treatment (Simeone and Ascierto, 2012). Ipilimumab, an antibody against cytotoxic T-lymphocyte (CTL) antigen, is a commonly used drug for treatment of stage four melanoma. This drug removes inhibition of CTLs

so they can target and destroy cancer cells (http://www.cancer.gov/cancertopics/pdq/treatment/melanoma/HealthProfessional//Page9#Reference9.6). Antibodies targeting Programmed Death-1 (PD-1) are similar to Ipilmumab in the sense that they act as a pharmacological antagonist on the inhibitory receptors, thereby unblocking an immune response. PD-1 receptors work to evade the immune response by interrupting the interactions of PD-1 with T and B lymphocytes, thereby having anti-tumour functions (Simeone and Ascierto, 2012). Such targeted therapies along with conventional therapies are the most promising treatment for metastatic melanoma. As understanding of perturbations of signal transduction pathways advances, there will be greater progress in therapies targeting particular mutations and irregularities of those pathways.

1.1.4 Signal Transduction and Malignant Melanoma

Malignant melanoma is characterized by frequent metastasis; however, specific changes that cause this malignancy have yet to be characterized (Damsky et al., 2011). Several oncogenes, tumour suppressor genes, and pathways are implied; for example, NRAS, which activates RAF kinases in response to growth factors is overactive in 15–20% of melanomas (Padua et al., 1984; Van t'Veer et al., 1989). P16 (INK4A) tumour suppressor expression is also lost by mutation, deletion, or transcriptional silencing of the CDKN2A locus in many melanomas (Yang et al., 2005). BRAF mutations are often found alongside P16 mutations. Phosphatase and tensin homolog (PTEN) mutations and deletions are also present in some

melanomas, coinciding with BRAF mutations (Yang et al., 2005; Daniotti et al., 2004; Curtin et al., 2005). Since these two mutations often occur together PTEN loss reflects the importance of two RAS-effector pathways in melanoma (Flaherty et al., 2012). Another genomic aberration associated with melanoma is the amplification of microphthalmia-associated transcription factor (MITF) (Flaherty et al., 2012). The occurrence of several different mutations implies that several signal transduction pathways are perturbed in melanoma.

Melanoma was one of the first cancer types associated with β-catenin/Wnt signaling mutations (Rubinfeld et al., 1997). However, the exact role of these mutations in melanoma has remained elusive (Lucero et al., 2010). Mutations in the Wnt signaling pathway that result in over-activation of β-catenin signaling are readily observed in melanomas, but the functional implications are unclear (Damsky et al., 2011). This project focuses on the implications of the β-catenin signaling pathway on melanoma progression.

Several in vivo and in vitro models have been established to study the implications of a deregulated Wnt signaling pathway in melanoma. Overactive β-catenin signalling along with a constitutively active phosphoinositide-3-kinase (PI3K) pathway has shown facilitation of melanoma development in a mouse model (Damsky et al., 2011).

The high incidence and low survival rate of melanoma make it an important area of study. Elucidation of the changes and dysregulation occurring in signal transduction pathways that leads to metastasis will allow identification of

molecular targets and thus efficacious therapies to treat metastatic disease (Smith et al., 2008).

Mutations in several growth regulatory pathways have been described in melanoma studies (Larue and Delmas, 2006), which through many mechanisms result in metastasis. Of particular interest to this project are mutations in the Wnt/β-catenin pathway as well as the PI3K pathway. Elevated levels of nuclear β-catenin are observed in ~30% of human melanomas (Larue and Delmas, 2006). The PI3K pathway is likely the most frequently deregulated pathway in melanoma, although the mechanism underlying the over-activation in most cases remains largely elusive (Lau and Ronai, 2011).

1.2 β-catenin

1.2.1 β-catenin: Structure and Function

β-catenin is a 781 amino acid protein encoded by the *CTNNB1* gene. It is highly conserved throughout species and shares 67% homology to the Drosophila Armadillo protein (Shapiro et al., 2009). β-catenin's primary structure is composed of two terminal domains; the N-terminal (NH_2) and C-terminal (COOH) domains, and a central domain (Figure 1.3). β-catenin's structure allows binding of specific partners at distinct sites across the terminal domains and the central domain. The β-catenin central Armadillo (ARM) domain, characteristic of the Armadillo/catenin family of proteins, is distinguished by a positively charged groove of densely packed α-helices (Huber et al., 1997) comprising of 12 imperfect repeats of 42 amino acids (total 550 amino acids) (Xing et al., 2008;

Huber et al., 1997).

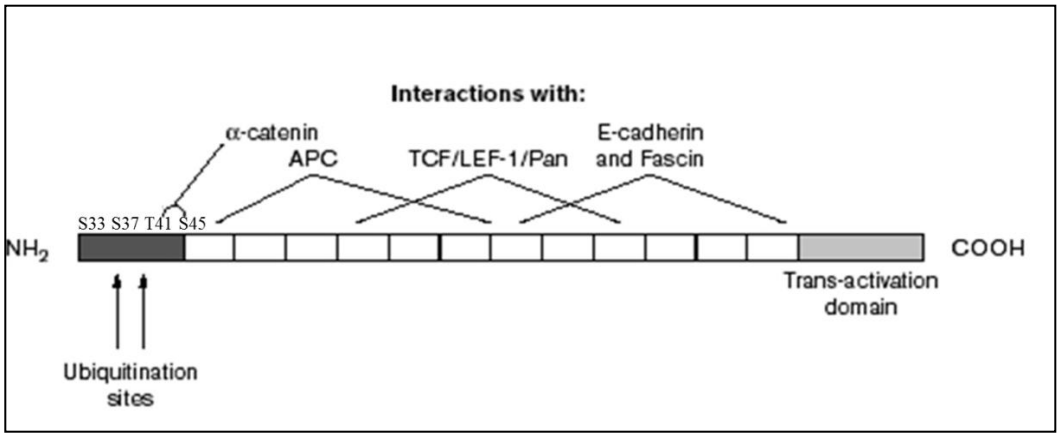

Figure 1.3: Schematic showing β-catenin structure in terms of binding to its partners. N-terminal shows sites of phosphorylation, marking β-catenin for ubiquitination and degradation. Armadillo repeats bind with several β-catenin partners such as; APC, TCF/LEF-1 and E-cadherin. C-terminal domain presents the transactivation domain of β-catenin **(**Hoover, B. A., 2005).

The crystal structure of the ARM repeat domain shows that each repeat consists of three helices, H1, H2, and H3 (Huber et al., 1997) and the repeats pack against one another to form a positively charged superhelix. This positively charged groove is ideal for β-catenin to bind its various negatively charged partners. When these interactors are post-translationally modified by phosphorylation, effectively increasing the magnitude of the negative charge, β-catenin's binding affinity with these interactors is augmented (Huber et al., 2001). The ARM domain folds into a single structural unit where its surface serves to bind the majority of β-catenin's partners, such as; cadherins, TCF/LEF transcription factors and APC (Xing et al., 2008).

The N-terminal domain (NTD) and C-terminal domain (CTD) of β-catenin are

less evolutionarily conserved relative to the central ARM domain. The NTD is important for the stability of the cytoplasmic levels of β-catenin while both the NTD and CTD are significant in β-catenin's role as a co-activator/transactivator of TCF/LEF transcriptional activity. The established role of the CTD in recruiting factors required for regulation of gene expression is dependent on the interaction with cellular partners at the proximal structured elements of this region, such as helix C, which directly follows the 12^{th} arm repeat (Maher et al., 2010). The functions for the more distal unstructured region of the CTD remain poorly defined. Furthermore, the acidic charge distribution of the NTD and CTD creates a tertiary structure that brings the NTD and CTD in close proximity to the largely basic ARM domain. Since the NTD and CTD are highly negatively charged and the structural groove of the ARM domain is highly positively charged it is likely that both the NTD and CTD tails of β-catenin interact with the groove of the ARM domain through non-specific charge interactions (Xing et al., 2008). The NTD and CTD serve as intramolecular chaperones of the ARM repeat domain which increases the binding specificity and prevents the self-aggregation of the armadillo repeat domain region (Xing et al., 2008). Post-translational modifications, such as phosphorylation pattern which change the charge of β-catenin may further result in conformational change or stabilization of the N and/or C tails causing a regulation in binding specific interactors (Xing et al., 2008).

The CTD also plays a role in the interaction of β-catenin with a number of nuclear factors including; TATA Binding Protein (TBP) (Hecht et al., 1999), Sox 17 and

13, histone deacetylase, SMAD4, the retinoic acid receptor, the CREB binding protein and related proteins (Piedra et al., 2001) as well as transcriptional inhibitors such as ICAT, and Chibby (Barker et al., 2001; Hecht et al., 2000).

At Cellular Membrane

At the cell membrane, β-catenin is an important component of the adherens junctions, where it links E-cadherin and α-catenin to the actin cytoskeleton. The adherens junction is essential in maintaining the seamless cell-cell interaction of the epithelial phenotype and provides the cell with structural integrity. The binding of E-cadherin to β-catenin spans the entire ARM region (Huber et al., 2001) although the actual sites of interaction are concentrated within ARM repeats 4-12 (Hulsken et al., 1994)). Tyrosine (Tyr) modification of β-catenin regulates the disassembly of adherens junctions and is regulated by phosphorylation of Tyr-654 of the final armadillo repeat which leads to decreased binding of E-cadherin and β-catenin (Roura et al., 1999). A possible mechanism by Piedra and collegues suggests that this may be due to decreased interaction between ARM and CTD with the phosphorylation of Tyr-654 (Piedra et al., 2001). Interestingly, this phosphorylation does not affect the association of nuclear factors such as TBP (binding site 639-729), nor TCF-4 (T-cell factor 4) at the CTD. This supports the fact that the CTD is an integral regulatory component which facilitates the interactions of β-catenin with E-cadherin (Piedra et al., 2001).

In the Cytoplasm and Nucleus

While β-catenin linked to E-cadherin is deemed to be highly stable, the cytosolic and nuclear pools are quite dynamic. The subcellular localization of β-catenin is largely regulated by direct competition of β-catenin's binding to E-cadherin and TCF. The N-terminal of TCF forms extensive contacts at ARM 3-9 of β-catenin which bears structural similarities to the E-cadherin-β-catenin interaction. To this end, overexpression of cadherins has been shown to inhibit the transcriptional activity of β-catenin (Gumbiner, 2000). Furthermore, binding to cadherins can effectively sequester β-catenin within the plasma membrane/cytoplasm and inhibit its signaling efficacy (Gottardi et al., 2001).

1.2.2 β-catenin / Canonical Wnt Pathway

β-catenin is a dual function protein. It plays a role in intercellular adhesion and in regulating gene expression. The latter role is associated with its oncogenic properties. Its second role is as a transcriptional co-activator of the canonical Wnt signaling pathway. The Wnt signal transduction pathway is an essential regulatory pathway that directs cell proliferation, cell polarity and cell fate determination (MacDonald et al., 2009). The following figure depicts both roles of β-catenin (Figure 1.4).

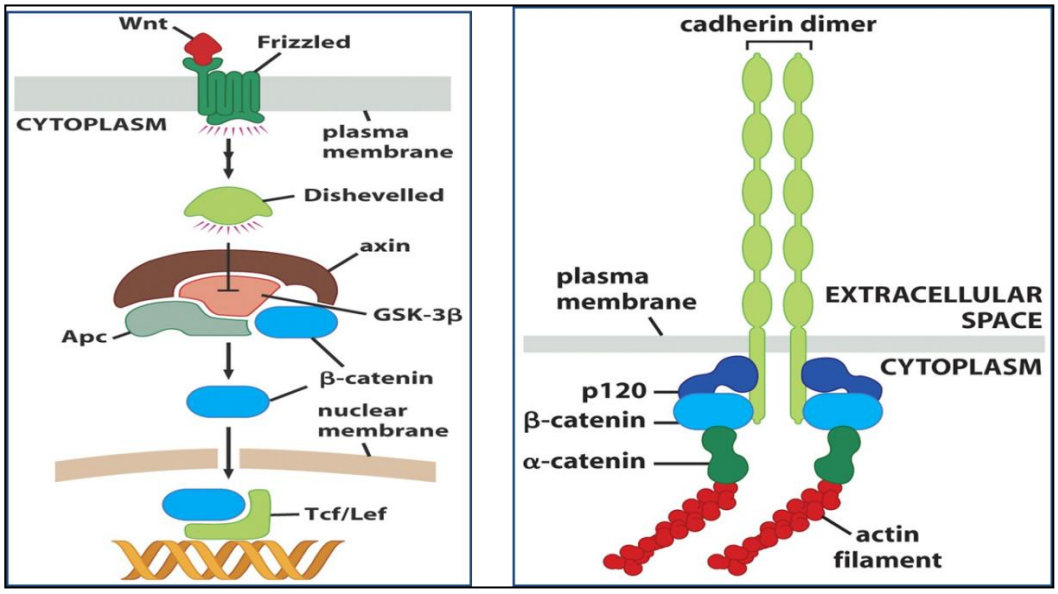

Figure 1.4: β-catenin as a dual-function protein. Left Panel: Shows the role of β-catenin in the canonical Wnt signaling pathway, serving as a transcriptional co-activator of TCF/LEF target genes. Right panel: Depicts β-catenin's role in cell-cell adhesion serving as a link between cadherins and actin cytoskeleton.

β-catenin's fate as an adhesion molecule or a transcriptional activator is determined by its intracellular stability. The Wnt pathway largely regulates the intracellular stability of β-catenin.

Pathway Inactivation

In the absence of extracellular Wnt factors, free cytoplasmic β-catenin levels are regulated by a multi-protein destruction complex comprising the scaffold protein Axin, the tumour suppressor Adenomatous Polyposis Coli (APC), Glycogen Synthase Kinase-3β (GSK3β) and Casein Kinase-1 (CK-1). Axin is the scaffolding protein at the center of the destruction complex, which binds and brings into proximity the other components. APC plays a key role in the

regulation of β-catenin turnover since cells containing a mutant APC have elevated β-catenin levels. GSK3β binds a central region within Axin, with a single Axin helix fitting into a hydrophobic groove in the C-terminus of GSK-3β, leaving the GSK3β active site free to phosphorylate β-catenin (Dajani et al., 2003). CK1 binds Axin and phosphorylates β-catenin at Ser45 in order to prime GSK3β phosphorylation at the more N-terminal residues (Ser33, Ser37 and Thr41) (Amit et al., 2002; Liu et al., 2006; Kimelman 2006). This phosphorylation creates a site for ubiquitination of β-catenin by E3 ubiquitin ligase β-transducin repeat-containing protein (β-Trcp), resulting in β-catenin's subsequent proteosomal degradation (MacDonald et al., 2009).

Pathway Activation

Wnts are secreted glycoproteins that bind to frizzled seven-transmembrane spanned receptors. There are 19 known Wnt ligands, three of which are known to stimulate the canonical Wnt pathway in humans, namely Wnt 1, 3 and Wnt8 (MacDonald et al., 2009). Particular Wnt ligands are responsible for embryonic development in several different species. A complete listing of the particular Wnts is described by Dr. Roel Nusse's laboratory (http://www.stanford.edu/group/nusselab/cgi-bin/wnt/). Wnt ligands bind to receptors which are coupled with heterotrimeric G proteins. In the canonical pathway, LRP 5/6, low-density lipoprotein receptors, are co-receptors of Wnt ligands. Upon binding of Wnt ligands, the activated Fz recruits the intracellular protein dishevelled (Dvl), which in turn recruits the axin–GSK3β complex to the

plasma membrane. Wnt-induced LRP6 phosphorylation is a key event in receptor activation (Tamai et al., 2004). Formation of this complex promotes the initial phosphorylation of LRP6 (Zeng et al., 2005, 2008). These phosphorylated sites serve as docking sites for Axin complex (Davidson et al., 2005; Tamai et al., 2004., Zeng et al., 2005) thereby recruiting Axin to LRP6 upon Wnt stimulation (Mao et al., 2001).

Further phosphorylation of LRP6 by CK-1 (Davidson et al. 2005; Zeng et al. 2008) results in the clustering of various proteins—including LRP6, Dvl, and Axin—to form what has been referred to as the LRP6 signalosome (Bilic et al. 2007). Formation of this complex from the phosphorylation of LRP5/6 leads to inhibition of the "destruction complex". De-activation of the destruction complex results in stabilization of β-catenin within the cytoplasm and its targeted entry into the nucleus, where it binds to the T-cell factor (TCF)/Lymphoid Enhancer Factor (LEF) family of transcription factors leading to transcriptional activation of Wnt target genes (Logan and Nusse, 2004).

The following figure represents the canonical Wnt signaling pathway, in the presence and absence of Wnt signals (Figure 1.5).

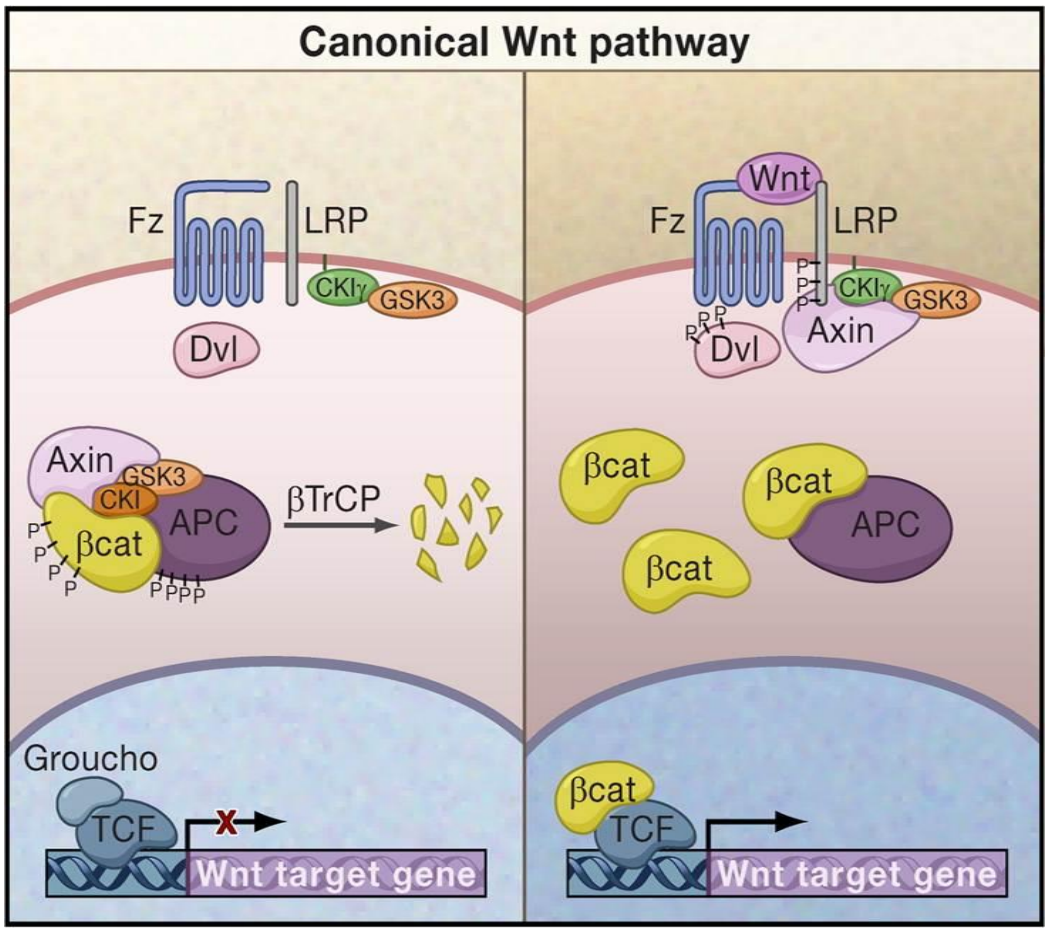

Figure 1.5: The Canonical Wnt Signaling pathway. Left panel: In the absence of Wnt ligands, β-catenin is phosphorylated by the destruction complex and degraded in the cytoplasm. Right panel: In the presence of Wnt ligands, the destruction complex is inactivated. Thereby allowing β-catenin to accumulate and further activated TCF target Wnt genes. (Clevers, 2006)

Within the nucleus, the CTD of β-catenin interacts with the TCF family of proteins, which anchor β-catenin to specific promoters for the transcription of Wnt target genes (Xing et al., 2003). Many of these target genes, such as cMyc, Cyclin D1, vascular endothelial growth factor-a (VEGFa) and matrix metalloproteases (MMPs) have implications in cell survival, cell proliferation, growth, cell cycle progression and invasion along with several others that can be

found on the following page: http://www.stanford.edu/group/nusselab/cgi-bin/wnt/target_genes. Since the canonical Wnt pathway regulates transcription of genes involved in cell cycle, growth and survival, uncontrolled activation of the pathway is highly significant in disease pathophysiology. Constitutive activation of the canonical Wnt pathway results in positive regulation of cell survival and negative regulation on cell death/apoptosis. These changes in cellular properties associated with elevated cellular β-catenin are associated with poor prognosis in many human cancers including adenocarcinoma of the prostate and breast as well as melanoma (MacDonald et al., 2009).

1.2.3 Active β-catenin

Upon Wnt activation, GSK3β associated with the axin scaffold is inhibited allowing β-catenin to evade degradation. The cytoplasmic accumulation of β-catenin is thought to ultimately result in its translocation to the nucleus. However, this translocation alone is not sufficient for β-catenin/TCF transcriptional activity (Mo et al., 2000; Staal et al., 2002). Staal and colleagues demonstrated that the increased half-life of β-catenin upon Wnt signaling was not a direct consequence of its stability (Staal et al., 2002). The phosphorylation status of the NTD of β-catenin upon Wnt signalling independently affected the signaling properties and half-life of β-catenin. In fact, it is not so much the accumulation of β-catenin per se but the dephosphorylation of specific amino acids at the NTD of β-catenin that is important in generating a transcriptionally active form of β-catenin (Staal et al., 2002; Maher et al., 2010). Maher and colleagues demonstrated that the cadherin

free form of β-catenin unphosphorylated at S37 and T41 (transcriptionally active-β-catenin (ABC)) is largely monomeric and located mainly within the nucleus. Active-β-catenin is found to be intrinsically more transcriptionally active than that of the non-phosphorylated β-catenin (Maher et al., 2010). The predominant nuclear accumulation of the active-β-catenin is due to its low concentration within the cell, which renders it less likely to be bound by the cadherins and α-catenin (Maher et al., 2010). Furthermore, β-catenin phosphorylated at three sites; S33, S37 and T41 is found to be more retained within the cytosol, as well as subject to increased nuclear export. Maher and colleagues also established that β-catenin phosphorylated at T41/S45 strongly co-localizes with active-β-catenin within the nucleus and is largely a cadherin-free form of β-catenin. This suggests that the nuclear form of β-catenin phosphorylated at Ser45 may also be a signaling/active form of β-catenin. Referring back to the Wnt pathway, β-catenin is phosphorylated at Ser45 by CK1 in a priming mechanism, allowing subsequent phosphorylation by GSK3β at Ser 33,37 and T41 (Liu et al., 2002). Therefore, it is possible that the priming of β-catenin at S45 by CK1 may be a temporal regulatory mechanism that couples β-catenin phosphorylation and degradation to β-catenin nuclear signaling. Since β-catenin phosphorylated at the three sites of phosphorylation by GSK3β does not completely overlap with β-catenin phosphorylated at serine 45 and threonine 41, suggests a possible spatial separation of the two kinase activities of GSK3β and CK1 (Maher et al., 2010). In addition to serving as a priming site for phosphorylation, the phosphorylation at Serine 45 may facilitate the phosphorylation pattern of β-catenin making it

transcriptionally active. However, this has to be investigated further as this idea is yet primitive (Maher et al., 2010).

High levels of nuclear phospho-β-catenin are associated with significantly worse overall survival (Lopez-Bergami et al., 2008). Using a phosphorylation specific antibody Kielhorn and colleagues determined that nuclear β-catenin staining was more prevalent in advanced melanomas (Kielhorn et al., 2003). This may be due to the specific phosphorylation pattern of β-catenin having specificity for TCF thereby allowing transcription of cancer causing genes.

1.2.4 Localization

A well-defined feature of active-β-catenin is that it is located exclusively in the nucleus (Staal et al., 2002). However, the mechanism of the nuclear localization of β-catenin is currently unknown. β-catenin does not contain a nuclear localization sequence (NLS) nor utilize the importin transport machinery (Krieghoff et al., 2006). However, nuclear export of β-catenin is established to be mediated by an intrinsic export signal and its interaction with APC. The retention of β-catenin within the nucleus is thought to be due to its interaction within the nucleus with TCF, BCL-9 and pygopous (Krieghoff et al., 2006). However, these interactions are not a prerequisite for β-catenin's localization into the nucleus as it has been demonstrated that the protein can successfully localize to the nucleus in the absence of these interactions. Overexpression of LEF/TCF has been shown to lead to β-catenin's accumulation in the nucleus (Behrens et al., 1998; Simcha et al., 1998). It has been suggested that the nuclear import of the β-catenin/LEF

complex is mediated by the NLS provided by LEF/TCF proteins. However, elevations in nuclear levels of β-catenin are observed even when the levels of LEF/TCF are low (Simcha et al., 1996, 1998). Therefore, mechanisms independent of LEF/TCF are likely to be important for regulating the nuclear import of β-catenin in vivo (Zhurinsky et al., 2000). Two groups have independently demonstrated a direct importin-independent nuclear import of β-catenin in a semi-permeabilized cell model (Fagotto et al., 1998; Yokoya et al., 1999), which could be mediated by the interaction between β-catenin and the Nup1 nucleoporin (Fagotto et al., 1998). However, to date no mandatory chaperone essential to the nuclear transport of β-catenin has been identified.

In summation, it is within the nucleus that β-catenin is specifically active-β-catenin and has its oncogenic role as it serves as a transcriptional co-activator of cancer promoting target genes.

1.2.5 β-catenin & Cancer

In carcinomas, the loss of β-catenin-E-cadherin complexes is an important step in disease progression. Loss of organization by disruption of epithelial complexes at adherens junctions is a common feature of invasiveness. Furthermore, deregulation of the Wnt signaling pathway at various levels, often leads to metastasis and cancer progression as Wnt target genes are responsible for controlling the regulation of cell cycle, proliferation and inhibition of apoptosis. A common effect of deregulated/activated Wnt pathway components is an over-expression of β-catenin. Many common cancers including, colorectal

cancer (CRC) (Polakis, 2000), hepatocellular carcinoma (Armengol et al., 2009), adrenal cancers (El Wakil and Lalli, 2011), breast cancer (Zardawi et al., 2009), Wilm's tumour (Tycko et al., 2007), several hematological malignancies (Ge and Wang, 2011) and melanomas (Larue and Delmas, 2006) have been found to have a deregulated Wnt pathway. Some of the causative factors of this deregulation are the loss of function mutations in APC or Axin (Laurent-Puig and Zucman-Rossi 2006), or mutations in the amino acids at the NTD of β-catenin which interfere with its phosphorylation and proteosomal degradation (Polakis, 2000). Truncating mutations in Axin cause nuclear accumulation of β-catenin in hepatocellular carcinomas (Satoh et al., 2000). Furthermore, APC is mutated in 85% of familial and sporadic CRCs (Neufeld et al., 2000). Mutations have also been found to occur in exon 3 of the β-catenin gene, affecting sites of phosphorylation by GSK3β, making β-catenin refractory to degradation (Morin et al., 1997).

The result of mutations in the Wnt pathway is an elevation of total cellular levels of β-catenin and the activation of β-catenin dependent TCF/LEF transcription which mediates its oncogenic effect in various tissues. However, high transcriptional activity of β-catenin in certain disease conditions cannot be attributed to mutations in β-catenin or components of the Wnt pathway. In support of this view point, β-catenin, recently identified as a candidate gene for melanoma progression, was found to be mutated in 5% of melanomas but constitutively active (nuclear expression and transcriptional activity) in 40-50% of melanomas (Larue and Delmas, 2006). This suggests the involvement of alternate regulatory mechanisms/pathways in controlling the oncogenic/transcriptional

properties of β-catenin. Since active-β-catenin is the transcriptionally relevant form of β-catenin, the pathway responsible for the generation of this form of β-catenin needs to be investigated.

1.2.6 β-catenin in Melanoma

Wnt-β-catenin signaling is up regulated in melanoma, and approximately 30% of melanoma exhibit increased nuclear β-catenin (Larue and Delmas, 2006). The high frequency of nuclear accumulation is not all attributable to mutations in the Wnt pathway. The discrepancy between these datasets prompts the investigation of putative mechanisms responsible for the excessive accumulation of nuclear β-catenin. The regulatory mechanism that regulates β-catenin's transcriptional activity of Wnt target genes needs further investigation. Determining how this nuclear pool of β-catenin is regulated by the Wnt pathway alongside other pathways to orchestrate the transcription of target genes is an area of study that needs much anticipated investigation. This would be a leap into the study of melanoma formation and tumour progression (Larue and Delmas et al., 2006).

A thorough understanding of the pathway will provide a look into cell specific molecular mechanisms involved in initiation and progression of melanoma. The goal of this study is to understand regulation of the β-catenin pathway in transforming melanocytes to malignancy.

β-catenin expression in melanoma has been shown to be different than many other cancers. Several studies using melanoma cell lines show a decrease in nuclear and cytoplasmic staining in malignant cell lines compared to a benign nevus stage

(Kageshita et al., 2001). This creates contradiction of β-catenin's expression pattern in other cancers where β-catenin levels are elevated as the cancer progresses, such as hepatoma, gastric and bladder cancers (Kageshita et al., 2001).

Little is known specifically about changes in active-β-catenin in melanoma progression, the pool of β-catenin relevant in the transcription of genes for the proteins that promote metastasis.

Demunter and colleagues showed that post-translational modifications of β-catenin rather than mutations in the *CTNNB1* gene itself are responsible for the altered distribution of β-catenin in the cell (Demunter et al., 2002). This study also draws the conclusion that loss of membranous β-catenin is not associated with its nuclear accumulation. This is another key point that indicates that two pools may be regulated by two different pathways.

Although, overall nuclear and cytoplasmic staining is reduced in the progression of primary to metastatic cells, phosphorylated β-catenin levels are increased. The fact that β-catenin serves many roles in the cell and has variability in its phosphorylation pattern may be an explanation as to why many studies measuring overall levels of β-catenin show an inverse relationship in melanoma progression and β-catenin levels. The fact that phospho-β-catenin is more prevalent in metastatic melanomas is consistent with the fact that β-catenin serves different roles and functions in a cell (Kiehlhorn et al., 2003). Kiehlhorn and colleagues suggests that phosphorylation specific antigen of β-catenin is correlated with a

better marker of disease progression than overall levels, which are masked with different pools of β-catenin.

Although the canonical Wnt pathway is well characterized in the regulation of cellular β-catenin levels, several investigations suggest that β-catenin may also be regulated by other signal transduction pathways via potential cross talk. In particular, the phosphotidylinositol-3 kinase (PI3K) pathway has been significantly implicated in the regulation of β-catenin (Persad et al., 2001). However, there are divergent views on the role of the PI3K pathway in the regulation of β-catenin. The regulation of β-catenin by the two pathways may be through direct crosstalk via a common component. Since GSK3β is a common component of both pathways, several studies suggest that the inactivation of GSK3β by AKT links the PI3K pathway to the Wnt pathway in a bipartite mechanism which subsequently regulates the cytoplasmic levels of β-catenin (Pap and Coopers, 1998). However, other studies propose that the Wnt and PI3K pathways remain distinct and variably regulate alternate pools of GSK3β (Ng et al., 2009).

The second way the PI3K/PTEN may regulate β-catenin is through phosphatase activities, regulating the dephosphorylation pattern of β-catenin which will be discussed later. This project focusses on the interplay between the Wnt and PI3K pathways in the regulation of β-catenin and the subsequent effect of this regulation on tumourigenesis and melanoma progression.

1.3 PI3K Pathway

1.3.1 Overview

The PI3K pathway is widely implicated in tumourigenesis. It serves a role in altering cellular functions in response to extracellular signals, and it is a central integrator of metabolism, survival and growth signals (Carracedo and Pandolfi, 2008). With respect to metabolism, various studies have shown the PI3K pathway has implications in insulin sensitivity (Katso et al., 2001).

There are four members identified in class 1 PI3Ks, divided by their mechanism of activation. Class 1A PI3K is comprised of a heterodimeric complex comprising of a regulatory subunit p85α and any of the three catalytic subunits; p110α, p110β and p110δ. Several membrane receptors, in particular G-protein coupled receptors, cytokines and those with tyrosine kinase activity activate class 1 PI3Ks. The binding of insulin like growth factor-1 (IGF-1) to its cognate receptor (IGF1-R) leads to activation of the receptor and autophosphorylation on tyrosine residues. This further leads to the recruitment of PI3K to the membrane via an adaptor molecule (Fresno Vara et al., 2004).

Upon recruitment to the plasma membrane, PI3K phosphorylates phosphoinositol bis phosphate (PIP2) at the D3 position of the inositol ring generating phosphoinositol tris phosphate (PIP3). PIP3 serves to recruit proteins containing the pleckstrin homology (PH) domain such as the serine-threonine kinases; AKT /protein kinase B (PKB), and phosphoinositide-dependent kinase 1 (PDK-1) to the plasma membrane. AKT is a central protein involved in normal and

pathological signaling. AKT gene amplification is found in cancers such as gastric, ovarian, pancreas and stomach cancers (Engelman et al., 2006). Structurally, AKT contains an N-terminal PH domain, a central catalytic domain and a C-terminal regulatory region. The PH domain binds specifically to D3-phosphorylated phosphinositides with high affinity (Fresno Vara et al., 2004). Upon recruitment to the plasma membrane, AKT is phosphorylated at two sites, specifically at Thr 308 by phosphoinositide dependent kinase 1 (PDK1) and Ser 473 by phosphoinositide dependent kinase 2 (PDK2). However, the exact mechanism of these phosphorylations is yet unclear (Fresno Vara, et al., 2004). Phosphorylation of AKT leads to its activation whereby it phosphorylates key downstream effectors. Of particular interest to this project is the inactivation of GSK3β, by its phosphorylation (Zhao and Vogt, 2008). AKT, through the phosphorylation of these target proteins, fulfills a role as a key regulator of a variety of critical cell functions including glucose metabolism, cell proliferation and survival (Carracedo and Pandolfi, 2008).

The following figure is a simplified look at components of the PI3K pathway that are of interest to this project (Figure 1.6).

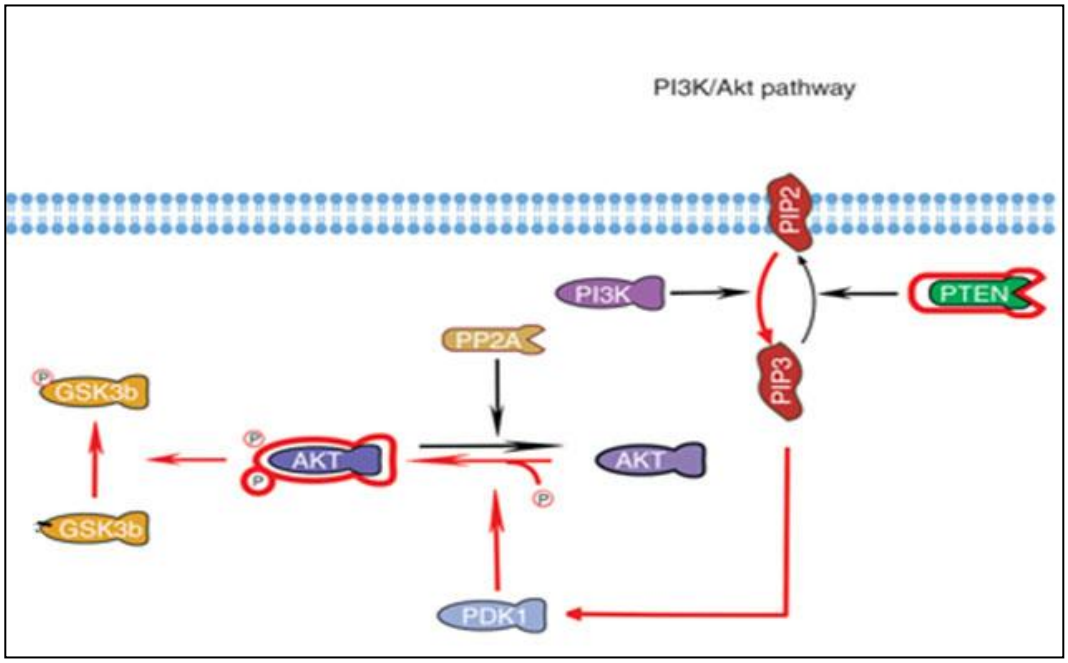

Figure 1.6: Simplified view of PI3K pathway. PIP2 at the plasma membrane is converted to PIP3 by PI3K and is negatively regulated by PTEN. This leads to phosphorylation of AKT by PDK1 which leads to phosphorylation of GSK3β. Kinase activity of PDK1 is opposed by phosphatase activity of PP2A.

Components of this pathway have been implicated in tumourigenesis and cancer progression at many levels such as excessive growth signals, insensitivity to growth inhibitory signals, evasion of apoptosis, limitless replicative potential, sustained angiogenesis, and tissue invasion and metastasis (Hanahan and Weinberg, 2000).

PI3K gene amplifications are frequently seen in ovarian and gastric tumours, and mutations of the pathway are common in breast, colorectal cancer and melanoma (Bader et al., 2005; Aziz et al., 2009). The most frequent mutations of PI3K are in its kinase domain and helical domain causing different impacts on PI3K targets (Zhao et al., 2008). Deregulation of the pathway is usually caused by oncogenic

activation of receptor tyrosine kinases. Alternatively, amplifications of genes encoding the catalytic unit of PI3K, and activating mutations in the regulatory subunit of PI3K, also cause excessive activation of the pathway (Zhao et al., 2008).

1.3.2 PTEN

PTEN (phosphatase and tensin homologue) is one of the most frequently lost or mutated tumour suppressors in cancer and is generally associated with advanced and metastatic disease (Zhang et al., 2012). PTEN is both a lipid and protein phosphatase. The significance of its protein phosphatase activity remains unknown and represents a gap in our understanding of the function of this important regulator of cell signaling (Zhang et al., 2012). A very recent study by Zhang and colleagues suggests that PTEN's protein phosphatase role is an auto-dephosphorylation event, thus having implications in PTEN's activity of itself (Zhang et al., 2012). The best known function of PTEN is as a lipid phosphatase, hydrolysing phosphoinositides at position 3' (Strambolic et al., 1998). PTEN can dephosphorylate the D3 position of PIP3 thus antagonizing signaling through the PI3K pathway (Maehama et al., 2001). PTEN can also dephosphorylate Tyr as well as Ser and Thr residues (Myers and Tonks, 1997). The lipid phosphatase role of PTEN effectively controls the activity of the PI3K pathway in regulating cell survival and growth via signaling from growth factor receptors and components of the extracellular matrix (Stambolic et al., 1998). Loss of PTEN results in suppression of apoptosis (Stambolic et al., 1998) and accelerated cell cycle

progression (Ramaswamy et al., 1999). The loss of PTEN is observed in many cancers (Li and Sun, 1997) and further germline alterations are associated with a group of syndromes known as PTEN hamartoma tumour syndromes, which are characterized by the presence of developmental and neurological defects and cancer susceptibility (Carracedo and Pandolfi, 2008). Loss of PTEN results in overactive AKT, which induces proliferation and promotes survival by inhibiting apoptosis (Datta et al., 1997).

1.3.3 PI3-Kinase and Melanoma

Deregulation of PI3K pathway is used by tumours to attain growth advantage and survival (Sansal and Sellers, 2004). The PI3K/PTEN pathway is one of the most deregulated pathways in melanoma. PTEN mutations are found in 30-40% of melanoma cell lines and 5-20% of primary melanomas (Guldberg et al., 2007; Tsao et al., 1998). Loss of expression or function of PTEN is due not only to mutation and allelic loss (Guldberg et al., 2007; Tsao et al., 1998), but functional inactivation by epigenetic silencing (Wu et al., 2003) or altered subcellular localization (Trotman et al., 2003). Absence or inactivity of PTEN deregulates the PI3K pathway and activates the downstream effector, AKT via its phosphorylation at two critical amino acids: Serine (Ser) 473 and Threonine (Thr) 308 (Chudnovsky et al., 2005). The resulting constitutive activation of AKT induces a sustained proliferative and anti-apoptotic cellular response. The importance of the PI3K pathway in malignant melanoma is underscored by the fact that over 60% of melanomas exhibit activated AKT (Dhawan et al., 2002).

A deregulated PI3K pathway can result in several cellular processes being upregulated, such as regulation of cellular growth, metabolism and proliferation. This is through downstream effectors such as Cyclin D3, VEGF, NFkB and MMPs which regulate cell cycle, angiogenesis, inflammation and invasiveness respectively (Lau and Ronai, 2011). Loss of the G1-S phase checkpoint is often seen in melanoma and allows cells to pass into the stage of cell proliferation without control (Sauroja et al., 2000). The role of the PI3K pathway in melanoma has been studied extensively and is a key player in melanoma progression. Ectopic expression of PTEN has been demonstrated to suppress melanoma cell growth and melanoma tumourigenicity and metastasis (Lopez-Bergami et al., 2008). A positive correlation has been determined in melanoma progression and phosphorylated/ activated AKT levels. Levels of phospho-AKT correlate inversely with disease-free survival and are associated with poor prognosis (Lopez-Bergami et al., 2008).

Chapter 2: Materials and Methods

(See appendix A for chemical list and appendix B for buffer recipes)

2.1 Cell Culture

2.1.1 Plasmid Preparation

Bacterial transformation was carried out using *E.Coli*. Competant *E.Coli* (BL21 DE3 purchased from New England Biolabs Product #C2527H) cells were thawed on ice for 15 minutes following which the plasmid (100ng) was added to the bacteria and incubated on ice for 30 minutes. The bacterial-plasmid mix was heated at 42^{o}C for one minute then cooled off on ice. 950µl of LB buffer was added to the heat shocked samples and incubated at 37^{o}C for one hour, after which bacterial cells were spread onto LB agar plates with ampicillin in a sterile manner. The plates were incubated overnight at 37^{o}C.

A colony was isolated from the plate and bacteria was cultured in LB Buffer with kanamycin at a final concentration of 50µg/ml or Ampicillin 100µg/ml depending on the antibiotic resistance of the plasmid. A single colony off the agar plates was first grown in 5ml of LB buffer with antibiotic. Tubes are incubated in 37^{o}C shaker at 200rpm overnight. A 1ml aliquot was then transferred to 50ml of LB buffer with antibiotic and continued to incubate in shaker. They were then grown once again overnight and then transferred to a volume of 100ml LB buffer with antibiotic.

Plasmids were then ready for purification using QIAGEN Plasmid Purification Kit Maxi (Catalogue # 12963)/Midi (Catalogue # 12943) Prep as per

manufacturer's protocol. Plasmid concentration was then measured using a mini spectrophotometer.

2.1.2 Restriction Digest and Agarose Gel Electrophoresis

Plasmid integrity was analyzed with a restriction digest and analyzed on an agarose gel. The TOPflash and FOPflash vectors were cut using *Bam* H1 (R0136 New England Biolabs) and Not I (R0189 New England Biolabs) restriction enzymes. The mix contained ddH_2O, DNA, 10X enzyme buffer (Buffer 3 from New England Biolabs) and 1µl of either or both enzymes. While the restriction digest incubated for two hours, a 1% Tris-Borate-EDTA (TBE) agarose gel was prepared with 1:10,000 SYBR dye (Invitrogen S33102). Following incubation 6X DNA loading dye was added to samples to bring to equal volumes then was loaded onto the gel. Samples were electrophoresed at 100V until dye reached 2/3 way along gel. Gel was viewed over UV light and imaged with Kodak Imager.

2.1.3 Cell Lines

The HEMa-LP cell line represents a primary human epidermal melanocytic cell line and was isolated from adult skin (Cascade Biologics™). Human Epidermal Melanocytes Lightly Pigmented (HEMa-LP) (c-024-5c) were grown in Medium 254 (M-254-500) supplemented with 10% Human Melanocyte Growth Supplement (HMGS) (s-002-5) and 10µg/ml gentamicin and 0.25µg/ml amphotericin B (R-015-010).

WM-35 cells, which were obtained from American Type Culture Collection (ATCC) (Special Wister Collection) were established from a primary superficial spreading melanoma in the radial growth phase taken from the scalp and neck of a patient from Sunnybrook Health Sciences Center, Toronto, Ontario from Dr. Robert Kerbel. These cells were grown in Hyclone's RPMI-1640 medium (SH30027.01) containing 10% Fetal Bovine serum and 1% penicillin/streptomycin (Invitrogen). WM-793B cells were also obtained from ATCC (Special Wister Collection) and were isolated from skin taken from a melanoma in the vertical growth phase lesion obtained from the sternum of a patient. These cells were grown in the same medium as WM-35 cells. A2058 cells, metastatic melanoma cell line, was obtained from the lymph node of a patient also obtained from ATCC. A2058 cells were cultured in Dulbecco's Modified Eagle Medium (DMEM++-) High Glucose 1X (Gibco 11995) with 10% Fetal Bovine Serum and 1% Penicillin/streptomycin. All cells were incubated in 5% CO_2 and 37^{o}C. Cell growth and confluency was checked every few days, and cells were passaged prior to 90% confluency.

2.1.4 Cell Passage

Cell medium was removed and cells were washed with 1X phosphate buffered saline (PBS) and the PBS was removed. 350µl of 0.25% Trypsin-EDTA was added to the cells, and the plate was incubated in cell incubator for one minute. After which cell medium containing fetal bovine serum (FBS) was added to the plate, to de-activate trypsin activity. An aliquot of cells was passed onto a new

plate with fresh growth medium. Fresh medium with 10%FBS and 1% Penicillin/Streptomyosin brought up the total volume to 10ml for a 60mm cell culture plate and 2ml for each 6-well plate.

2.1.5 Transient transfection of PTEN

A2058 cells were grown to 70% confluency and were transfected with 4 µg pEGFP-C3-hPTEN or pEGFP-C3 empty vector control. All transfections utilized Lipofectamine2000 (Invitrogen) according to manufacturer's protocols in Opti-MEM reduced serum medium. For each well of a 6-well plate the following conditions were used: 10µl of Lipofectamine 2000 was incubated in 240µl of OptiMEM for five minutes along with 4µg of plasmid in 250µl OptiMEM in a separate tube. After five minutes the two tubes were combined and mixed gently and allowed to incubate for another 20 minutes. Meanwhile, medium from the plates was removed and the plates were washed with OptiMEM. 1.5ml of OptiMEM was added to each well, following incubation the DNA/Lipofectamine/OptiMEM was added to the cells.

Cells were incubated at $37^{o}C$ at 5% CO_2 for 24 hours post transfection. Transfection efficiency was analyzed using fluorescence microscopy to detect GFP. pEGFP-C3 empty vector and no DNA transfections were used as controls. At 24 hours cells were lysed as per protocol (Section 2.1.7).

2.1.6 Cell Treatments with Inhibitors

2.1.6.1 Wortmannin Treatment

A2058 Cells were treated with 1µM Wortmannin (Sigma W3144) for 12 hours in DMEM (++-)/10% FBS/ 1%P/S. The medium was replaced every three hours and fresh Wortmannin was added. At 12 hours cells were lysed as per protocol. Control cells were incubated in the same volume of DMSO as cells treated with Wortmannin to serve as a vehicle control.

2.1.6.2 Wnt 3a Treatment

A2058 cells were treated with 150 and 300 ng/ml Recombinant Human Wnt-3a (R&D Systems Inc. 5036-WN) for 1, 3, 6, 9, 12, 18 and 24 hours in DMEM (++-)/10% FBS/ 1%P/S. Cells were then lysed as per protocol.

2.1.6.3 DKK-1 Treatment

A2058 cells were treated for 1, 2, 3, 4, 5, 6, 9, 24 hours using 10ng/ml, 50ng/ml, 100ng/ml, 250ng/ml, 500ng/ml and 1µg/ml Recombinant Human Dickkopf Homolog 1 (DKK1) (Invitrogen Gibco PHC9214) in the presence and absence of recombinant Wnt 3a. After treatment, cells were lysed as per protocol.

2.1.6.4 Sfrp-1 Treatment

A2058 cells were treated with recombinant Human sFRP-1 (R&D Systems Inc. 5396-SF) at a concentration of 1, 10, 100 nM (0.15, 0.75, 3.25 µg/ml respectively) for 8-9 hours. After treatment, cells were lysed as per protocol.

2.1.7 Preparation of Cell Lysates

Cells were washed with phosphate buffered saline (PBS) and lysed with 150µl lysis buffer per well of a 6 well plate. The lysis buffer contained 50mM Tris buffer (pH 8.0), 150mM NaCl, 1% NP-40, 0.5% sodium deoxycholate, 1mM phenylmethanesulfonylfluoride (PMSF), 5µg/ml leupeptin and 25 µg/ml aprotinin. A protease inhibitor cocktail was added to the lysis buffer to prevent protein degradation and to preserve the phosphorylation status of proteins by inhibiting proteases. Cells were homogenized with a 26Guage syringe, centrifuged at maximum speed at 4^{o}C for five minutes, and the clear supernatant was collected. Lysate was either used immediately or stored at -80^{o}C once protein concentration was determined.

2.1.8 Preparation of Nuclear and Cytosolic Extracts

Cytoplasmic and nuclear cell extracts were obtained using the NE-PER Pierce Kit (Thermo Scientific 78833) as per manufacturer's protocols with some modifications as follows.

Cells were trypsinized as per protocol and collected with 5ml of DMEM (++-)/10% FBS/ 1%P/S in a 15ml falcon tube. They were spun down at 500 x g for five minutes. The supernatant/medium was then removed and the pellet was washed by centrifugation with PBS three times for five minutes each at 500 x g. The PBS was discarded and the pellet was resuspended in 1ml of fresh PBS. Cells were counted using Allen Cell Coulter Counter. Cells were accordingly aliquoted depending on total cell count. A pellet of a minimum of two million

cells was vortexed with 200µl of ice cold CER I for 15 seconds in order to fully suspend pellet, then incubated on ice for 10 minutes. Then 22µl of ice cold CER II was added to the tube. The tube was once again vortexed for five seconds then incubated on ice for one minute, following another five second vortex. The tube was then centrifuged in a 4^{o}C centrifuge at maximum speed (16,000 x g) for five minutes. The supernatant was immediately transferred to a clean tube and was labelled as the cytoplasmic fraction. The pellet was washed three times, five minutes each with PBS to ensure no cytoplasmic contamination in the nuclear fraction. After the final wash the PBS was removed and the cells were suspended in 100µl of NER I. The sample was then homogenized using a 26Guage syringe. The sample was then left in a 4^{o}C rotator for one hour, and was vortexed every 15 minutes. After this, the sample was centrifuged in a 4^{o}C centrifuge at maximum speed for 10 minutes. The supernatant (nuclear fraction) was then collected and stored at -80^{o}C until further use. If more or less than two million cells were used, the volume of CER I, II and NER I was changed accordingly keeping the 200:11:100 volume ratio respectively consistent.

2.2 Protein Concentration Determination

Protein concentration of lysates were quantified by Bicinchoninic Protein Assay (Thermo Fischer Scientific Inc.). Protein concentrations were measured against BSA concentrations of 0, 50, 100, 200, 300 and 500ng/ml. A minimum r^2 value of 0.99 was sought to determine most accurate protein concentrations.

A 96-well plate was used for the assay, 10µl of a 1:10 dilution of the lysates and 10µl of the standards were added to the plate. 190µl of the assay mix was then added to the unknown concentration lysates as well as the standards and a blank. All samples were conducted in triplicates. The assay mix was a mixture of Reagent A and Reagent B, for every 5mls of Reagent A, 100µl of Reagent B were added.

The plate was incubated at 37^{o}C for half an hour after which the plate was read in a VersaMax Microplate reader.

2.3 Western Blot

15µg of cell lysate was combined with 6X loading buffer for a final volume of 20µl. The samples were placed in boiling water for two minutes, then vortexed and separated by 10% Tricine gel electrophoresis with inner and outer tris buffers. The samples were run alongside a molecular weight marker (Bio-Rad Precision Plus Protein Dual Colour Standard). Once the loading dye reached the bottom of the tricine gel the gel was removed and transferred at 4^{o}C onto polyvinylidene difluoride (PVDF) membranes (Millipore), which were first incubated in methanol for five minutes. PVDF membranes were blocked with 5% gelatin from cold water fish skin (Sigma G7041)/TBS-T and probed with specific primary antibodies followed by peroxidase-conjugated secondary antibodies (GE Healthcare UK Limited) and visualized using Western Lightning® Plus-ECL (PerkinElmer, LAS Inc.) using X-ray films. The following primary antibodies were used, diluted in 5% gelatin/TBS-T; anti-β-actin (1:5000), anti-β-catenin

(Cell Signaling) (1:2000), anti-active-β-catenin (Millipore) (1:1000), antiphospho-β-catenin (ser 45) (Cell Signaling) (1:1000), antiphospho-β-catenin (ser 33/37/thr 41) (Cell Signaling) (1:1000), anti-AKT (Cell Signaling) (1:3000), anti-PAKT (Ser 473) (Cell Signaling) (1:2000), anti-PTEN (Cell Signaling), anti-GFP (Santa Cruz) (1:2000), anti-Lamin B (Calbiochem) (1:2000), α/β tubulin (Cell Signaling) (1:5000). Following incubation in primary antibody, membranes were then incubated in secondary mouse/rabbit antibodies (GE Healthcare UK Limited) 1:10,000 dilution in 5% gelatin/TBS-T for 1 hour at room temperature. Blots were then visualized using Western-Lightning® Plus-ECL for one minute (PerkinElmer, LAS Inc.) and were visualized by X-ray film (Kodak BioMax/ Fujifilm Super RX).

Densitometric analysis was performed by Image J software. Histograms are an average of three or more independent experiments, reported as a fold-change of control (which is set at 1). Statistical analysis was performed by a student's t-test ($p<0.05$) and Mann-Whitney Rank Sum test ($p<0.05$) using SigmaPlot (v12) software.

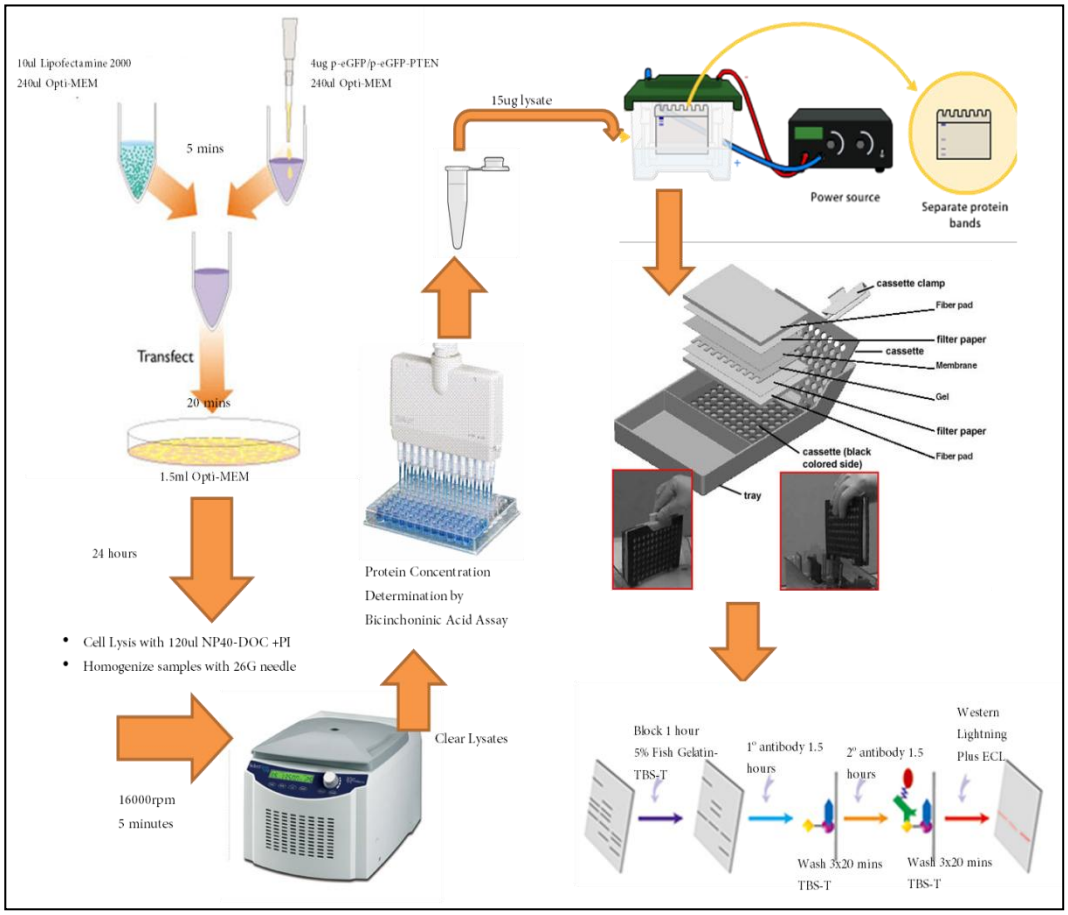

Figure 2.1: Summary of transfection to western blot protocols. Figure is a representation of methodology used in PTEN plasmid transfection, preparation of cell lysates, protein determination, gel electrophoresis and western blot analysis.

2.4 Protein: DNA interaction Assays

2.4.1 Luciferase Assay

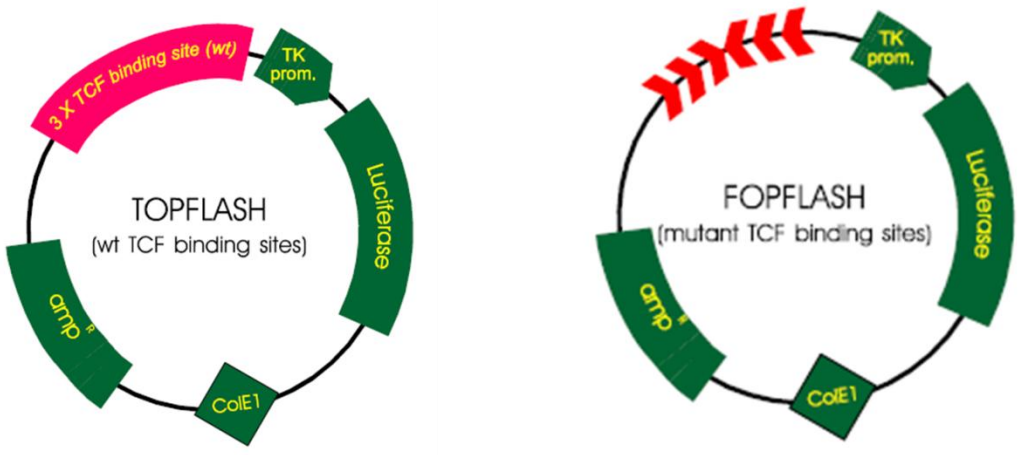

Figure 2.2 TOPflash and FOPflash Plasmid: Left: shows TOPflash plasmid with three wild-type TCF binding sites. Right: shows FOPflash plasmid with mutant sites.

Cells were transfected with PTEN, pEGFP empty vector, pTOPFLASH pFOPFLASH (Reporter Kit 17-285 Millipore), and pRenilla according to the methods below.

Transfection Protocols:

Method 1:

Night before transfection cells were incubated in growth medium (DMEM with 10% FBS) lacking antibiotics. On the day of transfection, cells were washed with PBS and incubated in 2ml of fresh medium without antibiotics and were left in cell incubator until transfection mix was ready. 10µl of Lipofectamine 2000 was

mixed with 240µl of Opti-MEM, and in another tube 2µg of TOPflash/FOPflash plasmid, 0.01µg pRenilla plasmid with and without 2µg GFP/PTEN was mixed in 250µl of Opti-MEM. After five minutes both tubes were mixed and let to incubate for another 20 minutes. The 500µl transfection mix was added directly to each corresponding well of the six well plates (with a final volume of 2.5ml). The cells were incubated at 37^{o}C at 5%CO_2. After 24 hours of transfection, the medium was changed to growth medium lacking antibiotics (DMEM ++- with 10% FBS). Cells were incubated for another 48 hours.

Method 2:

A2058 cells were grown in DMEM with 10% FBS to about 60% confluency. The medium was replaced with 1.5ml Opti-MEM medium. 10µl of Lipofectamine 2000 was mixed with 240µl of Opti-MEM, and in another tube 2µg of TOPflash/FOPflash, 0.01µg pRenilla with and without 2µg GFP/PTEN was mixed in 250µl of Opti-MEM. After five minutes both tubes were mixed and let to incubate for another 20 minutes. The transfection mix was added to the cells and allow to transfect for 24 hours. After a further 24 hours of incubation the medium was replaced with DMEM with 10% FBS and allowed to incubate another 24 hours.

Method 3:

Night before transfection incubate cells were growth medium (10% FBS) lacking antibiotics. On the day of transfection, cells were washed with PBS and incubated in 2ml of fresh medium without antibiotics and were left in cell incubator until

transfection mix was ready. 10µl of Lipofectamine 2000 was mixed with 240µl of Opti-MEM, and in another tube 0.2-0.6µg of TOPflash/FOPflash plasmid, 0.001µg pRenilla plasmid with and without 4µg GFP/PTEN was mixed in 250µl of Opti-MEM. After five minutes both tubes were mixed and let to incubate for another 20 minutes. The 500µl transfection mix was added to directly to each corresponding well of the six well plates (with a final volume of 2.5ml). The cells were incubated at 37^{o}C at 5%CO_2. After 5-13 hours of transfection the medium was replaced with DMEM with 10% FBS and 1% P/S. The cells were incubated for another 36-48 hours.

Method 4:

Cells were transfected for 24 hour transfection with Fugene HD (Promega E2311) with a transfection reagent:DNA ratio of 2:1, 3:1,4:1,6:1. TOPflash/FOPflash was used in increasing concentrations of 0.2µg-0.6µg with 0.001-0.003µg pRenilla with and without 3-4 µg of PTEN/GFP plasmid. Cells were lysed after the 24 hour transfection.

Method 5:

Cells were transfected for 12 hour transfection with Fugene HD (Promega E2311) with a transfection reagent:DNA ratio of 2:1, 3:1,4:1,6:1. TOPflash/FOPflash was used in increasing concentrations of 0.2µg-0.6µg with 0.001-0.003µg pRenilla with and without 3-4 µg of PTEN/GFP plasmid. After 12 hours of transfection cells were incubated in DMEM with 10% FBS and 1% P/S for a further 36 hours, after which they were lysed.

Method 6:

Cells were transfected for 24 and 48 hours with 1,3,5µg TOPflash/FOPflash and 0.005, 0.015, 0.025 µg pRenilla plasmid respectively and a 3:1 Fugene HD: DNA ratio in Opti-MEM.

Method 7:

Cells were transfected for 36 hours with 2.5µg TOPflash/FOPflash with and without 3µg PTEN/GFP plasmid and a 3:1 Fugene HD: DNA ratio in Opti-MEM.

Method 8:

Cells were transfected for 48 hours with Lipofectamine 2000 as per protocol with 1-3µg TOP/FOPflash with and without 1-4µg PTEN/GFP in Opti-MEM medium.

Method 9:

Cells were transfected for 48 hours with Fugene HD:DNA ratio of 3:1 with 1,3,5µg TOPflash/FOPflash 0.005,0.015,0.025 µg pRenilla respectively and 1-2µg TOPflash/FOPflash, 0.005,0.010 µg pRenilla respectively and 2-3µg PTEN/GFP.

Following transfection by one of the above mentioned methods 1-9, cells were passively lysed with 1X Passive Lysis Buffer (Part of Promega Dual Luciferase Reporter Assay System) and were assayed according to manufacturer's

instructions (Promega Dual Luciferase Kit). The instrument used was a BMG FLUOstar Omega (Cross Cancer Institute Dr. Mary Hitt's Lab).

2.4.2 Electrophoretic Mobility Shift Assays (EMSA)

Post-transfection cells were trypsinized and suspended in medium and then pelleted. A cell count was done using the Allen Lab Coulter Counter. Equal number of cells was used for extractions. Nuclear Extracts were prepared using a Nuclear/Cytoplasmic Extraction Kits (Pierce) as described previously.

2.4.2.1 Infrared Dye 700: Electrophoretic Mobility Shift Assays

As a substitute for radioactive EMSAs, an alternative assay was carried out using a wild-type TCF binding oligonucleotide (pTOPFLASH sequence (Integrated DNA Technologies) (sense 5'-5IRD700/ TGC CGG GCC CTT TGA TCT GCT-3') (anti sense 5IRD700/ AGC AGA TCA AAG GGC CCG GCA-3') and mutant TCF binding oligonucleotide (pFOPFLASH sequence sense 5'-/5IRD700/AGC GGC CAA AGG GGC CCG GCA -3') (antisense 5IR700/TGC CGG GCC CCT TTG GCC GCT-3') with an infrared 700 dye. 5µg of nuclear extract was used in a binding reactions consisting of components Li-Cor Odyssey Infrared EMSA Kit components (829-07910): (10X Binding Buffer (100mM Tris, 500mM KCl, 10mM DTT; pH 7.5)), (25mM DTT, 2.5% Tween®), (Poly dIdC, 1µg/µl in 10mM Tris, 1mM EDTA; pH 7.5), (200mM EDTA, pH 8.0), 1% NP-40, 100mM $MgCl_2$.

The binding reaction along with the 50nM sense and 50nM antisense oligonucleotide was incubated at room temperature for 25 minutes at room temperature. After which the samples were equalized with 10X Orange Loading Dye (Licor Odyssey Infrared EMSA Kit). The samples were run on a 5% non-denaturating acrylamide (30:0.8; acrylamide:bis-acrylamide) gel. During the incubation period, the gel was pre-run at 90V for 30 minutes. The running buffer was 0.5X Tris-Borate-EDTA (TBE). Following the pre-run, the samples were loaded and the gel was run at 100V until loading dye reached bottom.

The gel was visualized using an Infrared Li-Cor Odyssey Gel Reader (IDT Core Dr. Richard Fahlman's Lab).

2.5 Immunofluorescence

Cells were transiently transfected as per protocol. 24 hours post transfection cells were trypsinized and added to coverslips at the bottom of a 6-well plate. Cells were allowed to grow for one day. Cells were then washed with PBS and fixed with 4% formaldehyde in PBS for 15 minutes. They were then washed three times with PBS five minutes each. Cells were permeablized with 100% cold methanol at -20^{o}C for 20 minutes. They were washed once again, and then blocked in 1% BSA in PBS for one hour at room temperature. Followed by incubation in primary antibody for four hours at room temperature. They were thoroughly washed with PBS, then incubated in Alexa Fluor ® 555-conjugated secondary antibody (Invitrogen) for visualization for one and half hours at room temperature, followed by more washing. Cells were observed with

immunofluorescence imaging using Carl Zeiss laser scanning confocal microscope (Cross Cancer Institute) and analyzed by LSM510 software.

2.6 Quantitative Real Time PCR

2.6.1 RNA Extraction

**All procedures from this point on were done in RNAse-free/sterile environment.

Treated cells were trypsinized as per protocol, and were then counted using Allen Cell Counter. Between $1x10^5$ and $1x10^6$ cells were used for RNA extraction. RNA was extracted using Qiagen RNAeasy kit (Catalogue #74104), following their protocol for 'Animal Cells Spin' section (P.27-30 of manual) with step 3 homogenization being performed with a 26Guage needle. Once RNA was extracted, its concentration was measured using a mini spectrophotometer. If RNA purity was an optical density reading of 1.8-2.0, it was further used for cDNA preparation.

2.6.2 cDNA Preparation

Prior to reverse transcription, the 2µg of RNA was purified of DNA contamination using Deoxyribonuclease I, Amplification Grade (Invitrogen 18068-015). The protocol was followed as supplied with the product, however all volumes were doubled to have a final volume of 22µl instead of 11µl as would be in the written protocol. After this the RNA was ready for reverse transcription using Superscript II reverse transcription (Invitrogen 18064) as per protocol with

once again doubling all the volumes. After this the concentration of the prepared cDNA was measured using a spectrophotometer. Once again a purity of 1.8-2.0 was sought. Samples were then frozen at -80^{o}C until use.

2.6.3 PCR

The PCR reaction was performed using Taq DNA polymerase (Invitrogen 10966) protocol. The samples were then analyzed by agarose gel electrophoresis as described earlier.

2.6.4 Primer Design for qPCR

In order to make optimal primers for qPCR the Real Time PCR software from Integrated DNA Technologies (IDT) was used. Some points to determine optimal primers that were considered were: to have a melting temperature between 60-62^{o}C, have a GC content less than 50% and have a length between 18-30 bases. This tool allowed easy primer design using the NCBI gene accession number of the target gene. SciTools OligoAnalyzer 3.1 (IDT) was used to determine these physical properties of the primers. These primers were then ordered through IDT services. They were stored at -20^{o}C.

2.6.5 Quantitative Real-Time PCR

Total RNA was extracted using RNeasy Kit (QIAGEN catalogue #74104) as per manufacturer's protocol. The extracted RNA (1µg) was used for reverse transcription of Oligo (dt) (Invitrogen) and Superscript II reverse transcription (Invitrogen). Real time quantification of MMP-2, cyclin D1, and VEGFa were

assessed using power SYBR Green PCR Master Mix (Applied Biosystems). GAPDH was used as the endogenous control. Samples were amplified with a precycling hold at 95˚C for 10 minute, then 40 cycles of annealing and extension at 95^{o}C for 15 seconds followed by 60˚C for one minute. The following primers were used: MMP-2: sense (5'- ACC CAT TTA CAC CTA CAC CAA G -3'); MMP-2: anti-sense(5'- TGT TTG CAG ATC TCA GGA GTG -3'); MMP-9: sense (5'- CGA ACT TTG ACA GCG ACA AG -3'); MMP-9: anti-sense (5'- CACTGA GGA ATG ATC TAA GCC C-3'); Cyclin D1: sense (5'- CAT CTA CAC CGA CAA CTC CAT C-3'); Cyclin D1: anti-sense; (5'- TCT GGC ATT TTG GAG AGG AAG- 3') VEGF-A: sense (5'-AGTCCAACATCACCATGCAG -3'); VEGF-A: (5'TTCCCTTTCCTCGAACTGATTT-3') anti-sense; GAPDH: sense (5'- TCAACGACCACTTTGTCAAGCTCA -3'); GAPDH: anti-sense;(5`-GCTGGTGGTCCAGGGGTCTTACT-3`). Measurements were performed with Applied Biosystems 7900HT Fast Real Time PCR System using SDS 2.3 software. Gene expression was determined using the ΔΔct method normalized to GAPDH-binding transcript levels. Data was analyzed using RQ (relative quantity) Manager software. The manual method of calculation is attached as anppendix (Courtesy of Kunimasa Suzuki Molecular Biology and Biochemistry Core Facility University of Alberta, Alberta Diabetes Institute). Histograms are reported as a percentage of the control, which is set at 100%.

2.7 Invasion Study: BD Biocoat™ Matrigel™ Invasion Chamber

To study the invasiveness of cells a Matrigel invasion assay was carried through at per manufacturer's protocol (BD Biosciences Biocoat Matrigel invasion chamber 24-well Cat No. 354480). At room temperature, the inserts and wells were hydrated with Dulbecco's Modified Eagle Medium (DMEM++-) High Glucose 1X (Gibco 11995) for two hours in a humidified cell incubator at $37^{o}C$ and 5% CO_2. During the rehydration time, cell suspensions were prepared with $1.25x10^{5}$cells/ml from three control groups; untreated cells, cells with transfection reagent and cells transfected with empty GFP vector, along with the experimental group cells transfected with pEGFP-PTEN following 24 hour transfection in DMEM ++-. Following rehydration the inserts were transferred to wells with chemoattractant DMEM++- with 10% FBS. The cell suspension was added to the inserts, and the BD Biocoat Invasion Chambers were incubated in a humidified culture incubator for 24 hours at $37^{o}C$ and 5% CO_2 atmosphere.

Following incubation, non-invasive cells were removed by scrubbing the top of the insert gently with a moistened cotton swab. Inserts were then stained with a staining/fixing dye (4% paraformaldehyde, 0.1% crystal violet in PBS) for 2 minutes after which the insert was passed through two beakers of water to remove excess dye. The inserts were then air dried. Once dry the insert with the invading cells was removed by the tip of a sharp scalpel blade. It was then rotated and fix to a slide with Permount. A cover slip was placed on top of the membrane to

remove air bubbles. The cells were counted at 200X magnification in a blinded manner.

Chapter 3: Results

3.1 β-catenin Profile in Melanoma Progression

This study used a panel of cell lines representative of the various stages of melanoma progression: primary melanocytic line (HEMa-LP); radial growth phase (RGP) (WM35); vertical growth phase (VGP) (WM793) and metastatic melanoma (A2058). To study the alterations in β-catenin through progression of melanoma to metastasis, β-catenin/active-β-catenin expression levels along with subcellular distribution were evaluated throughout melanoma progression.

Western blot (WB) analysis revealed that HEMa-LP and WM35 cells showed low expression of β-catenin, while WM793 and A2058 cells showed significantly higher levels of β-catenin (Figure 3.1a). These results were confirmed by immunofluorescence (IF) analysis (Figure 3.1b). IF showed that along with increasing levels of β-catenin in melanoma progression, β-catenin also changed in localization. HEMa-LP and WM35 cells showed β-catenin expression localized at the cellular membrane. WM793 cells showed increased levels of cytosolic expression and A2058 cells showed β-catenin throughout the nucleus and cytosol in high levels along with complete delocalization from the plasma membrane.

3.2 PI3-K profile in Melanoma Progression:

To elucidate a potential mechanism by which β-catenin levels are regulated, levels of PTEN were evaluated, as representative of the PI3K pathway. The tumour suppressor and negative regulator of PI3K, PTEN is mutated in 30-50% of melanomas (Wu et al., 2003). Therefore it was important to see the expression of PTEN in progression of melanoma, to see the status of the PI3K pathway at the level of PTEN. Hema-LP and WM-35 cell lines showed expression of PTEN, however WM793 and A2058 cells were PTEN-null, as measured by western blot analysis (Figure 3.1a). This pathway in particular was looked at because previous studies have shown that the PI3K pathway plays a role in regulating levels of active-β-catenin (Sharma et al., 2002 and Persad et al., 2001).

These results collectively suggest that as melanoma progresses levels of β-catenin as well as active-β-catenin increase, while PTEN expression is lost. This suggests a potential inverse relationship between a deregulated PI3K pathway and elevated β-catenin levels.

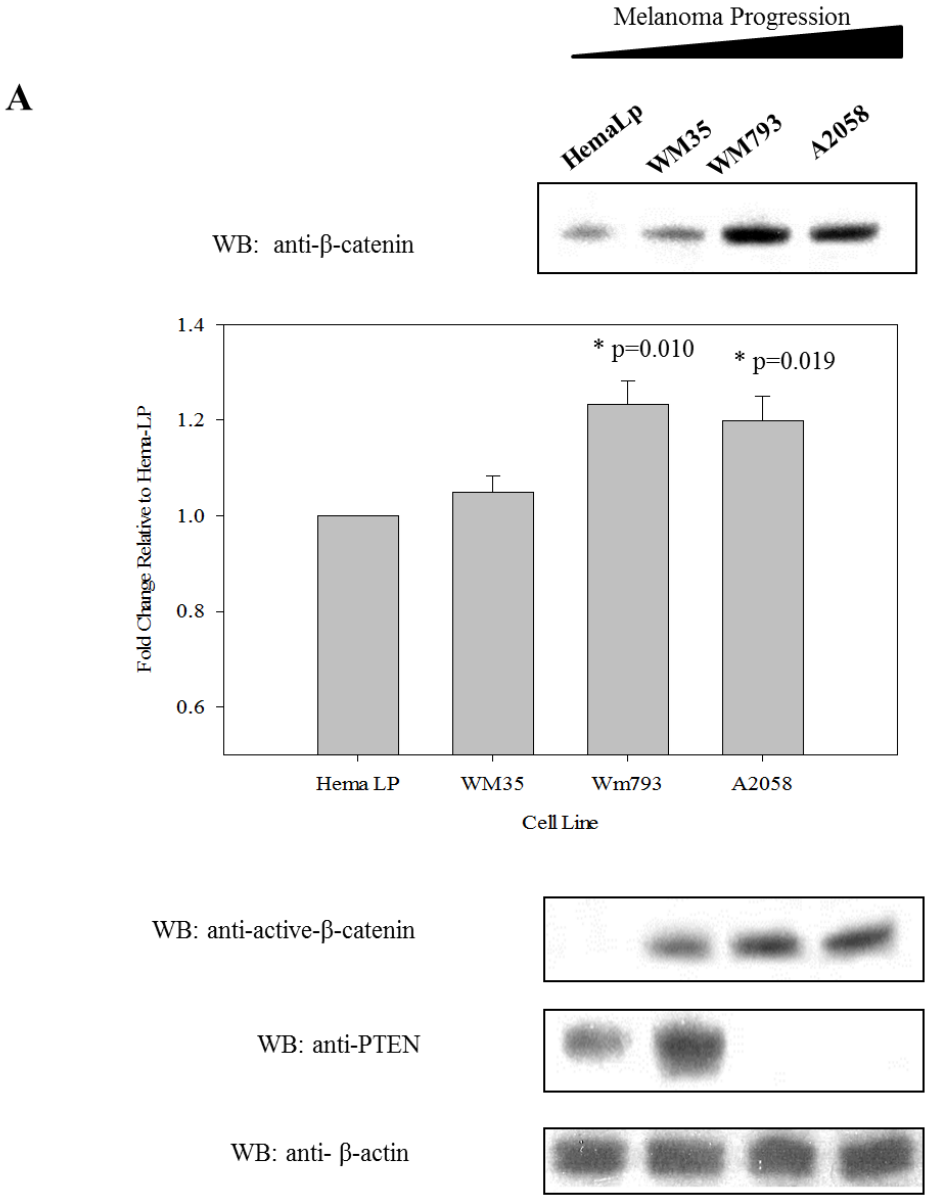

Figure 3.1: Expression of β-Catenin is elevated in melanoma progression. (A) Western Blot Analysis of Expression profile of β-Catenin, Active-β-Catenin and PTEN and densitometric analysis of β-Catenin in normal melanocytes (Hema-LP), radial (WM-35) and vertical (WM-793) growth phase, and metastatic (A2058) melanoma cell lines.

B

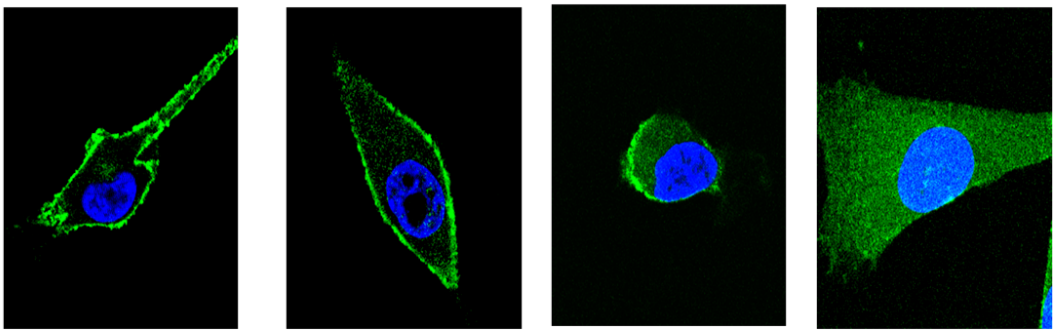

Hema-LP **WM-35** **WM-793** **A 2058**

Figure 3.1: Localization of β-Catenin is elevated in melanoma progression. (B) Immunofluorescence analysis of β-Catenin (green) localization in normal melanocytes (Hema-LP), radial (WM-35) and vertical (WM-793) growth phase, and metastatic (A2058) melanoma cell lines. β-catenin loses localization from cell membrane as melanoma progresses. β-catenin is expressed in nucleus (blue DAPI) and cytoplasm of metastatic cells.

3.3 Decrease of Active-β-catenin and total cellular β-catenin upon reintroduction of PTEN in PTEN-null A2058 Cells

My previous results showed that PTEN-null melanoma cells expressed high levels of total cellular β-catenin which was dispersed throughout the entire cell. Active-β-catenin, which was also expressed in high levels was mainly localized in the nucleus. In order to evaluate whether the PI3K/PTEN pathway regulated the observed increase in β-catenin levels with melanoma progression, we studied alterations in β-catenin levels in PTEN-null cells transfected with wild-type PTEN. PTEN-null A2058 cells were transiently transfected with 4µg of pEGFP-PTEN. Four forms of β-catenin; two phosphorylated forms, total cellular β-catenin and active-β-catenin, were evaluated by western blot analysis and immunofluorescence.

A time dependent analysis of PTEN transfection showed a decrease in both β-catenin and active-β-catenin levels between 24 and 48 hours post transfection (Figure 3.2). However to avoid excess cell death which was observed post 24 hours, the following transfections were carried out for 24 hours.

Levels of active-β-catenin (Figure 3.3b) decreased upon reintroduction of PTEN as did levels of total cellular β-catenin (Figure 3.3a) when compared to control cells and cells transfected with an empty GFP vector. Levels of both forms of phosphorylated β-catenin (serine33/37 threonine 41) (Figure 3.3c) and (serine 45) (Figure 3.3d) were unaffected by reintroduction of PTEN, suggesting that the PI3K pathway may not be involved in the post-translational modification of β-

catenin. To ensure proper loading, a western blot for the loading control β-actin was carried out (Figure 3.3e). There was a decrease in level of phospho-AKT while levels of AKT remained constant in PTEN transfected cells, showing that the transfected PTEN was inhibiting the PI3K pathway (Figure 3.3e). Since western blot analysis showed that PTEN affects levels of active-β-catenin as well as total cellular β-catenin, it was imperative to see changes in localization as well.

IF confirmed the changes in levels of β-catenin as well as active-β-catenin. Active-β-catenin, which was mainly located in the nucleus of control cells (untreated) showed significantly decreased levels in the PTEN transfected cells (Figure 3.4c). β-catenin was dispersed throughout the cell and expressed in high levels in control A2058 cells. Upon PTEN reintroduction β-catenin levels significantly decreased and β-catenin was mainly localized in the cellular membrane. This was similar to the expression pattern observed in primary cells, as shown in Hema-LP (Figure 3.4a/b).

Evaluation of nuclear and cytosolic fractions by western blot analysis confirmed the decrease in levels of nuclear β-catenin. Cytoplasmic and nuclear samples were free of contamination as confirmed by blotting for nuclear purity by Lamin B and cytoplasmic purity by α/β tubulin. (Figure 3.3f)

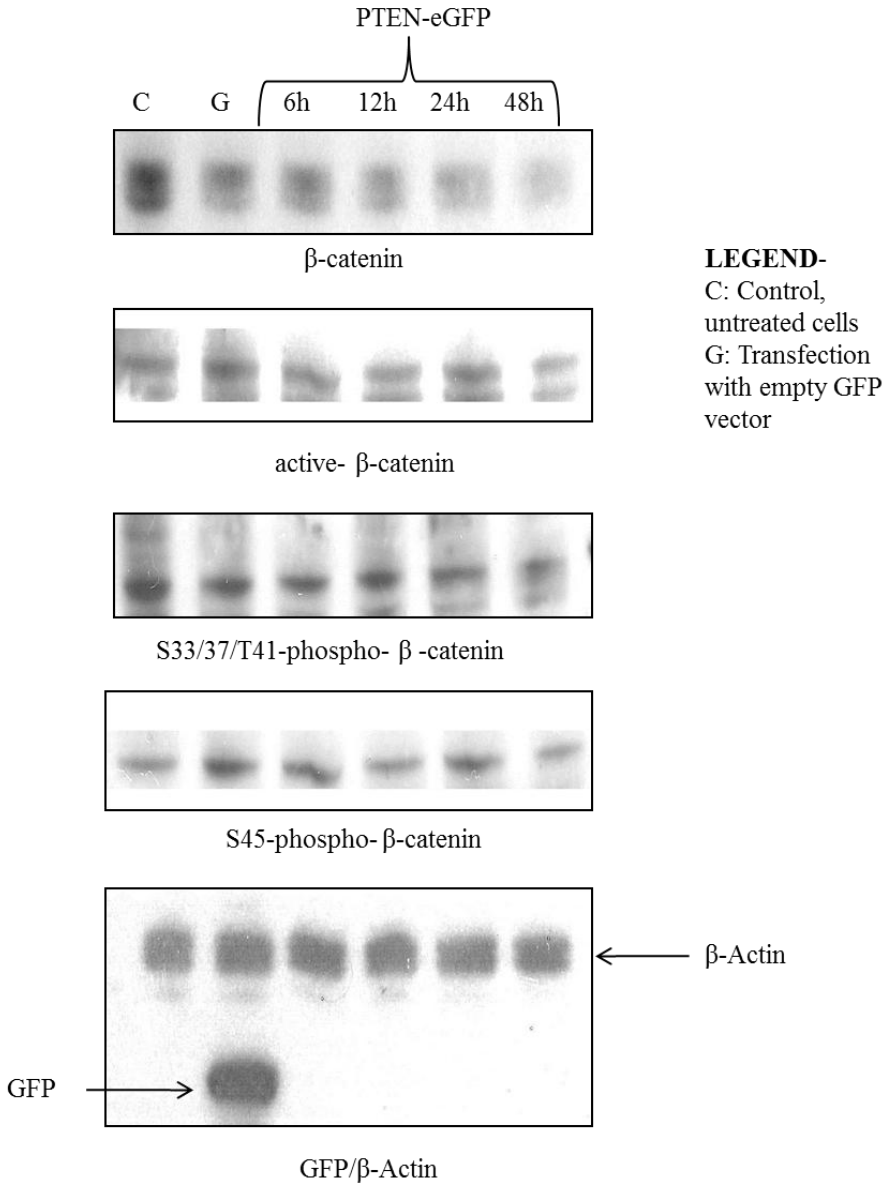

Figure 3.2: β -Catenin Levels in Time Dependent PTEN Transfection of A2058 Cells. Levels of total β-catenin, Active- β -Catenin decrease 24-48 hours post PTEN transfection. Levels of, Ser 33,37, Thr41 and Ser45 Phospho-B-Catenin are unchanged with 6,12,24,48 hours of PTEN transfection in metastatic PTEN-null cells.

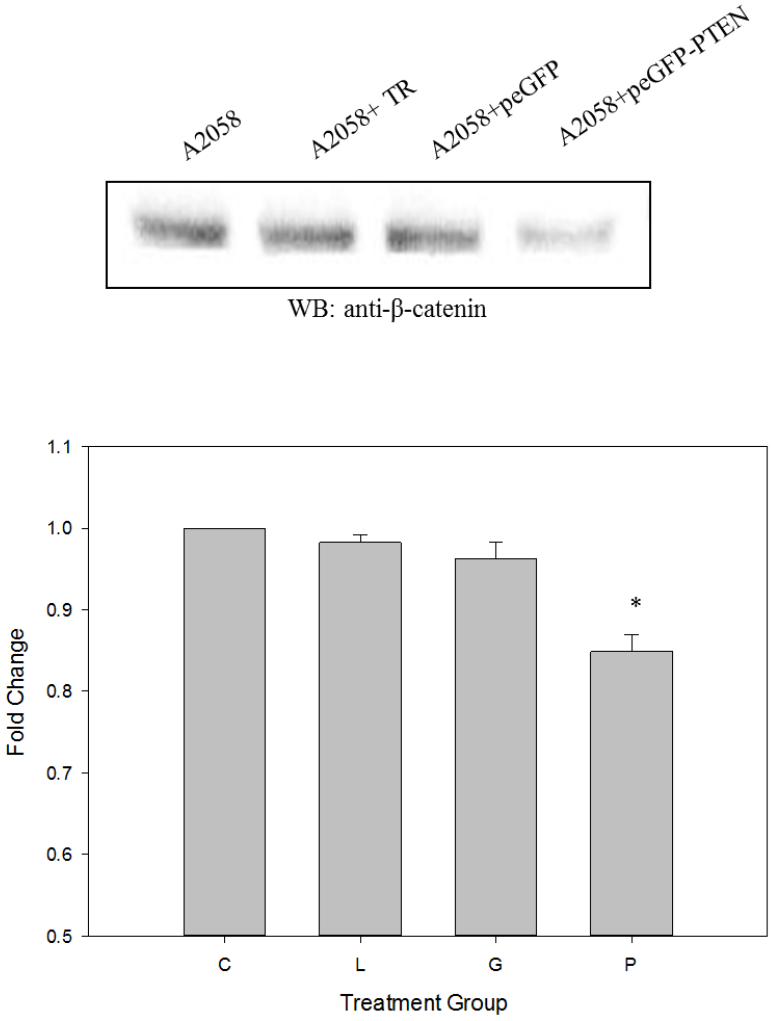

Figure 3.3 A: PTEN re-expression decreases β-Catenin protein in PTEN null melanoma cells (A2058). Western blot analysis and densitometric analysis reveals PTEN transfected A2058 cells show a significant decrease ($p= 0.002$) in levels of β-catenin 24hours post transfection.
C: Untreated A2058 cells; L: A2058 cells with Lipofectamine 2000 transfection reagent;
G: A2058 transfection with empty GFP vector; P: A2058 transfection with PTEN-eGFP plasmid

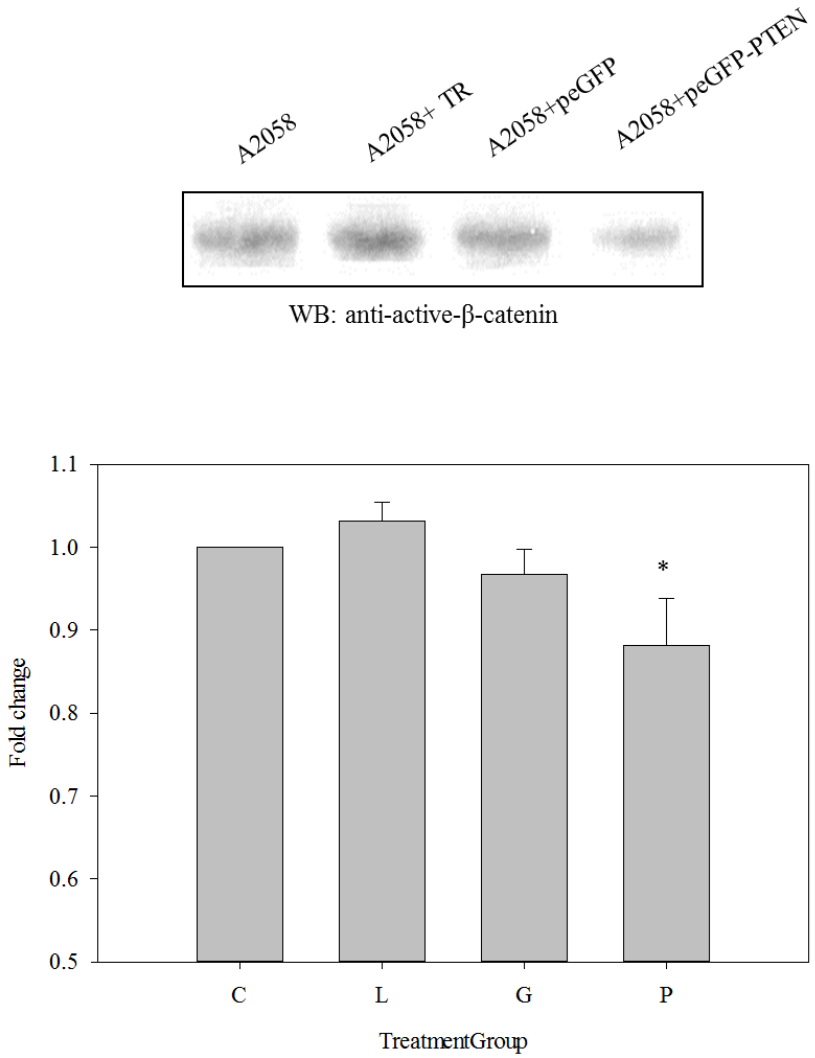

Figure 3.3 B: PTEN re-expression decreases Active-β-Catenin protein in PTEN null melanoma cells (A2058). Western blot analysis and densitometric analysis reveals PTEN transfected A2058 cells show a significant decrease (p=0.032) in levels of Active-β-catenin.24 hours post transfection.
C: Untreated A2058 cells; L: A2058 cells with Lipofectamine 2000 transfection reagent;
G: A2058 transfection with empty GFP vector; P: A2058 transfection with PTEN-eGFP plasmid

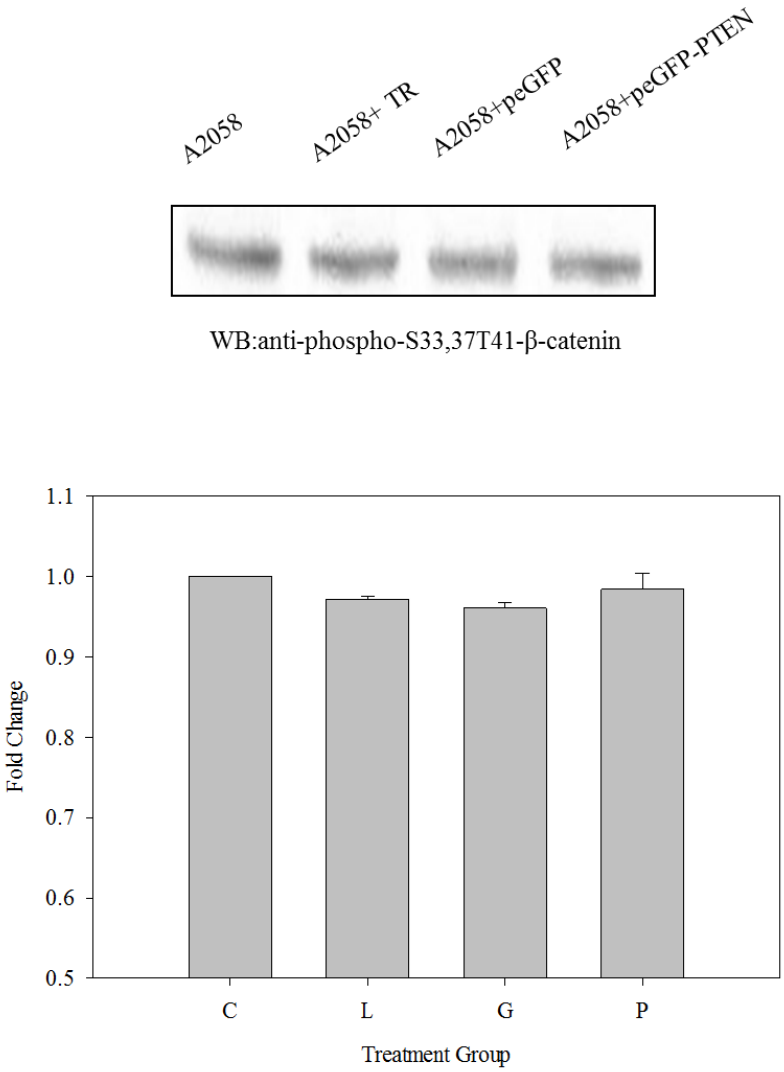

Figure 3.3C: PTEN re-expression shows no change in levels of β-Catenin Phosphorylation. Western blot analysis and densitometric analysis shows PTEN transfected A2058 cells show no change in level of phosphorylation of β-catenin at Serine 33,37 and Threonine 41 sites 24 hours post transfection.
C: Untreated A2058 cells; L: A2058 cells with Lipofectamine 2000 transfection reagent;
G: A2058 transfection with empty GFP vector; P: A2058 transfection with PTEN-eGFP plasmid

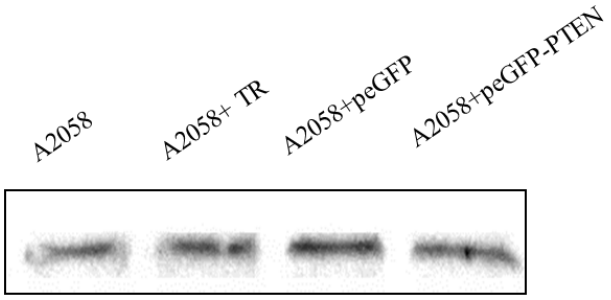

WB: anti-phospho-S45-β-catenin

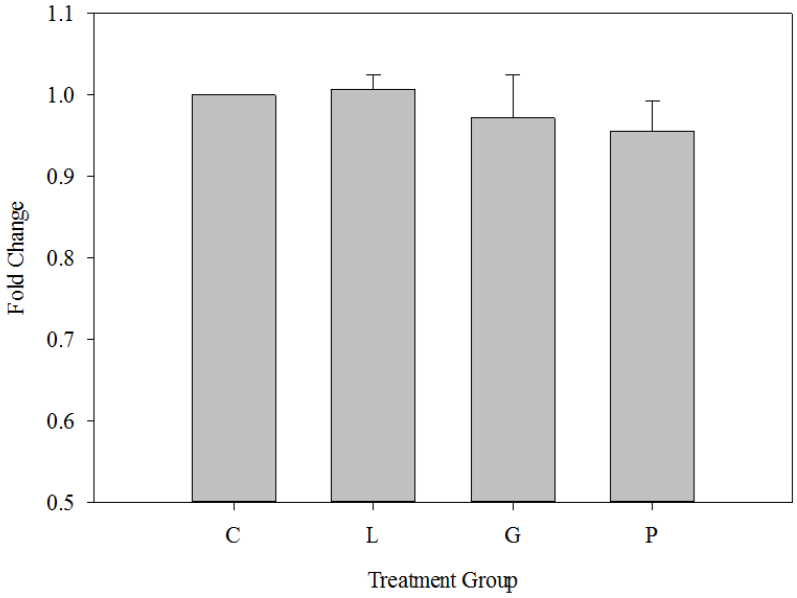

Figure 3.3D: PTEN re-expression shows no change in levels of β-Catenin Phosphorylation. Western blot analysis and densitometric analysis shows PTEN transfected A2058 cells show no change in level of phosphorylation of β-catenin at Serine 45, 24 hours post transfection.
C: Untreated A2058 cells; L: A2058 cells with Lipofectamine 2000 transfection reagent;
G: A2058 transfection with empty GFP vector; P: A2058 transfection with PTEN-eGFP plasmid

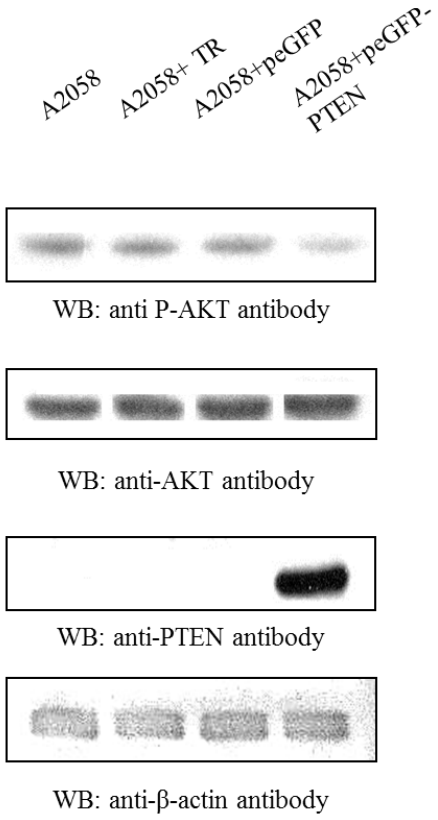

Figure 3.3E: PTEN re-expression shows direct effects on downstream AKT phosphorylation in PTEN null melanoma cells (A2058). (E) PTEN transfected A2058 cells show AKT-Ser473-P levels decreased and total AKT levels remained unchanged PTEN expression showing inhibition of PI3K activity. Presence of PTEN at 81 kda shows presence of PTEN-eGFP revealing effective plasmid transfection and consistent β-actin levels show accurate loading conditions.

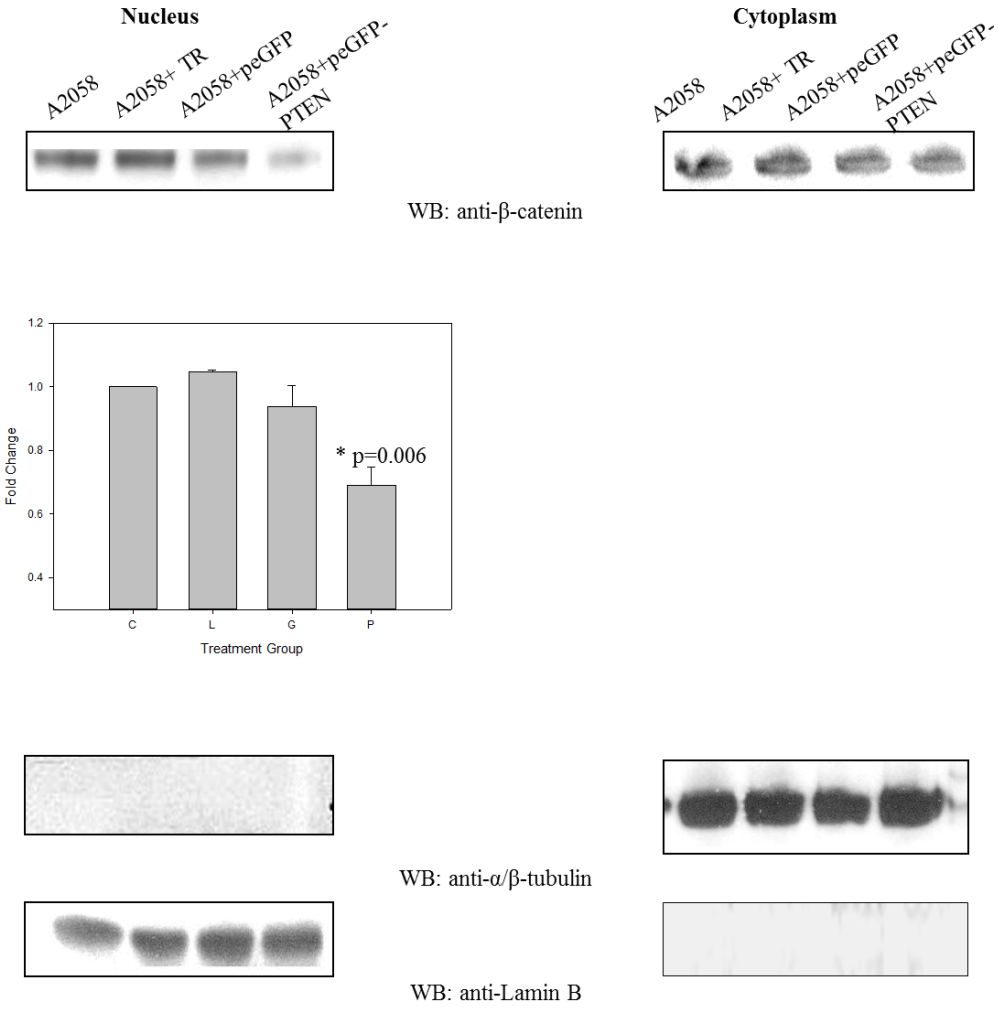

Figure 3.3F: PTEN re-expression decreases nuclear β-Catenin protein level.
Western blot analysis and densitometric analysis shows PTEN transfected A2058 cells results in a significant decrease in β-Catenin in nuclear fraction ; cytoplasmic fraction shows no change. Blots for anti-α/β-tubulin serve as a loading control for cytoplasmic fraction and Lamin B serves as a loading control for nuclear fraction.

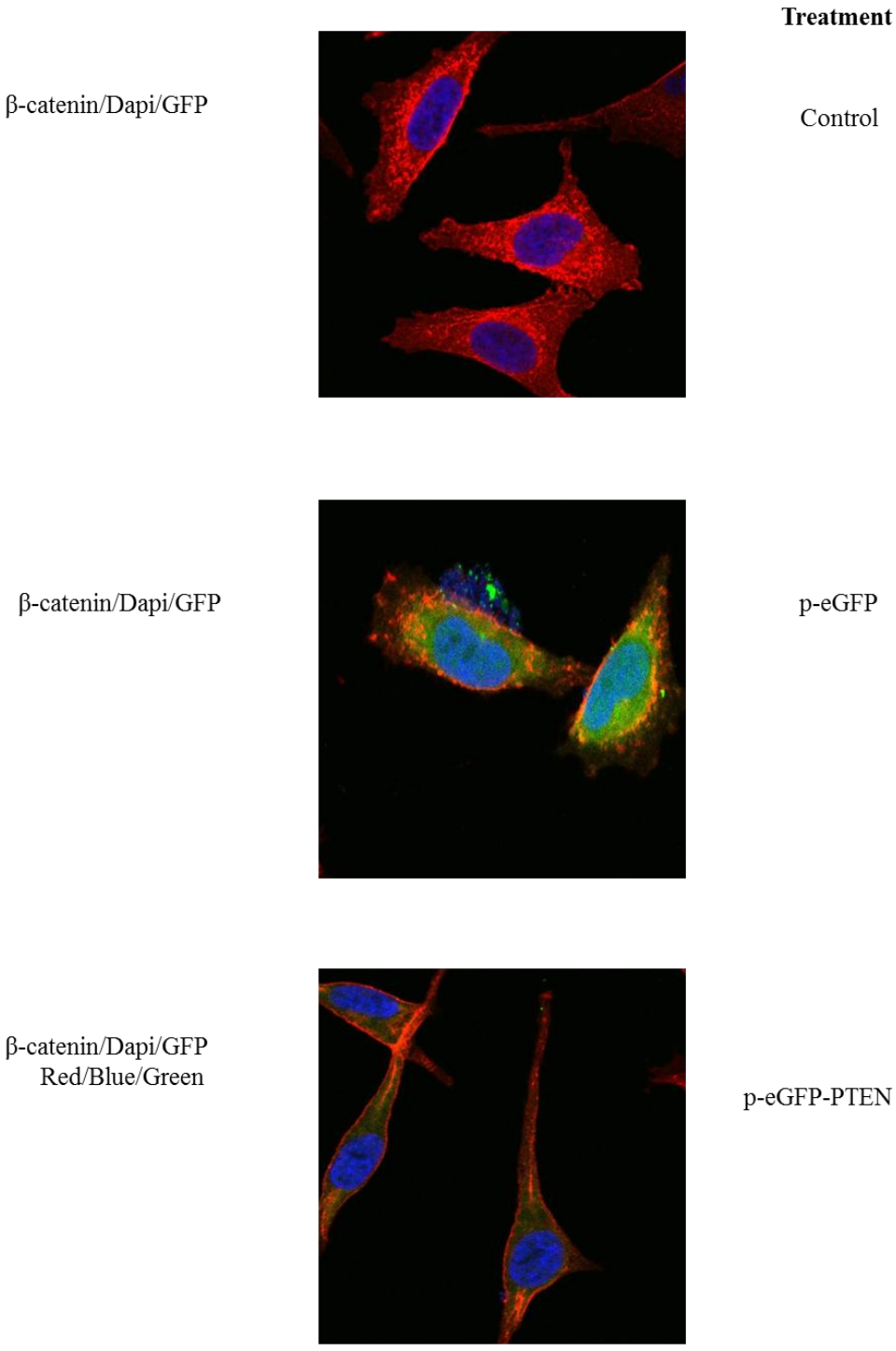

Figure 3.4A: Immunofluorescence analysis of β-catenin confirms decrease expression following re expression of PTEN: A) Multi-Cell View β-Catenin (Red) shows decrease in nuclear and cytosolic levels and localization to cellular membrane 24 hours post PTEN transfection.

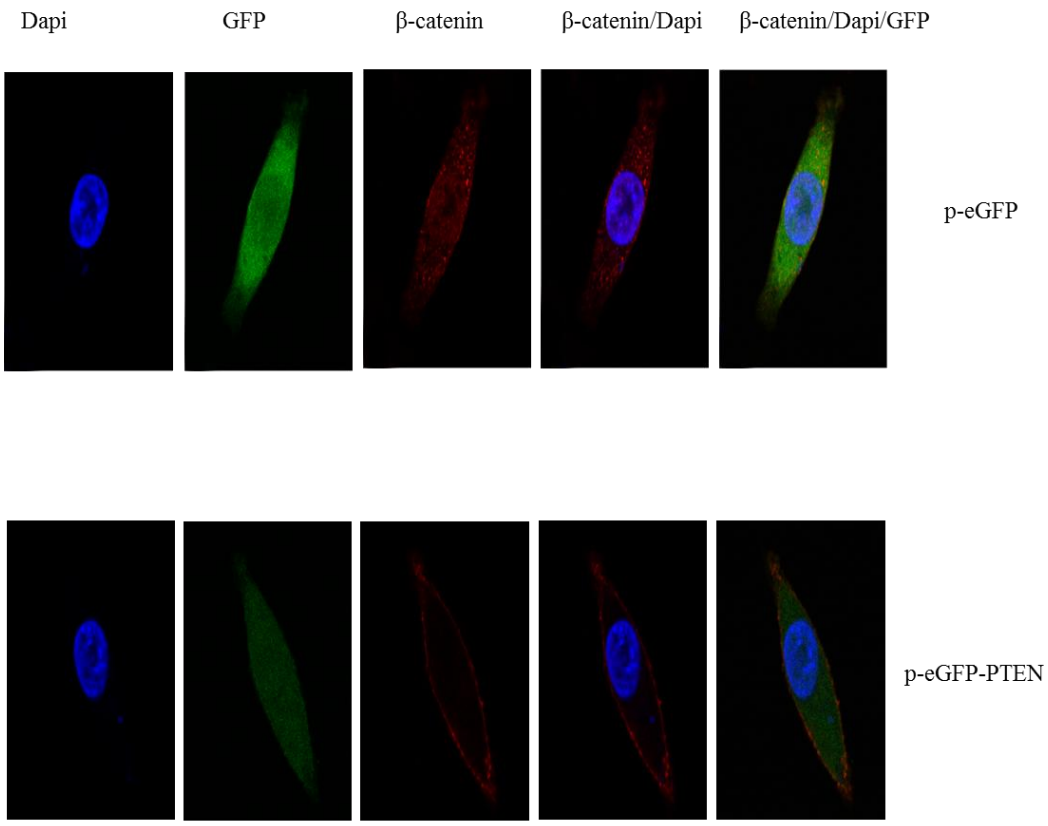

Figure 3.4B: Immunofluorescence analysis of β-catenin confirms decrease expression following re expression of PTEN: Single Cell View: β-Catenin (Red) shows decrease in nuclear and cytosolic levels and localization to cellular membrane 24 hours post PTEN transfection.

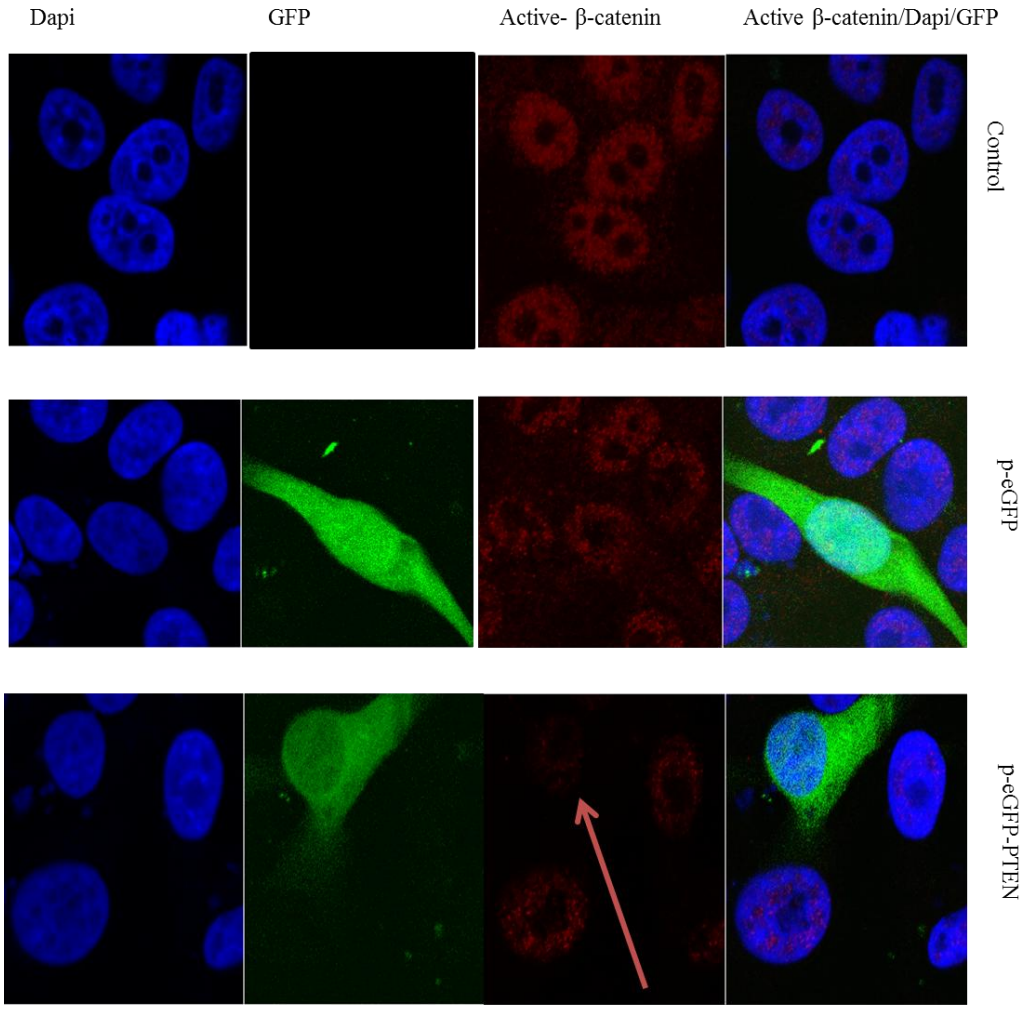

Figure 3.4C: Immunofluorescence analysis shows significant reduction of active-β-catenin following PTEN re expression in PTEN-null melanoma cells (A2058): Multi-cell view shows presence of active-β-catenin exclusively in the nucleus of control A2058 cells. 24 hours post PTEN transfection Active- β -Catenin levels diminish significantly.

3.4 Inhibition of the PI3K pathway by drug treatment confirms effect of PTEN reintroduction in PTEN-null cells

To further confirm changes in levels of β-catenin by the PTEN/PI3K pathway, A2058 cells were treated with the PI3K inhibitor, Wortmannin, which inhibits the pathway at the level of PI3K. A time dependent experiment was carried out to observe the effects of Wortmannin on PI3K inhibition, at the level of P-AKT, which showed that inhibition of the pathway occurred within one hour of treating A2058 cells with 1μM of Wortmannin (Figure 3.5a). This experiment also revealed that the drug was effective in growth medium with serum more than without serum, shown by lower levels of P-AKT and was effective for no more than four hours of treatment, as levels of P-AKT started to increase. This provided the effective dose and time for the following experiments.

With using 1μM of Wortmannin for a time span of 12 hours, levels of total β-catenin significantly decreased 6-12 hours following treatment (Figure 3.5b). Active-β-catenin levels decreased 9-12 hours post-treatment (Figure 3.5c). Levels of both serine-33/37/thr 41-phosphorylated β-catenin (Figure 3.5d) and serine-45 (Figure 3.5e) were not affected by the drug treatment. Levels of P-AKT (Figure 3.5f) decreased within one hour of drug treatment and levels of AKT (Figure 3.5f) did not change once again confirming effective inhibition of the PI3K pathway by Wortmannin.

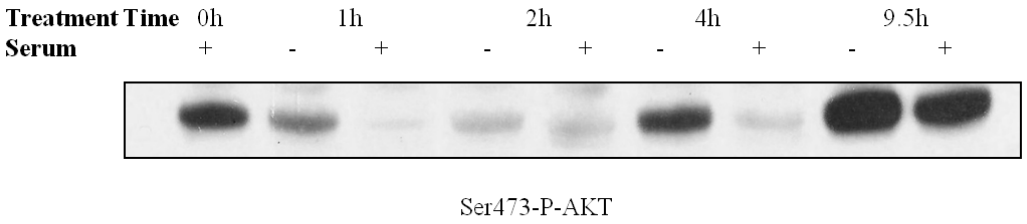

Figure 3.5: (A) Time Dependent Effects on PI3-K inhibition by Wortmannin on A2058 cells. Western Blot of P-Akt levels with Wortmannin (1uM)Treatment to determine effective time of PI3K inhibition by Wortmannin (t=0, 1, 2, 4, 9.5hrs) in A2058 PTEN-null metastatic melanoma cells. Drug shows greater inhibition in medium with growth factors compared to serum-free conditions. Effective inhibition upto 4 hours as measured by levels of Ser473-phoshpho-AKT.

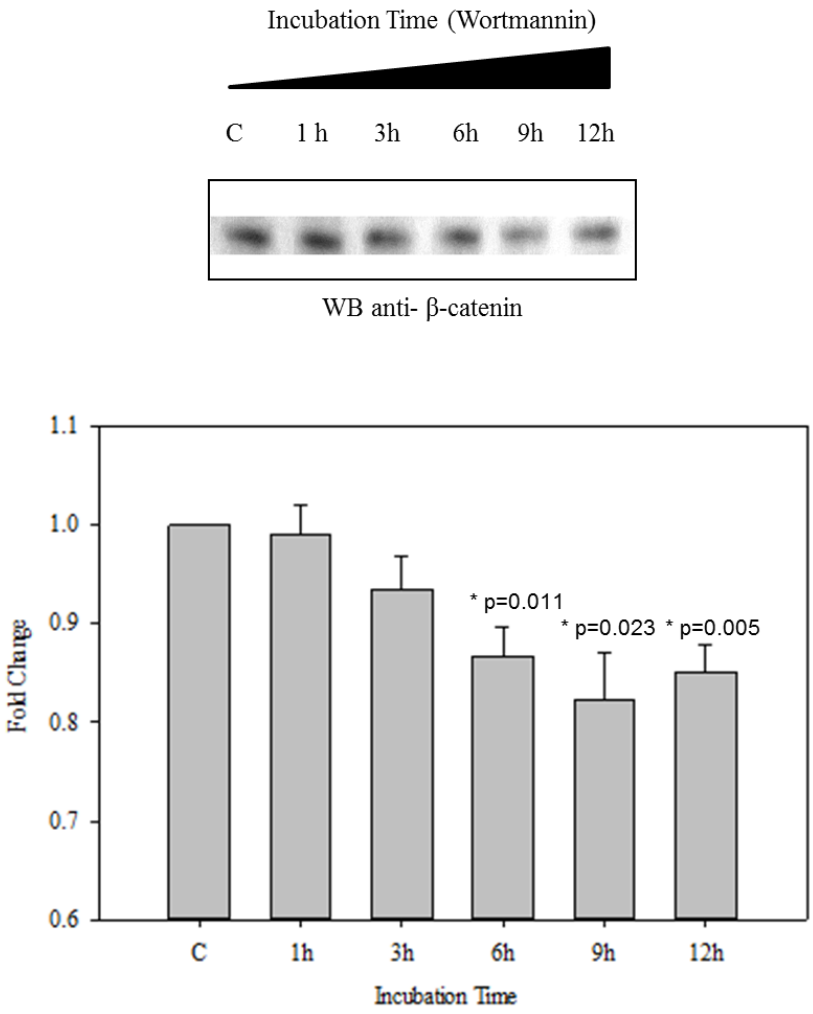

Figure 3.5: (B) Inhibition of the PI3-K pathway with 1μM Wortmannin reduces expression of total β-catenin. Inhibition of PI3K by drug treatment in A2058 cells results in decreased β-catenin 6-12 hours post treatment.

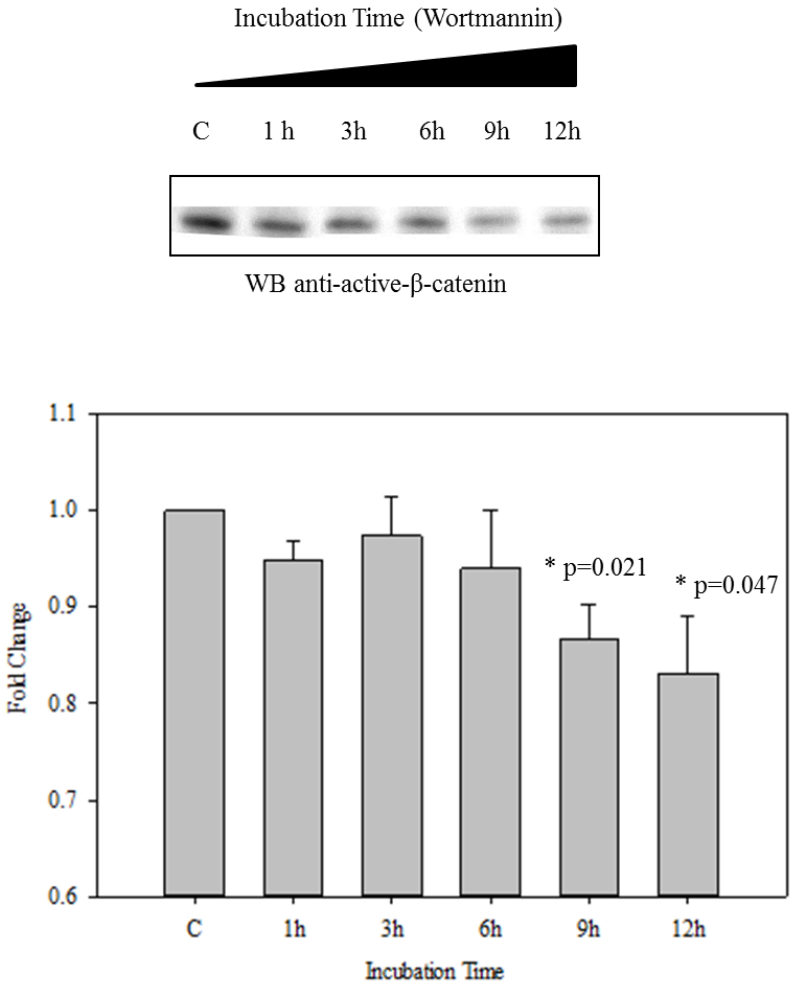

Figure 3.5: (C) Inhibition of the PI3-K pathway with 1μM Wortmannin reduces expression of active-β-catenin. Inhibition of PI3K by drug treatment in A2058 cells results in decreased Active-β-catenin 9-12 hours post-treatment..

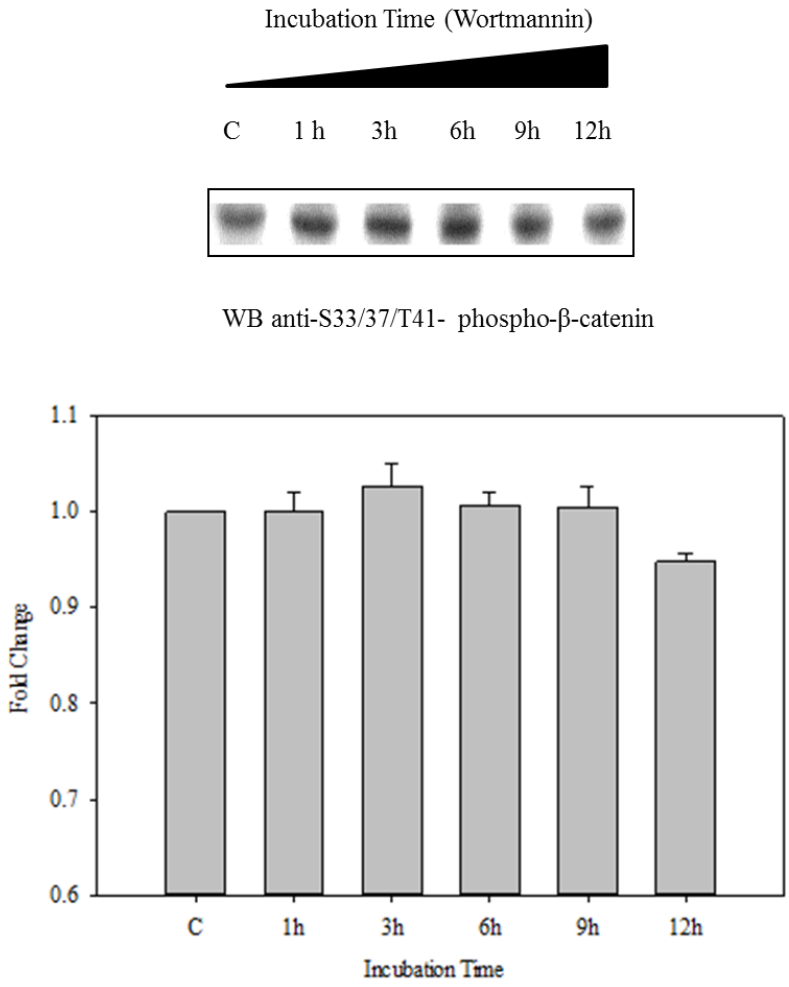

Figure 3.5: (D) Inhibition of the PI3-K pathway with 1μM Wortmannin has no effect on the phosphorylation of β-Catenin. Inhibition of PI3K by drug treatment in A2058 cells causes no change in level of phosphorylation of β-Catenin at Serine 33/37 and Threonine 41 over time course of 1-12 hours of Wortmannin treatment.

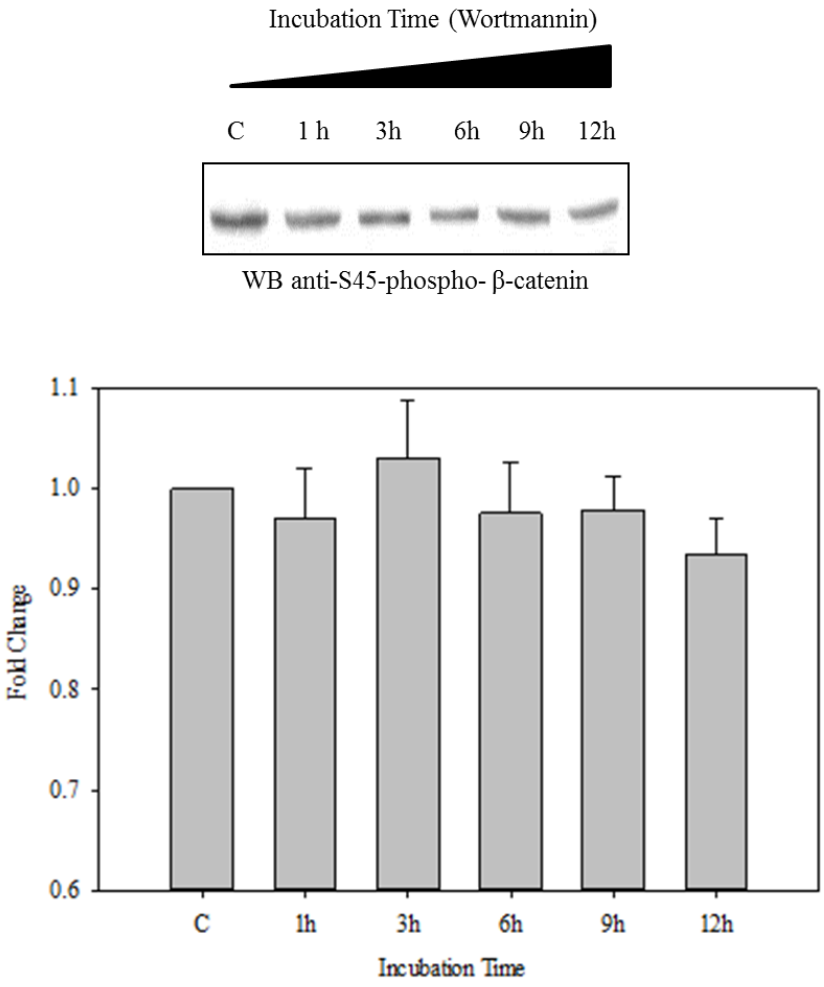

Figure 3.5: (E) Inhibition of the PI3-K pathway with 1μM Wortmannin has no effect on the phosphorylation of β-Catenin . Inhibition of PI3K by drug treatment in A2058 cells results in no significant change in levels of β-Catenin phosphorylation at serine 45 over a range of 1-12hours of drug treatment.

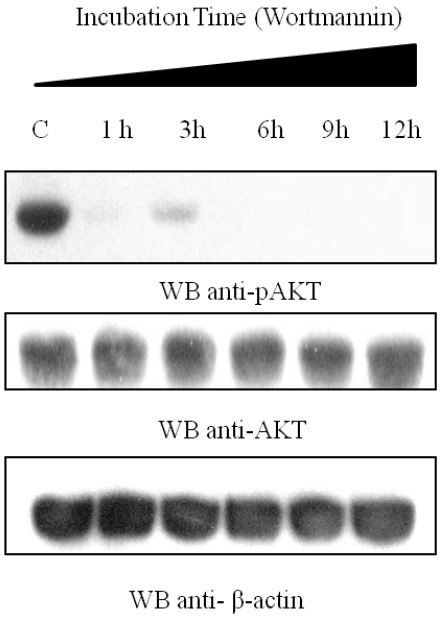

Figure 3.5: (F) Inhibition of the PI3-K pathway with 1μM Wortmannin is effective with drug replenishment every three hours. Inhibition of PI3K by drug treatment in A2058 cells results in AKT-S473-P depletion with treatment; and AKT is unchanged when the drug is replenished every three hours upto 12 hours. B-Actin serves as a loading control.

3.5 Effect of Wnt activation on β-catenin in A2058 Cells

To this point, we have seen how inhibiting the PI3K pathway both by addition of the negative regulator PTEN or by chemical inhibition, decreases levels of active-β-catenin as well as total cellular levels of β-catenin through a yet unknown mechanism. Our next experiment was to see the effect of the canonical Wnt pathway on regulation of active-β-catenin. Stimulating the canonical pathway by addition of recombinant Wnt 3a resulted in an increase in levels of β-catenin at 12 hours of treatment, confirmed at two concentrations (150ng/ml (Figure 3.6a/c) and 300ng/ml (Figure 3.6b)). There was a decrease in levels of phosphorylation of β-catenin at serine 45 (Figure 3.6c) and serine 33/37/threonine 41 (Figure 3.6c), which occurred at an earlier time point, 9-12 hours. Although this decrease in levels of phosphorylation was observed over multiple experiments the results were not statistically significant. Interestingly levels of active-β-catenin were unchanged in a stimulated Wnt environment (Figure 3.6a-c) at all-time points, suggesting regulation of active-β-catenin at a different level other than the canonical Wnt pathway. This showed that different pools of β-catenin may be regulated in different manners dependent or independent of the canonical Wnt pathway. Thereby the next step was to see changes in β-catenin by inhibition of the canonical Wnt pathway.

After seeing effects of Wnt stimulation, several experiments were carried through to inhibit the canonical Wnt pathway with the inhibitors, DKK-1 and Sfrp-1. These experiments were carried out at different doses and times of treatment with

and without addition of recombinant Wnt 3a. Inhibition of the Wnt pathway showed no effect on active-β-catenin (incomplete results not shown). However a decrease in levels of total β-catenin was observed. Changes in phosphorylated β-catenin and active-β-catenin were harder to detect. (Results were incomplete and not conclusive)).

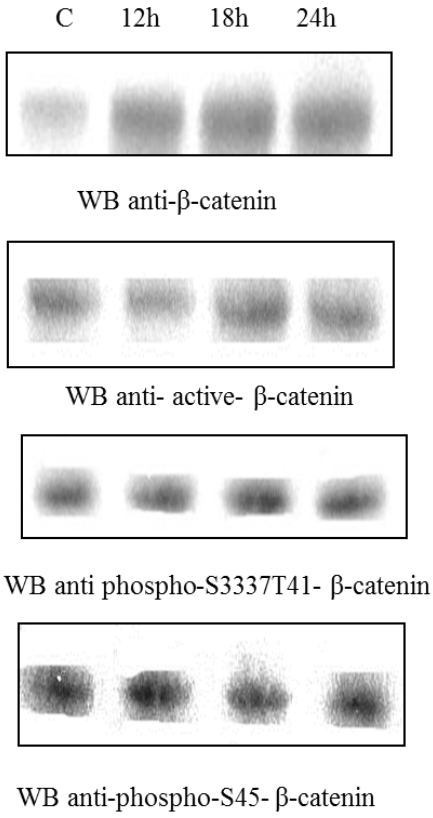

Figure 3.6: Time Dependent Effects of Recombinant Wnt 3a Treatment of A2058 Metastatic Melanoma Cells: (A) Western Blot and Densitometric Analysis showing changes in Levels of total cellular β-Catenin, Active-β-Catenin, Ser33/37,T41 and S45-Phospho-β-Catenin after 12,18,24 hours of 150ng/ml Recombinant Wnt Treatment. Wnt 3a addition shows significant increase only in levels of total β-Catenin 12-24 hours after treatment, and shows no change in active as well as phosphorylated pools of β-catenin.

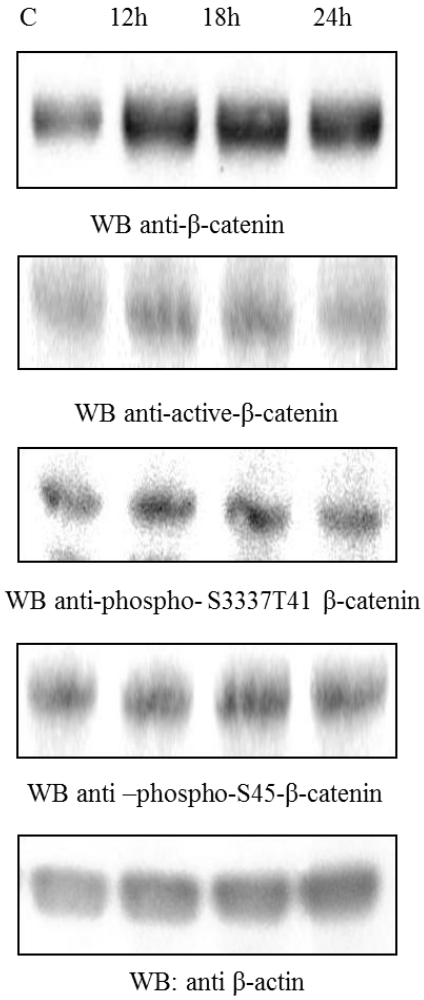

Figure 3.6: Time Dependent Effects of Recombinant Wnt 3a Treatment of A2058 Metastatic Melanoma Cells: (B) Western Blot and Densitometric Analysis showing Changes in Levels of total cellular β-Catenin, Active-β-Catenin, Ser33/37,T41 and S45-Phospho-β-Catenin after 12,18,24 hours of 300ng/ml Recombinant Wnt Treatment. Wnt 3a addition shows significant increase only in levels of total β-Catenin 12-24 hours after treatment, and shows no change in active as well as phosphorylated pools of β-catenin.

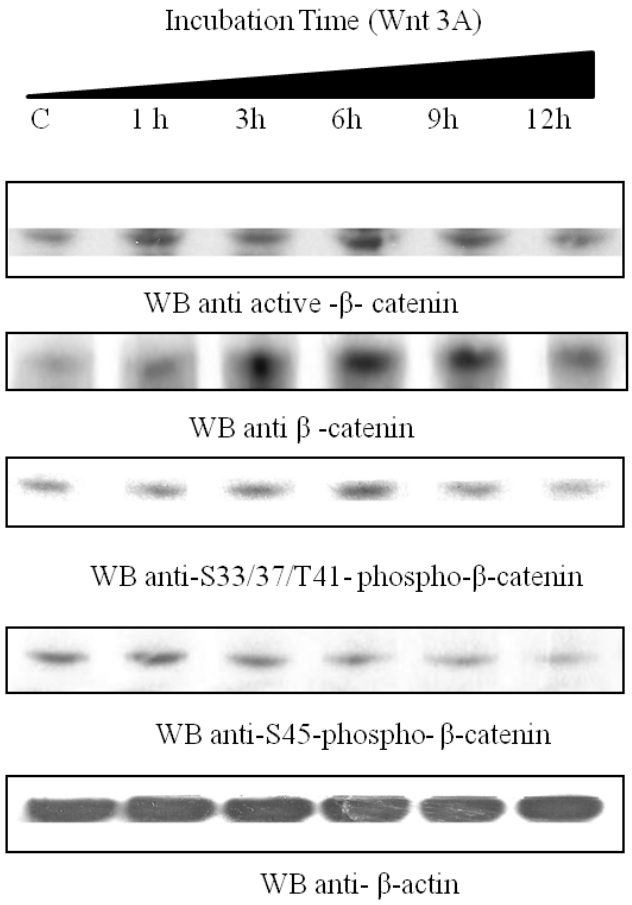

Figure 3.6: Wnt 3a regulates affects expression of β-catenin and its phosphorylation independent of active-β-catenin. (C)
Western Blot Analysis shows 150ng/ml of Recombinant Wnt 3a results in increase in total B-catenin within 1 hour of treatment. Levels of phosphorylation at Serine 33,37,T41 and S45 decrease 9-12 hours post treatment. Levels of active-β-catenin shows no change.

3.6 Downstream effect of PI3K's regulation of β-catenin-TCF Binding

3.6.1 Electrophoretic mobility shift assay (EMSA)

Carrying out an EMSA allowed investigation of how PTEN affects complex formation between β-catenin protein and DNA with a TCF sequence. A short DNA sequence was synthesized with specific TCF binding sites. The sequence was labeled with an infrared dye that was measured at 700nm wavelength. (Synthesis by Integrated DNA Technologies)

A2058 cells were transfected with PTEN for 24 hours, the purified nuclear fraction of these cells was bound to the synthesized DNA sequence of either a wild-type or mutant TCF binding sequence. Four samples were prepared; untreated control A2058 cells, cells in the presence of transfection reagent, cells transfected with an empty vector pEGFP and pEGFP-PTEN transfected cells. All nuclear lysates showed strong protein-DNA complex formation with DNA containing wild-type TCF binding sites. Comparing the three controls to the PTEN transfected lysate, there was an extra light band lower than the TCF bound band in all the samples (Figure 3.8). Samples that were bound with mutant TCF binding sequences bound very minimally with nuclear samples. This reflected the specificity of nuclear samples/TCF binding.

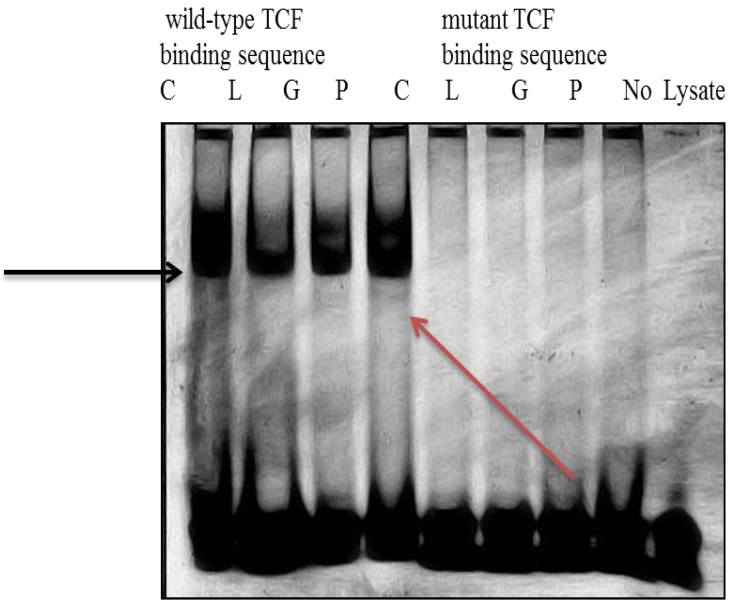

Figure 3.7: Infrared Electrophoretic Mobility Shift Assay Shows TCF-β-catenin complex formation in Metastatic Melanoma Cells: In the presence of a wild-type TCF binding sequence binding/complex formation (black arrow) is observed in a conditions of A2058 cells, however a lower band (red arrow) is observed in A2058 cells transfected with PTEN. No binding is observed in presence of a mutant TCF binding oligonucleotide.

C: Untreated A2058 cells; L: A2058 cells with Lipofectamine 2000 transfection reagent;
G: A2058 transfection with empty GFP vector; P: A2058 transfection with PTEN-eGFP plasmid

3.6.2 Luciferase

A luciferase assay was carried out to obtain a readout of β-catenin and TCF transcriptional activity. The wild-type TCF binding plasmid was TOPflash, which contained three TCF binding sites, and the negative control FOPflash had mutant sites. This assay is used readily to measure Wnt signaling at the transcriptional level of β-catenin/TCF. This is crucial to measure the specificity and functional effect on β-catenin. Changes observed in TOPflash activity are a direct readout of β-catenin's downstream transcription. Several studies were carried out to optimize results of the TOPflash luciferase experiments. The main dilemma in these experiments was that once an additional plasmid (GFP or PTEN) was transfected along with the TOPflash/FOPflash and pRenilla, luminescent values were negligible. Not only were these values lower in the presence of PTEN, which is expected since active-β-catenin values are lower, but they are also lower in the presence of an empty vector. The optimal transfection reagent for which highest luminescence for TOPflash was obtained when cells were transfected with Fugene HD (Promega) with a 3:1 transfection reagent: DNA ratio. It was difficult to determine conclusive results from these experiments as none of the data obtained was consistent in three experiments.

3.7 Effect of PTEN reintroduction in A2058 Cells on Downstream β-catenin/Wnt downstream target Genes

Since we have confirmed that the PI3K pathway, at the level of PI3K and PTEN affects active-β-catenin expression resulting in reduced binding of β-catenin with TCF (through presence of lower band in EMSA), it was imperative to study the effect that inhibition of the PI3K pathway has on the transcription of downstream Wnt target genes. PTEN-null A2058 cells were transfected with or without pEGFP-PTEN for 24-48 hours and the changes in cellular mRNA expression of selected Wnt target genes (cyclin D1 (Figure 3.9b), VEGF-a (Figure 3.9a), and MMP-2 (Figure 3.9c)) were measured with real-time quantitative polymerase chain reaction (RT-qPCR); GAPDH was used as an endogenous control to normalize results. mRNA expression of all three genes decreased in A2058 cells with PTEN transfection, compared to transfection with an empty GFP vector.

All three genes showed similar changes in mRNA expression pattern. Compared to transfection with an empty GFP vector, 24 hours of transfection with PTEN resulted in a significant decrease in mRNA expression of the target genes. The decrease was sustained for 48 hours after transfection. This is convincing evidence that the PI3K pathway has a functional effect on β-catenin, in that it not only decreases active-β-catenin expression along with β-catenin:TCF complex, but also on the transcription of downstream β-catenin: TCF target genes.

A western blot analysis looking at the protein expression of VEGF-A and cyclin D1 (Figure 3.9d) also confirmed a decrease at the protein level. This showed that

the effects of β-catenin were not exclusive to the transcription of these genes, but further affected the translation, having an effect on the protein level.

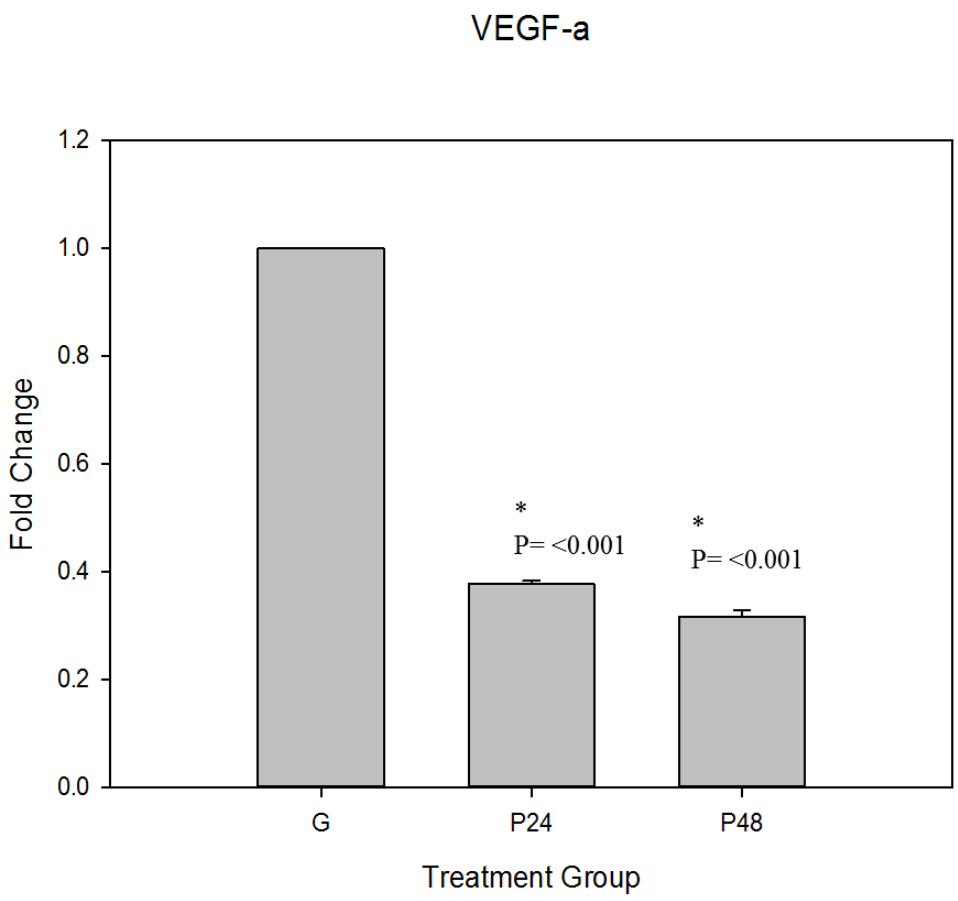

Figure 3.8A :PTEN re-introduction shows decrease in mRNA levels of Wnt target genes. mRNA expression levels of VEGF-a is decreased in 24-48 hours post PTEN transfected A2058 cells as measured by QRT-PCR using GAPDH as a reference gene. G: GFP treatment; P24: 24 hours of PTEN transfection; P48: 48 hours of PTEN transfection

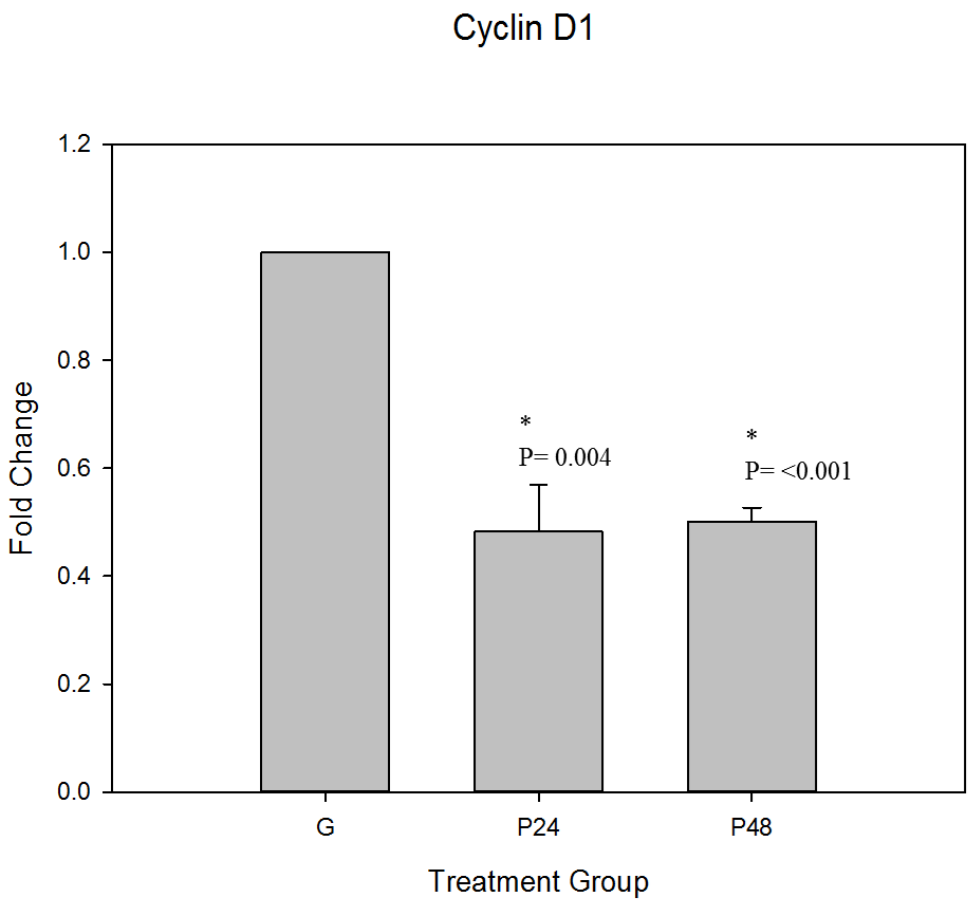

Figure 3.8B:PTEN re-introduction shows decrease in mRNA levels of Wnt target genes. mRNA expression levels of Cyclin D1 is decreased in 24-48 hours post PTEN transfected A2058 cells as measured by QRT-PCR using GAPDH as a reference gene. G: GFP treatment; P24: 24 hours of PTEN transfection; P48: 48 hours of PTEN transfection

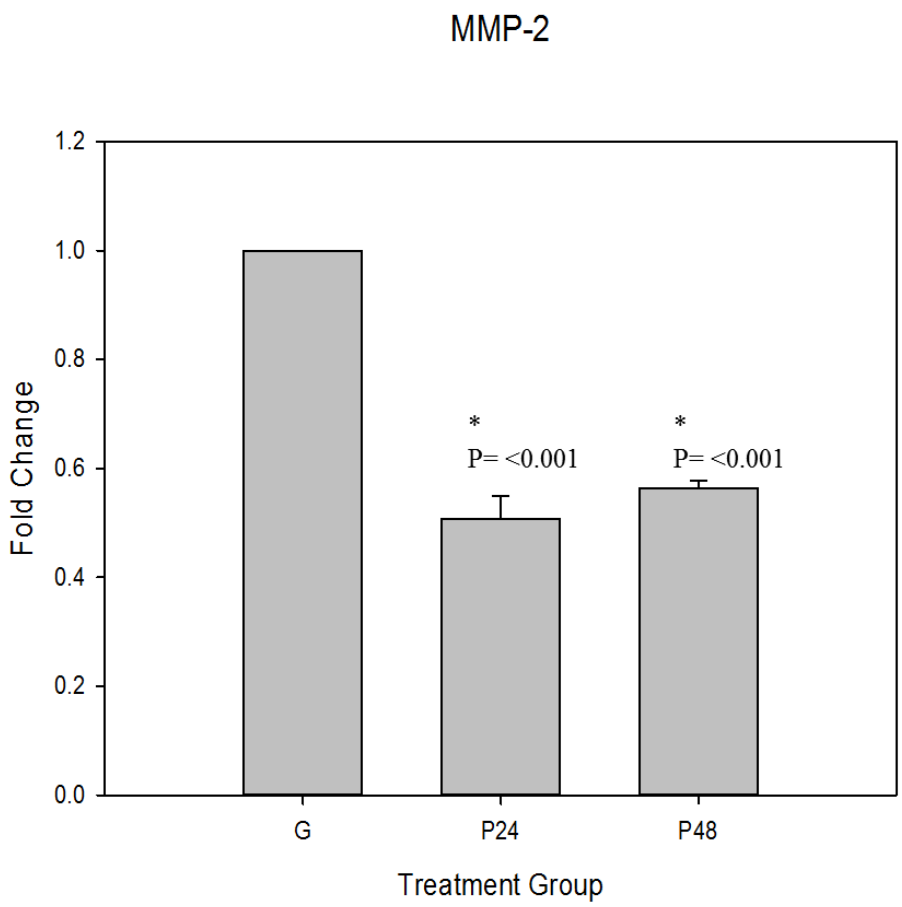

Figure 3.8C:PTEN re-introduction shows decrease in mRNA levels of Wnt target genes.
mRNA expression levels of MMP-2 is decreased in 24-48 hours post PTEN transfected A2058 cells as measured by QRT-PCR using GAPDH as a reference gene.
G: GFP treatment; P24: 24 hours of PTEN transfection; P48: 48 hours of PTEN transfection

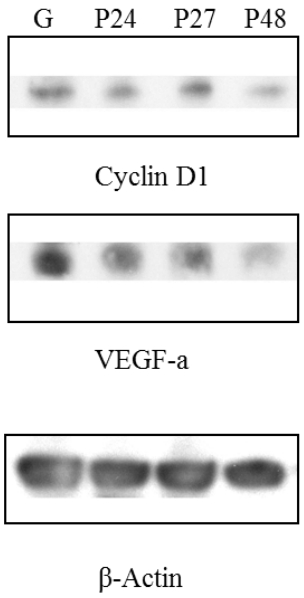

Figure 3.8D: PTEN reintroduction in PTEN-null A2058 Cells decreases protein expression of Wnt target genes. Western Blot analysis decreases Cyclin D1 and VEGF-a expression 24-48 hours post PTEN transfection.
G: GFP treatment; P24: 24 hours of PTEN transfection; P27: 27 hours of PTEN transfection; P48: 48 hours of PTEN transfection

3.8 PI3K and Invasiveness

To show the functional effect of a deregulated PI3K pathway in A2058 cells, we carried out a matrigel invasion assay to measure changes in invasiveness of the cells. The attachment to and penetration of basement membranes by tumour cells is required to complete the metastatic cascade which culminates in the establishment of tumours to distant sites of the body beyond their primary location. Therefore, basement membranes are critical barriers to the passage of disseminating tumour cells. Matrigel invasion assays can be used to measure the degree of invasiveness across a basement membrane.

Upon PTEN reintroduction cells decreased in invasiveness by 48% (Figure 3.11), compared to control PTEN-null metastatic melanoma cells. This confirmed the importance of the PI3K pathway on invasiveness and metastatic potential of these melanoma cells.

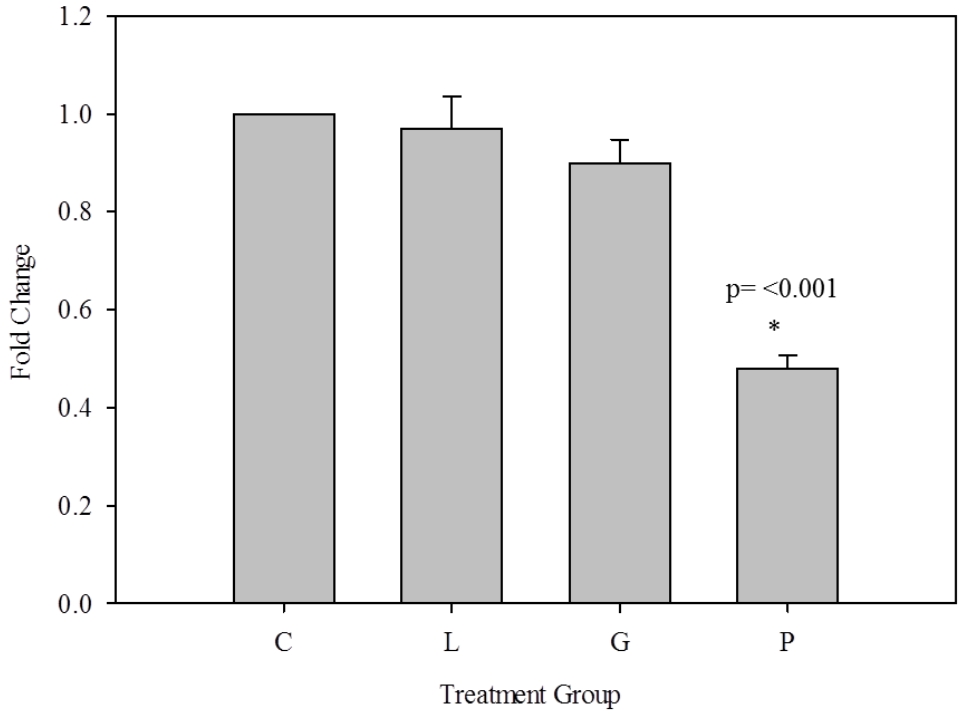

Figure 3.9: PTEN re expression in A2058 cells decreases invasiveness. Matrigel invasion assay reveals a significant decrease (p=<0.001) comparatively in PTEN expressing cells versus PTEN-null A2058 cells.

Chapter 4: Discussion

The aim of this study was to characterize β-catenin's changes that occur as melanoma progresses and to delineate the pathway that is regulating β-catenin's expression, localization and activity. Initially it was imperative to study the molecular changes that occur as melanoma progresses through distinct stages leading to metastasis. This allows for an understanding of pathways that are deregulated causing up or down regulation of genes that cause loss of control of cellular functions causing a melanoma to lead to metastasis and hard to treat stage.

This study was carried out using four cell lines correlating with four distinct phases of melanoma. The findings taken together created a model that could be used to study melanoma progression from normal melanocytes to metastatic melanoma (HEMa-LP, WM-35, WM-793 and A2058). Each cell line was obtained from separate patients and was isolated from distinct stages (described in Chapter 2). Although the transition of these cell lines from HEMa-LP to A2058 showed a gradual progression of melanoma, the cell lines were distinct and were grown in different conditions in comparison to each other. Using these cell lines provided an initial understanding of the changes that occur in β-catenin profile as melanoma progresses, however more investigations on different cell lines must be followed. To further justify this study it is necessary to use cell lines derived from the same patient from sites showing different stages of melanoma. This may be a future direction of this study.

Studying changes in β-catenin activity and levels in these cell lines provided an understanding of how β-catenin levels are changing from primary cells leading to metastasis. A hyper active Wnt signaling pathway is found in many cancers and plays an important role in tumourigenesis (Omholt et al., 2001). Increased β-catenin levels correlate with increased invasion and poor prognosis in many cancers. Since active-β-catenin is the specific form of β-catenin that plays the tumourigenic role in the Wnt pathway, it was imperative to study active-β-catenin expression alongside the expression of overall β-catenin.

De-regulation of the Wnt/ β-catenin pathway resulting in high levels of active-β-catenin is often observed in metastasis. Activation of the Wnt/β-catenin pathway, shown by increased nuclear/cytosolic localization, is frequently reported in melanoma (Rimm et al., 1999). Loss of localization of β-catenin from the cytosolic membrane to nuclear/cytosolic localization is observed in one third of melanomas (Rimm et al., 1999).

Many studies suggest that nuclear β-catenin expression is decreased in increasing metastatic cancers compared to primary cancer and is associated with a better prognosis (Chien et al., 2009). Bachman and colleagues show that there is a shift from nuclear to cytoplasmic expression in malignant tumours (Bachman et al., 2005). Another study by Kageshita and colleagues shows that melanoma shows a loss of β-catenin expression in the malignant stages in contrast to many other cancers (Kageshita et al., 2001). Although these studies looked specifically at nuclear expression, it should be made clear that in our studies we were looking at

the status of active-β-catenin. Transcriptionally active-β-catenin is not only nuclear but has a specific phosphorylation pattern, as it is dephosphorylated at Ser37 and Thr41 (Staal et al., 2002). Therefore Wnt signals are transmitted exclusively through N-terminally dephosphorylated β-catenin (Staal et al., 2002). To better understand the controversy of β-catenin levels in melanoma compared to other cancers a better understanding of active-β-catenin is needed. In this study we found an increase in active-β-catenin through progression from melanocytes to metastatic melanoma.

The active-β-catenin antibody was generated using the first 100 amino acids sequence of human β-catenin. It was established using deletion constructs to have a H**S**GAT**T**TAP residues 36-44 thus harbouring dephosphorylated S37 and T41 (Staal et al., 2002). This phosphorylation pattern of active-β-catenin has been shown to be present in transcriptionally active-β-catenin by studies looking at TCF mediated transcription (Maher et al., 2010; Staal et al., 2002).

There is currently no molecular explanation for why this dephosphorylation pattern creates an active signaling form of β-catenin, opposed to other forms of β-catenin. One explanation for this may be that phosphorylation at these sites may disrupt interactions with β-catenin and the TCF/LEF promoter sequence, therefore the desphosphorylation allows for binding of β-catenin to the TCF promoter without hindrance (Daughtery and Gottardi, 2007). The findings of Staal and colleagues confirm that it is not merely the accumulation/levels of β-catenin that correlates with transduction of Wnt signals, however it is the phosphorylation

pattern (Staal et al 2002). The fact that accumulation of β-catenin, which is controlled by Wnt signals, and the transcription of Wnt target genes are separate events as per the phosphorylation status of β-catenin we must allude to the mechanism that functions in controlling active-β-catenin.

It is active-β-catenin that forms a bipartite complex with members of the TCF family of transcription factors. This further results in transcription of genes involved in promoting carcinogenesis by driving proliferation, migration and tumour vascularization (Maher et al., 2010).

Since our studies showed that levels of total cellular β-catenin as well as the active form of β-catenin increase with melanoma progression, these elevated levels are an indication of a possibly overactive canonical Wnt pathway. The implications of this are excessive cell proliferation and a causal effect in increased cell invasiveness due to the nature of the Wnt signaling in transcription of target genes regulating these processes.

Since western blot analysis revealed elevated protein levels of β-catenin in WM793 and A2058 cells, it was important to see how the localization patterns of β-catenin change throughout the cell lines since β-catenin has distinct roles in the cell depending on its localization. As melanoma progressed to metastasis, β-catenin lost its localization from the cellular membrane and was dispersed in the cytoplasm and nucleus with increased expression as well. This change in localization has implications in metastasis because as β-catenin is lost from the plasma membrane, cells lose cell-cell adhesion as β-catenin alongside the

cadherin family of proteins functions at adherens junctions. The increase in cytoplasmic and nuclear levels serves a role as a transcriptional co-activator for TCF in regulating Wnt target genes and has implications in cancer progression.

Although β-catenin is a dual function protein, its functions in the cell have been shown to be regulated by different mechanisms depending on its localization. For example, cadherin loss of function has been shown to be independent of enhanced β-catenin signaling (Gottardi and Gumbiner, 2004) and Wnt activation does not typically alter cell-cell adhesion. β-catenin's role in the Wnt signaling pathway as a result of TCF driven transcription was of concern to this project.

After establishing the changes in levels and localization of β-catenin through melanoma progression the next step was to study the specific pool of β-catenin that is involved in the transcriptional role of Wnt genes, which is active-β-catenin. Active-β-catenin expression was absent from HEMa-LP cells and levels increased progressing from radial to vertical to metastatic phases.

This showed a clear correlation of active-β-catenin with progression of melanoma. It is likely that since active-β-catenin is responsible for acting as a transcriptional co-activator of TCF target genes, metastasis is a result of the upregulation of Wnt target genes that control cellular processes such as cell proliferation. The pattern of active-β-catenin levels throughout melanoma progression can have many implications in terms of therapeutics in metastatic disease. If cancer progression, in this case melanoma progression shows a positive correlations with active-β-catenin levels, then the signal transduction pathway that is deregulated, which is

causing levels of active-β-catenin to be deregulated must be elucidated. Once this mechanism of regulation is found, and then mechanisms to perturb or reverse this deregulation can lead to future studies.

As previously discussed over 30% of melanomas express high levels of nuclear β-catenin, however the number of melanomas with β-catenin mutations is significantly less (Rimm et al., 1999). Other malignancies such as prostate cancer show that increased nuclear β-catenin levels and high TCF is not all attributable to mutations in β-catenin (Persad et al., 2001) or the degradation complex, specifically APC (Persad et al., 2001). This means that this accumulation of β-catenin cannot be the result of solely β-catenin mutations and is likely regulated by another mechanism or pathway.

A potential mechanism may be the PI3-K pathway as there lays an inverse relationship between β-catenin/ active-β-catenin levels and PTEN in melanoma progression. The loss of PTEN leads to a constitutively active PI3K pathway, leading to excessive cell proliferation, increased invasiveness and loss of apoptosis (Engelman et al., 2006). Persad et al., have previously shown direct regulation of nuclear β-catenin by PTEN/PI3-K pathway (Persad et al., 2001). It should be noted that A2058 cells also express a mutation in BRAF and p53 along with PTEN. Over activation of BRAF is associated with induced cellular defense mechanisms against activated oncogenes to subsequently result in cell senescence. Its cooperation with an overactive PI3K pathway, as in the A2058 cells, effectively promotes melanoma progression (Hao et al., 2012).

PTEN is one of the most frequently mutated tumour suppressor genes in human cancer (Salmena et al., 2008). It has both lipid phosphatase and protein phosphatase activity. Although the tumour-suppressive function of PTEN has mainly been attributed to its lipid phosphatase activity, a role for PTEN protein phosphatase activity in cell-cycle regulation has been suggested as well (Wu et al., 2003). Loss of expression or mutational inactivation of PTEN is paramount to sustained proliferative and anti-apoptotic response often observed in malignancy (Hao et al., 2012). PTEN is located on chromosome ten on the q arm, and loss of heterozygosity of chromosome 10q is found in 30-50% of melanomas (Wu et al., 2003). PTEN loss leads to constitutive phosphorylation and activation of AKT, which leads to many downstream effects leading to reduction of apoptosis and increased cell survival (Stahl et al., 2003).

Several pathways including Wnt/β-catenin and PI3K have implications in cancer progression resulting in metastasis. As cells gain a mesenchymal phenotype they acquire motility and properties of invasiveness (Larue et al., 2005). A deregulated PI3K pathway, leading to overexpression of downstream β-catenin target genes such as VEGF is often implicated in increased invasiveness (Larue et al., 2005). To measure the effects of β-catenin on the metastatic potential of melanoma cells, an invasion assay was carried through. Since A2058 cells are PTEN null, we compared the invasiveness of these cells to A2058 cells transfected with PTEN.

The fact that introduction of PTEN decreased invasiveness by almost half (48%) was significant. Nuclear accumulation of β-catenin in metastatic cells, as observed in A2058 cells, has many implications; as it is prominent at the invasive front, in a

high density area of inflammatory cells that surround a primary cancer mass (Suzuki et al., 2008). Activation of the PI3K pathway is important for normal cellular metabolism and growth and progression of certain types of cancers (Bowen et al., 2009). Both these events together; the loss of PTEN, leading to PI3K over activation and elevated active-β-catenin are significant events leading to invasiveness and metastasis. This was displayed in A2058 cells which showed high level of invasiveness and penetration through the basement membrane. Nuclear accumulation of β-catenin at the invasive front is associated with metastasis (Huang and Du, 2008), this provides a possible connection PI3K and β-catenin in promoting metastasis.

Since there was a significant decrease in the number of cells with the ability to move across a basement membrane with the presence of PTEN, one has to appreciate that it may be a combined effect of loss of PTEN and over active β-catenin that caused increased invasiveness in A2058 cells. Since both the Wnt and PI3K pathways have many downstream effectors and roles in the cell, the precise change that caused the decreased in invasiveness needed further investigation.

To see how β-catenin plays a role in invasiveness of these melanoma cells, we further investigated the changes occurring in pools of β-catenin following PTEN reintroduction in A2058 cells. Re-introduction of PTEN into PTEN-null (A2058) cells not only resulted in decreased expression of total endogenous levels β-catenin but also changed in localization to the cell membrane similar to the localization in primary melanocytes. From sub-cellular fractionation I also

observed a decrease specifically in the nuclear pool of β-catenin. A previous study by Persad and colleagues has shown that PTEN re-expression in PTEN null prostate cancer cells decreases levels of nuclear β-catenin (Persad et al., 2001). Since these changes are parallel and suggest PTEN's regulation of β-catenin is mainly in the nuclear pool.

What is interesting and needs to be investigated further is the fact that I did not detect changes in levels of phosphorylated β-catenin, while total endogenous levels are decreased. Due to the dynamic nature of the Wnt signaling pathway in order for total levels to decrease, at an earlier time point there should be an increase in phosphorylation which results in an increase in degradation. One explanation for this may be that since a 24 hour transfection time was used for all experiments and was the time point where changes in levels of total endogenous β-catenin were detected, the changes in phosphorylation may have been missed. Although several experiments were done at earlier time points, due to the nature of difficult and accurate band detection of phosphorylated β-catenin, a conclusive result was not observed. In order to see changes in the phosphorylation pattern of β-catenin more experiments at very close time points ranging from 0 to 24 hours need to be conducted. Another way to detect this phosphorylation pattern would be to conduct immunofluorescence; however there is a lack of antibodies suited for immunofluorescence for phospho-β-catenin. Similar experiments done in PTEN null prostate cancer cells have shown an increase in levels of phosphorylation of β-catenin along with an increase in degradation (Persad et al., 2001). One explanation for this regulation is depicted in the following figure.

Since GSK3β is a common component of both the canonical Wnt pathway and the PI3K pathway, it may be suggested that the PI3K pathway has effects on β-catenin accumulation via GSK3β, regulating β-catenin's degradation (Figure 4.1).

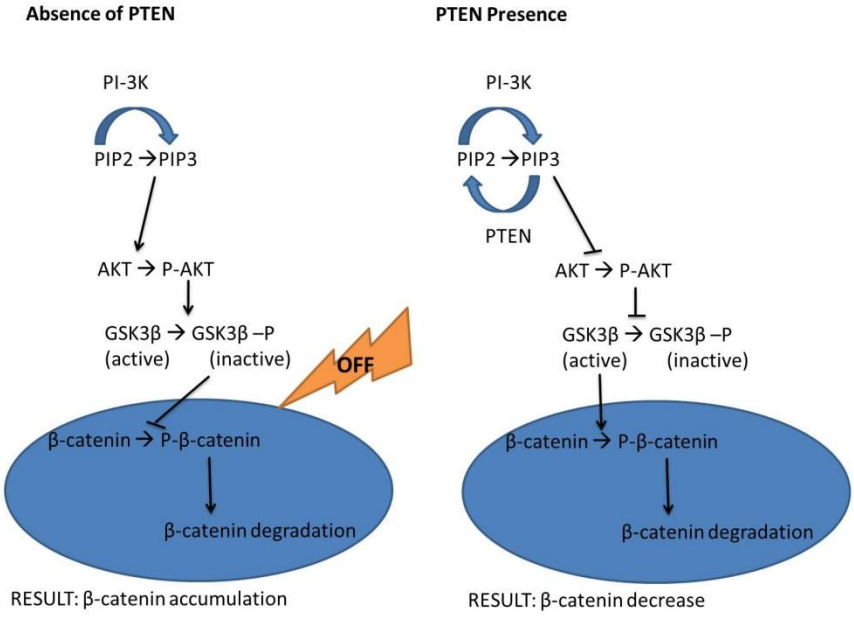

Figure 4.1: GSK3β as a common mediator of Wnt and PI3K signaling. Schematic shows a possible mechanism to link the canonical Wnt and PI3-K pathways with a common pool of GSK3β.

However, several studies argue against this hypothesis. It has been shown that less than 10% of total GSK3β in the cell is associated with Axin, engaging with the canonical Wnt signaling pathway (Lee et al., 2003; Benchabane et al., 2008). Whether GSK3β is a convergence point between the two pathways that is regulating the effects of the PI3K pathway on β-catenin must be further investigated and is a controversial topic. Although most of the scientific

arguments refute this hypothesis, GSK3β with mutations in its phosphorylation site which is phosphorylated by AKT has been shown to inhibit Wnt signaling (McManus et al., 2005; Ng et al., 2009; Doble et al., 2007). Ng and colleagues have demonstrated that Axin in the Wnt pathway shields GSK3β from being affected by other pathways such as PI3K (Ng et al., 2009). If GSK3β could be selectively inhibited in each pathway, there may be a lead into this model however chemical inhibitors of GSK3β are not selective and inhibit total endogenous GSK3β.

Since a decrease was observed in specifically the nuclear β-catenin pool we further looked into the change in active-β-catenin. PTEN introduction in A2058 cells further showed a decrease in active-β-catenin. Immunofluorescence analysis confirmed this finding and revealed that active-β-catenin is localized mainly in the nucleus of the cell. Even though all nuclear β-catenin is not active, the distinct pool of active-β-catenin is exclusively nuclear. Although we saw that the PI3K/PTEN pathway had an effect on expression of active-β-catenin the mechanism by which this regulation takes place has yet to be concluded. Further studies are necessary that look at this, whether it is a dephosphorylation event at the sites of S37 and T41 or a direct feedback into the canonical Wnt pathway via a common mediator. Protein phosphatases that have a role in both the Wnt and PI3K pathways are potential regulators of active-β-catenin formation and a potential cross regulatory effector between the PI3K and Wnt pathway. Screenings done by Zhang and colleagues on several phosphatases have defined PP2A as the putative phosphatase that dephosphorylates β-catenin at Serine 37

and Threonine 41 by its regulatory unit PR55α (Zhang et al., 2009), resulting in active-β-catenin. PP2A is a heterotrimeric protein, consisting of a structural, regulatory and catalytic subunit (Westermarck and Hahn, 2008). PP2A is a serine/threonine phosphatase downstream of TOR signaling which is affected by the PI3K/AKT pathway as it inactivates AKT by dephosphorylation (Guenin et al., 2008). Its role in Wnt signaling is conflicting as it interacts with multiple components of the Wnt pathway (Guenin et al., 2008). Since inhibition of the PI3K pathway, at the level of PTEN showed an effect on expression of active-β-catenin, it was imperative to test the effect via another mode of PI3K pathway inhibition.

There are two commonly used chemical inhibitors of the PI3K pathway at the level of PI3K; LY294002 and Wortmannin. Wortmannin has been shown to be a more specific inhibitor of class 1 PI3-kinases than LY294002 (Gharbi et al., 2007). For more specificity, Wortmannin was used for this study as it is a potent irreversible inhibitor of the catalytic p110α subunit of PI3K. It inhibits PI3K by a nucleophillic reaction mechanism (Shpretner et al., 1996). Replication of the data obtained from PTEN transfection by the use of Wortmannin confirmed that the alterations in PI3K pathway do in fact affect β-catenin activity and show that the effects were not PTEN specific. Several experiments were conducted to measure effective dose and time of drug treatment. After this was established another factor to take into consideration was the activity time of the drug and the time that it took to see changes in β-catenin. Following several studies we saw that Wortmannin was only effective, measured by P-AKT knockdown, for up to three

hours post treatment. Due to this, the drug was replenished every three hours in order to effectively inhibit the PI3K/PTEN pathway. This experiment was done for a period of 12 hours in order to see changes in β-catenin.

An experiment done prior to the replenished conditions revealed that P-AKT levels were depleted within an hour of Wortmannin treatment and increased after approximately four hours. The levels of P-AKT were higher in cells without serum than those with serum. This is explained by the mechanism of the PI3K pathway. In the presence of growth factors, stimulators of the pathway, the PI3K pathway is activated (Courtney et al., 2010), and since these cells lack PTEN, levels of P-AKT remain elevated. Therefore the effects of a PI3K inhibitor are amplified in a pathway which is activated at the same time. This was observed, as the decrease in P-AKT was more prominent in cells with a stimulated PI3K pathway (Figure 3.5a).

After carrying through dose and time dependent set of experiments to find ideal conditions for Wortmannin treatment and its effects on β-catenin the ideal concentration of Wortmannin was found to be 1μM. At 1μM there was a balance between minimal cell death and inhibition of the PI3K pathway, reflected by a decrease of P-AKT levels. The results of this experiment were parallel to the effects of PTEN reintroduction in PTEN-null metastatic cells. These experiments confirmed that the PI3K pathway regulates expression of active-β-catenin as well as total endogenous β-catenin. Once again, no change was seen in the phosphorylated β-catenin. It is well known that the canonical Wnt signaling pathway is responsible for the constant cycle of β-catenin. In the absence of Wnt

ligands β-catenin levels are monitored by the destruction complex. However the regulation of active-β-catenin may be independent of the events of the canonical Wnt signaling pathway. The mechanism by which the PI3K pathway is regulating active-β-catenin is a future direction of this project and must be further investigated. There may be two possible mechanisms of how the PI3K pathway regulates active-β-catenin The first may be a possible crosstalk between the PI3K and Wnt Signaling pathway as mentioned in Section 3.3.2 by a common mediator, GSK3β. The other may be through a protein phosphatase that regulates both pathways, the protein phosphatase 2A (PP2A). Zhang and colleagues showed that β-catenin phosphorylation and degradation may be separate events due to the activity of phosphatases opposing the kinase activity of the destruction complex (Zhang et al., 2009). Sablina and colleagues found that PP2A dephosphorylates β-catenin at Serine 37 and Threonine 41, creating active-β-catenin form (Sablina et al., 2010). PP2A may provide a possible link in the PI3K pathway regulating active-β-catenin. This model suggested that the PI3K pathway does not affect the accumulation or localization of β-catenin, but more so its de-phosphorylation.

Since we have seen that the PI3K pathway plays a role in regulating expression of active-β-catenin, it was important to study which aspects of β-catenin are regulated by the canonical Wnt pathway. We found that although the Wnt pathway regulates the levels, accumulation and degradation pattern of β-catenin, it does not control the expression of active-β-catenin. Interestingly, active-β-catenin is dephosphorylated at two specific sites, whose phosphorylation status is controlled by GSK3β in a Wnt mediated fashion. Since in the absence of Wnt

signals, GSK3β as a part of the destruction complex phosphorylates β-catenin at three sites; Serine 33,37 and Threonine 41, it is thought-provoking that active-β-catenin shows a specific non-phosphorylated pattern at two of these specific sites, Ser 37 and Thr 41. Although this alludes to a potential regulation of active-β-catenin in a Wnt controlled fashion, it is interesting that the recombinant Wnt ligand 3a, which is an activator of the canonical Wnt pathway showed no effect on levels of active-β-catenin. This may be because although the Wnt pathway controls the phosphorylation of β-catenin (van Noort et al., 2002), its dephosphorylation may be independent of Wnt signaling. In the progression of melanoma to metastasis, active-β-catenin expression may be independent of the Wnt pathway.

A decrease in levels of phosphorylated β-catenin preceding an increase in overall levels of total endogenous β-catenin confirmed effective Wnt 3a treatment showing activation of the canonical Wnt pathway. This confirmed that stimulation of the canonical Wnt pathway, leads to deactivation of the destruction complex, thereby decreasing the phosphorylation and degradation of β-catenin. As a result total levels of β-catenin accumulate within the cell.

Several preliminary studies were carried out to optimize effective dose and time of Wnt 3a treatment. The greatest increase in levels of total β-catenin was seen at 150ng/ml and 300ng/ml after 12 hours of incubation. This set of experiments was done at time points of 12 to 24 hours. At these time points no change was seen in levels of phosphorylated β-catenin (Figure 3.6a/b). This was most likely due to

the fact that the phosphorylation changes precede changes in total levels of β-catenin, therefore this lead to looking at time points starting one hour post treatment at the dose of 150ng/ml of recombinant Wnt 3a. This experiment was carried out at shorter time intervals and at 9-12 hours the phosphorylated levels of β-catenin at all four sites, Serine 33,37,45 and Threonine 41 showed a decrease (Figure 3.6c). This eludes to the fact that the phosphorylation, destruction and accumulation of total cellular levels is controlled by the canonical Wnt pathway. Changes in active-β-catenin are likely regulated by another mechanism, such as the PI3K pathway.

Once the changes in active-β-catenin following PTEN transfection were confirmed it was imperative to see further downstream changes in B-catenin and TCF DNA. EMSA was an assay established to detect DNA binding proteins (Fried and Crothers, 1987). It is known that β-catenin interacts with transcription factors of the TCF/LEF family and subsequently activates genes that are responsive to TCF/LEF family members (Giese et al., 1995; Behrens et al., 1996; Clevers and Grosschedl, 1996; Molenaar et al., 1996; van de Wetering et al.,1997). Therefore, we analyzed the ability of β-catenin to form complexes with a TCF consensus oligonucleotide in the presence of PTEN (Persad et al., 2001) by carrying out an EMSA.

We first determined the TCF sequence that was required for optimal specificity of binding. Once control A2058 cells and samples transfected with PTEN were bound to the TCF DNA they were run on a non-denaturing gel to measure

differences in the migration of the protein-DNA complexes. The following table summarizes the advantages of using IR labeled oligonucleotides versus radioisotopes.

Near-Infrared	**Radioisotype**
Easy access and disposal	Regulatory restrictions, disposal hassle and cost
Labeled oligos have extended stability	Short half-life of label
Non-hazardous	Hazardous
Wet gel imaged while still between gel plates	Gel drying and film/phoshor-screen exposure required
Fast, convenient detection of probe	Time-consuming, inconvenient detection
Gel can be replaced and run longer if needed	Gel run time cannot be extended
Results available in less than two hours	Experiment typically takes more than one day

Figure 4.2: Advantages of Near-Infrared Fluorescent EMSA detection
(LiCor Oddyssey)
[http://www.licor.com/bio/applications/odyssey_applications/emsa_gel_shift_assay.jsp]

Since all the samples bound very strongly to the wild-type sequence as opposed to negligible binding with the mutant sequence, showed that there is in fact TCF binding in these samples. These results were also confirmed in a radioactive

EMSA prior to carrying out an infrared EMSA (results not shown). Since prior results show that active-β-catenin is expressed in all samples (control and PTEN-transfected) it should be expected that there is β-catenin-TCF complex formation as well. In the presence of nuclear active-β-catenin, the lysates were expected to bind TCF transcription factors. This would be further confirmed by a super shift assay with an active-β-catenin antibody added to the binding reaction; however this was not conducted in these experiments. Since the PTEN transfected sample had reduced active-β-catenin levels it was expected that there would be less β-catenin:TCF complex formation in these samples. However the intensity of the band showing the complex did not have measurable differences in this sample compared to controls. However, there was an observed band which was lower than the intense bands across all samples. This was interesting because it can be interpreted in different ways. As PTEN transfected samples show decreased levels of active-β-catenin, they would also have less β-catenin-TCF complex formation. However, if this was the case the main band should have appeared less intense than the other bands, not show an additional band running faster on the gel. An additional band in an EMSA could be explained by the presence of a lighter complex causing the complex to move faster on the gel. These results bring some discrepancy to the expected results of the EMSA. Another explanation for this may be that since β-catenin and TCF binding involve a number of other components that work as the transcriptional machinery transcribing TCF target genes, the loss of these components may lead to a smaller/faster-moving complex. In other words when there is less active-β-

catenin available to bind TCF transcription factors to transcribe Wnt target genes, less transcription takes place and thereby all necessary components of the transcription complex may not be present. A similar experiment in PTEN-null prostate cells by Persad and colleagues has shown reduced levels of complex formation in cells transfected with PTEN (Persad et al., 2001). A possible explanation for why a lack of change in the intensity of the main band was not detected may have been because the overall intensity of the bands was quite high due to overexposure. This experiment would have to be re-done with an even more dilute concentration of nuclear extract and TCF binding oligonucleotide as the infrared signal is very strong. The over expression of the bands may be masking the small decrease in the PTEN transfected samples.

Since the EMSA showed decreased complex formation between β-catenin:TCF, it was necessary to study more specific effects of β-catenin transcriptional activity using TCF binding sequences. To correlate with the high levels of active-β-catenin observed in untreated A2058 cells, and the subsequent decrease observed with PTEN introduction, we wanted to see if this decrease would further decrease β-catenin/TCF transcriptional status. However due to several difficulties with the luciferase/TOPflash assay, the luciferase data obtained from all the studies was not consistent in any way from one experiment to another. Several difficulties were encountered, one of which was very low transfection efficiency with a triple plasmid transfection. It was very difficult to obtain an optimal transfection with high PTEN transfection efficiency along with pTOPflash along with keeping minimal background obtained with the pRenilla plasmid. Another problem that

was encountered was the unexplainable high pFOPflash readings. Since this plasmid had mutant TCF binding sites it was very confusing why the readouts would be higher than those of the wild-type pTOPflash plasmid. The only way to identify the presence of a pTOPflash or pFOPflash plasmid was by the higher signal or low signal respectively of luciferase readings. However since the readouts were quite unreliable, this may provide a false negative indication of transfection status. Lastly, one other thing that was of concern in these experiments was high values for the pRenilla readings. As this plasmid is transfected at very low concentrations, simply to normalize the background readings, a minimal readout should be observed to be reliable.

It was unfortunate that none of the experiments provided an ideal set of results. Since active-β-catenin is complexed to TCF, and induces activity of genes containing TCF DNA binding site in their promoter region (Persad et al., 2001) it would have been interested to see how PTEN has an effect on β-catenin mediated transactivation. Optimization of this experiment is a future direction of this project as it will provide the most accurate read out on the effect of the PI3K pathway on β-catenin:TCF activity.

Since PTEN introduction in A2058 cells has been shown to decrease invasiveness and active-β-catenin levels and further decrease β-catenin:TCF complex formation, we looked at the effect on downstream Wnt target genes. A quantitative real-time PCR was carried out to determine changes in selected Wnt target genes, following PTEN transfection in PTEN null cells. Since my data

confirmed that in fact the PI3K pathway does have a role in regulating active-β-catenin, it was imperative to measure the effects in downstream β-catenin/TCF target genes, to ensure a functional effect. The selected genes Wnt target genes that were studied were VEGF-a, cyclin d1 and MMP-2.

The effect of Wnt signaling on matrix metalloproteases has mainly been studied in T-cells, where blocking Wnt signaling has been shown to reduce T-cell migration due to decreased metalloprotease expression (Wu et al., 2007). Inhibition of the Wnt pathway in prostate cancer cells also shows decreased activity and protein levels of MMP-2 (Zi et al., 2005). The metalloproteases are seen as direct target of Wnt/TCF activation (http://www.stanford.edu/group/nusselab/cgi-bin/wnt/target_genes). Therefore the mRNA expression of these genes was used as a marker of the downstream effects of PI3K regulation on active-β-catenin.

Another downstream Wnt target gene is VEGFa, a key regulator of tumour angiogenesis. VEGFa has implications in endothelial proliferation, tube formation, enhanced tumour neovascularization and angiogenesis (Dilek et al., 2010). Due to its nature VEGFa is overexpressed in the vast majority of cancers (Dilek et al., 2010). Mutations in the Wnt pathway leading to overexpression of β-catenin have been shown to cause elevation of VEGFa and inhibition of the Wnt pathway has caused a down regulation in promoter activity as well as mRNA expression of VEGF in colon cancer cells (Zhang et al., 2001). PI3K mediated activation of AKT has also been shown to increase VEGF mRNA expression

(Zhang et al., 2001). Zhang and colleagues suggested a cooperative mechanism of VEGF regulation between the Wnt pathway and the PI3K pathway.

β-catenin –TCF dependent gene targets are responsible for cell cycle regulation and development. Cyclin D1 is a cell regulatory protein that is expressed at high levels during the G1 phase of the cell cycle. Cyclin D1 binds to cyclin dependent kinases and proliferating cell nuclear antigens (Dilek et al., 2010). Cyclin D1 has major implications in uncontrolled cell cycle regulation from G1 to S phase, therefore is also a protein found often overexpressed in many cancers.

The high expression of these three genes, which are regulated by the Wnt signaling pathway, has major implications in cellular processes leading to cancer progression and loss of control in cell growth. Since these genes are regulated by β-catenin acting as a transcriptional co-activator of TCF, the fact that inhibiting a dysregulated PI3K pathway by introducing PTEN, has an effect on these genes is very intriguing. Therefore it is very important to study how the expression of these genes can be down regulated as it may provide an outlook into the control of these genes. The results of my project have shown a direct correlation between deregulation of the PI3K pathway and the status and functional roles of active-β-catenin. Although the mechanism by which these two pathways are connected is a future direction of this project.

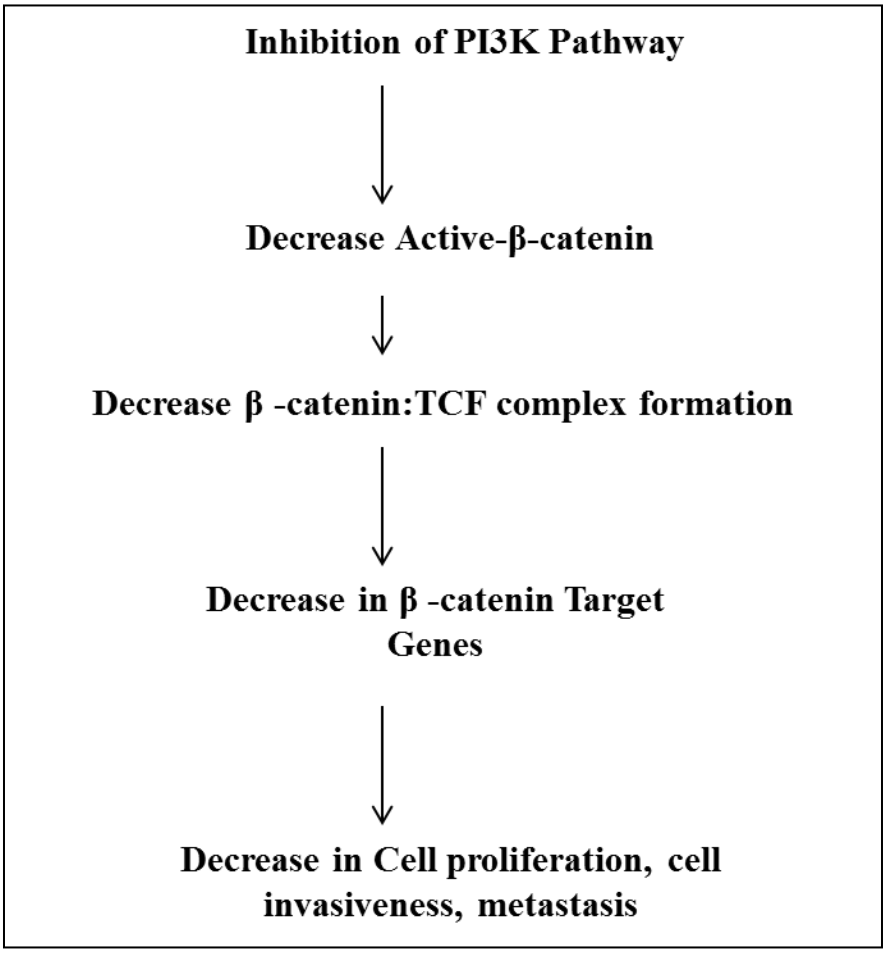

Figure 4.3: Schematic showing reasoning of investigation: Stepwise strategy showing effects of PI3K pathway on active-β-catenin and thereby cellular processes such as invasion.

Chapter 5: Concluding Remarks and Future Directions

5.1 Concluding Remarks

From the studies conducted in this thesis project, we investigated a possible regulatory pathway, the PI3K pathway, to jointly regulate β-catenin expression and localization in metastatic melanoma. The loss of PTEN and its relationship to β-catenin levels was a novel area of study, and therefore was the focus of this project. We have shown in two ways, PTEN transfection and drug treatment, that inhibition of the PI3K pathway decreased active-β-catenin expression. We have also seen that while the canonical Wnt pathway affected the phosphorylation, degradation and accumulation of total cellular β-catenin levels it did not have an effect on active-β-catenin. How the PI3K pathway affects active-β-catenin expression is yet to be investigated. Immunofluorescence analysis also confirmed these results, as active-β-catenin which showed localization mainly in the nucleus of the cell diminished with introduction of PTEN. Further investigation into the downstream effect on β-catenin:TCF complex formation was investigated and an EMSA revealed a band shift, which may allude to decreased β-catenin:TCF complex formation as a result of PTEN re introduction. Furthermore the effects of PTEN/PI3K were seen on downstream Wnt/β-catenin target genes, as mRNA expression of MMP-2, VEGFa and cyclin D1 decreased as a result of PTEN transfection. As the result of this decreased expression of Wnt target genes, PTEN also substantially decreased invasiveness of metastatic melanoma cells. These results all put together show convincing evidence that the PI3K pathway regulates active-β-catenin expression by a yet unknown mechanism. And this has

further implications in the functions of active-β-catenin. Figure 5.1 provides a summary of this thesis project.

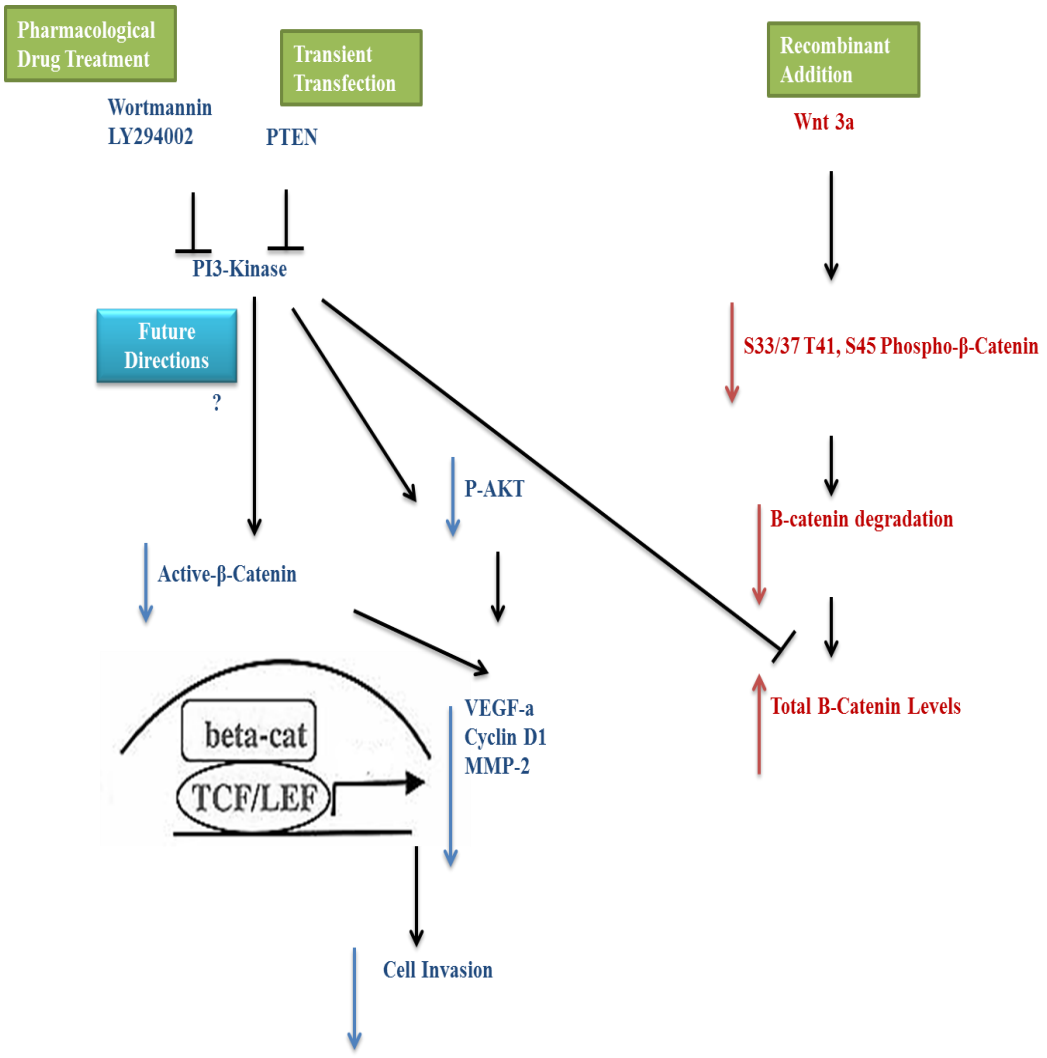

Figure 5.1: Project Summary.

5.2 Future Directions

The kinases that phosphorylate β-catenin as a part of the canonical Wnt signaling pathway leading to its degradation or accumulation have been extensively studied. However the mechanism that regulates the formation of active-β-catenin, causing its dephosphorylation at Serine 37 and Threonine 41, is yet to be determined. Since we have seen that the PI3K pathway plays a role in this regulation, the next step is to determine how this phosphorylation/ dephosphorylation pattern is regulated. Looking at how PP2A affects active-β-catenin through progressive melanoma cell lines would provide a possible look into providing a link between the PI3K and Wnt pathways. Also since PTEN and Wortmannin both showed a decrease in total endogenous levels of β-catenin, their effects on the phosphorylation status of β-catenin also need to be confirmed at earlier time points. Secondly, since there was difficulty with obtaining data from the luciferase/ TOPflash experiments it is very important to optimize this experiment. As this will provide the most accurate read-out of the effect of the PI3K pathway on active-β-catenin's role as a transcriptional co-activator, driving synthesis of TCF target genes. If the exact mechanism by which active-β-catenin is regulated is uncovered, this could have promising potential for targeted therapeutics with an intervention halting metastasis.

References

Grossman, D., and Altieri, D.C. Drug resistance in melanoma: mechanisms, apoptosis, and new potential therapeutic targets. *Cancer Metastasis Rev.* **20(1-2),** 3-11 (2001).

Helmbach, H., Rossmann, E., Kern, M.A., et. al. Drug-resistance in human melanoma. *Int J Cancer*. **93(5)**, 617-622 (2001).

Soengas, M.S., and Lowe, S.W. Apoptosis and melanoma chemoresistance. *Oncogene*. **22(20),** 3138-3151 (2003).

Kim, I.K., Lane, A.M., and Gragoudas, E.S. Survival in patients with presymptomatic diagnosis of metastaic uveal melanoma. *Arch Ophtalmol.* **128(7)**, 871-875 (2010).

Haass, N.K., Smalley, K.S., and Herlyn, M. The role of altered cell-cell communication in melanoma progression. *J. Mol. Histol.* **35(3),** 309-318 (2004).

Haass, N.K., Smalley, K.S., Herlyn, M., et. al. Adhesion, migration and communication in melanocytes and melanoma. *Pigment Cell Res.* **18(3),** 150-159 (2005).

Piris, A., Mihm, M.C Jr., and Duncan, L.M. AJCC melanoma staging update: impact on dermatopathology practice and patient management. *J Cutan Pathol.* **38(5),** 394-400 (2011).

Hao, L., Ha, J.R., Kuzel, P., et. al. Cadherin switch from E- to N- cadherin in melanoma progression is regulated by the PI3K/PTEN pathway through Twist and Snail. *Br J Dermatol*. **166(6),** 1184-1197 (2012).

Hirohashi, S. Inactivation of the E-cadherin-mediated cell adhesion system in human cancers. *Am J Pathol.* **153(2)**, 333–339 (1998).

Simone, E., and Ascierto, P.A. Immunomodulating antibodies in the treatment of metastatic melanoma: The experience with anti-CTLA-4, anti-CD137, and anti-PD1. *Journ of Immunotoxicology.* **9(3),** 241-274 (2012).

Damsky, W.E., Curley, D.P., Santhanakrishnan, M., et. al. β-catenin signaling controls metastasis in Braf-activated Pten-deficient melanomas. *Cancer Cell.* **20(6),** 741-754 (2011).

Padua, R. A., Barrass, N., and Currie, G. A. A novel transforming gene in a human malignant melanoma cell line. *Nature.* **311(5987)**, 671–673 (1984).

van 't Veer, L. J., Burgering, B.M., Versteeg, R., et. al. N-ras mutations in human cutaneous melanoma from sun-exposed body sites. *Mol. Cell. Biol.* **9(7)**, 3114–3116 (1989).

Yang, G., Rajadurai, A., and Tsao, H. Recurrent patterns of dual RB and p53 pathway inactivation in melanoma. *J. Invest. Dermatol.* **125(6)**, 1242–1251 (2005).

Daniotti, M., Oggionni, M., Ranzani, T., et. al. BRAF alterations are associated with complex mutational profiles in malignant melanoma. *Oncogene.* **23(35)**, 5968–5977 (2004).

Curtin, J. A., Fridlyand, J., Kageshita, T., et. al. Distinct sets of genetic alterations in melanoma. *N. Engl. J. Med.* **353(20)**, 2135–2147 (2005).

Flaherty, K.T., Hodi, F.S., Fisher, D.E., et. al. From genes to drugs: targeted strategies for melanoma. *Nat Rev Cancer.* **12(5),** 349-61 (2012).

Rubinfeld, B., Robbins, P., El-Gamil, M., et. al. Stabilization of beta-catenin by genetic defects in melanoma cell lines. *Science.* **275(5307),** 1790-1792 (1997).

Lucero, O.M., Dawson, D.W., Moon, R.T., et. al. A re-evaluation of the "oncogenic" nature of Wnt/beta-catenin signaling in melanoma and other cancers. *Curr. Oncol. Rep.* **12(5)**, 314-318 (2010).

Smith, A.G., Beaumont, K.A., Smit, D.J., et. al. PPARgamma agonists attenuate proliferation and modulate Wnt/ β-catenin signalling in melanoma cells. *Int J Biochem Cell Biol.* **41(4),** 844-852 (2009).

Larue, L., and Delmas, V. The WNT/Beta-catenin pathway in melanoma. *Front Biosci.* **11,** 733-742 (2006).

Lau, E., and Ronai, Z.A. Chapter 7 Altered Signal Transduction Pathways in Melanoma. In Bosserhoff, A., *Melanoma Development (*137-163). New York: Springerwien. (2011).

Shapiro, L., and Weis, W.I. Structure and Biochemistry of Cadherins and Catenins. *Cold Spring Harb Perspectives in Biology*. **1(3),** 1-21 (2009).

Huber, A.H., Nelson. W.J., and Weis, W.I. Three-Dimensional Structure of the Armadillo Repeat Region of β-Catenin. *Cell.* **90(5)**, 871-872 (1997).

Xing, Y., Takemaru, K., Liu, J., et. al. Crystal Structure of a Full-Length beta-catenin. S*tructure.* **16(3),** 478-487 (2008).

Hoover, B.A. Beta-catenin mediated Wnt signaling as a marker for characterization of human bone marrow-derived connective tissue progenitor cells. *The Journal of Young Investigators.* **12(5),** (2005).

Huber, A.H., and Weis, W.I. The structure of the beta-catenin/E-cadherin complex and the molecular basis of diverse ligand recognition by beta-catenin. *Cell.* **105(3),** 391-402 (2001).

Maher, M.T., Mo, R., Flozak, A.S., et. al. Beta-Catenin Phosphorylated at Serine 45 is Spatially Uncoupled from Beta-Catenin Phosphorylated in the GSK3 Domain: Implications for Signaling. *PLoS One* **5(4),** (2010).

Hecht, A., Litterst, C.M., Huber, O., et al. Functional characterization of multiple transactivating elements in beta-catenin, some of which interact with the TATA-binding protein in vitro. *The Journ of Biol Chem.* **274(25)**, 18017-18025 (1999).

Piedra, J., Martinez, D., Castano, J., et. al. Regulation of Beta-Catenin Structure and Activity by Tyrosine Phosphorylation. *The Journ of Biol Chem.* **276(23),** 20436-20443 (2001).

Barker, N.A., Hurlstone, H., Musisi, A., et al. The chromatin remodelling factor Brg-1 interacts with beta-catenin to promote target gene activation. *J EMBO.* **20(17)**, 4935-4943 (2001).

Hecht, A.K., Vleminckx, M.P., Stemmler, M.F., et. al. The p300/CBP acetyltransferases function as transcriptional coactivators of beta-catenin in vertebrates. *J EMBO.* **19(8),** 1839-1850 (2000).

Hülsken, J., Birchmeier, W., and Behrens, J. E-cadherin and APC complete for the interaction with beta-catenin and the cytoskeleton. *The Journ of Biol Chem.* **174**, 2061-2069 (1994).

Roura, S., Miravet, S., Piedra, J., et al. Regulation of E-cadherin/Catenin association by tyrosine phosphorylation. *The Journ of Biol Chem.* **274(51),**36734-36740 (1999).

Gumbiner, B.M. Regulation of cadherin adhesive activity. *J. Cell Biol.* **148(3)**, 399–404 (2000).

Gottardi, C.J., Wong, E., and Gumbiner, B.M. E-cadherin suppresses cellular transformation by inhibiting beta-catenin signaling in an adhesion-independent manner. *The Journ of Cell Biol.* **153(5),** 1049-1060 (2001).

MacDonald, B.T., Tamai, K., and He, X. Wnt/beta-catenin signaling: components, mechanisms, and diseases. *Dev Cell.* **17(1),** 9-26 (2009).

Dajani,R., Fraser, E., Roe, S.M., et.al. Structural basis for recruitment of glycogen synthase kinase 3beta to the axin-APC scaffold complen. *EMBO J.* **22(3),** 494-501 (2003).

Amit, S., Hatzubai, A., Birman, Y., et. al. Axin-mediated CKI phosphorylation of beta-catenin at Ser 45: a molecular switch for the Wnt pathway. *Genes Dev.* **16(9)**, 1066–1076 (2002).

Liu, J., Xing, Y., Hinds, T.R., et. al. The third 20 amino acid repeat is the tightest binding site of APC for beta-catenin. *J Mol Biol.* **360(1),** 133–144 (2006).

Kimelman, D., and Xu, W. beta-catenin destruction complex: insights and questions from a structural perspective. *Oncogene*. **25(57),** 7482-7491 (2006).

Tamai, K., Zeng, X., Liu, C., et. al. A mechanism for Wnt coreceptor activation. *Molecular cell*. **13(1),** 149-156 (2004).

Zeng, Y.A., Rahnama, M., Wang, S., et. al. Inhibition of Drosophila Wg Signaling Involves Competition between Mad and Armadillo/beta-Catenin for dTcf Binding. *PLoS One.* **3(12),** 1-9 (2008).

Davidson, G., Wu, W., Shen, J., et. al. Casein kinase 1 gamma couples Wnt receptor activation to cytoplasmic signal transduction. *Nature.* **438(7069),** 867-872 (2005).

Mao, J., Wang, J., Liu, B., et. al. Low-density lipoprotein receptor-related protein-5 binds to Axin and regulates the canonical Wnt signaling pathway. *Molecular cell*. **7(4),** 801-809 (2001).

Bilic, J., Huang, Y.L., Davidson, G., et. al. Wnt induces LRP6 signalosomes and promotes dishevelled-dependent LRP6 phosphorylation. *Science.* **316(5831),** 1619-1622 (2007).

Logan, C.Y., and Nusse, R. The Wnt signaling pathway in development and disease. *Annu. Rev. Cell Dev. Biol.* **20,** 781-810 (2004).

Clevers, H. Wnt/beta-catenin signaling in development and disease. *Cell.*469 (2006).

Xing, Y., Clements, W.K., Kimelman, D., et al. Crystal structure of a beta-catenin/ axin complex suggest a mechanism for the beta-catenin destruction complex. *Genes Dev.* **17(22),** 2753-2764 (2003).

Mo, R., Chew, T., Maher, M.T., et.al. The Terminal Region of Beta-Catenin Promotes Stability by Shielding the Armadillo Repeats from the Axin-scaffold Destruction Complex. *The Journ of Biol Chem.* **284(41)**, 28222-28231 (2000).

Staal, F.J., Noort Mv, M., Strous, G.J., et. al. Wnt signals are transmitted through N-terminally dephosphorylated beta-catenin. *EMBO reports.* **3(1),** 63-68 (2002).

Liu, C., Li Y., Semenov, M., et. al. Control of beta-catenin phosphorylation/degradation by a dual-kinase mechanism. *Cell Press.* **108(6),** 837-847 (2002).

Lopez-Bergami, P., Fitchman, B., and Ronai, Z. Understanding signaling cascades in melanoma. *Photochem Photobiol*. **84(2),** 289-306 (2008).

Kielhorn, E., Provost, E., Olsen, D., et. al. Tissue Microarray-Based Analysis Shows Phospho-Beta-Catenin Expression In Malignant Melanoma Is Associated With Poor Outcome. *Int J. Cancer.* **103(5),** 652-656 (2003).

Krieghoff, E., Behrens, J., and Mayr, B. Nucleo-cytoplasmic distribution of beta-catenin is regulated by retention. *J Cell Sci.* **119,** 1453–1463 (2006).

Behrens, J., Jerchow, B.A., Wurtele, M., et. al. Functional interaction of an axin homolog, conductin, with beta-catenin, APC, and GSK3-beta. *Science.* **280(5363),** 596-599 (1998).

Simcha, I., Shtutman, M., Salomon, D., et. al. Differential Nuclear Translocation and Transactivation Potential of Beta-Catenin and Plakoglobin. *The Journ of Cell Biol.* **141(6),** 1433-1448 (1998).

Simcha, I., Geiger, B.,Yehuda-Levenberg, S., et. al. Suppression of tumorigenicity by plankoglobin: an augmenting effect of N-cadherin. *The Journ of Cell Biol.* **133(1),** 199-209 (1996).

Zhurinsky, J., Shtutman, M., and Ben-Ze'ev, A. Differential mechanisms of LEF/TCF family-dependent transcriptional activation of beta-catenin and plankoglobin. *Mol and Cell Biol.* **20(12),** 4238-4252 (2000).

Fagotto, F., Gluck, U., and Gumbiner, B.M. Nuclear localization signal-independent and importin/karyopherin-independent nuclear import of Beta-catenin. *Current Biology.* **8(4),** 181-190 (1998).

Yokoya, F., Imamoto, N., Tachibana, T., et. al. Beta-catenin can be transported into the nucleus in a Ran-unassisted manner. *Mol Biol Cell.* **10(4)**, 1119-1131 (1999).

Polakis, P. Wnt Signaling and cancer. *Genes Dev.* **14(15),** 1837-1851 (2000).

Armengol, C., Cairo, S., Fabre, M., et. al. Wnt signaling and hepatocarcinogenesis: the hepatoblastoma model. *Int J Biochem Cell Biol.* **43(2),** 265–270 (2011).

El Wakil, A., and Lalli, E. The Wnt/beta-catenin pathway in adrenocortical development and cancer. *Mol Cell Endocrinol.* **332(1-2),** 32–37 (2011).

Zardawi, S.J., O'Toole, S.A., Sutherland, R.L., et. al. Dysregulation of Hedgehog, Wnt and Notch signalling pathways in breast cancer. *Histol Histopathol.* **24(3),** 385–398 (2009).

Tycko, B., Li, C.M., and Buttyan, R. The Wnt/beta-catenin pathway in Wilms tumors and prostate cancers. *Curr Mol Med.* **7(5),** 479–489 (2007).

Ge, X., and Wang, X. Role of Wnt canonical pathway in hematological malignancies. *J Hematol Oncol*. **3,** 33 (2011).

Laurent-Puig, P., and Zucman-Rossi, J. Genetics of hepatocellular tumors. *Oncogene*. **25(27),** 3778–3786 (2006).

Satoh, S., Daigo, Y., Furukawa, Y., et. al. AXIN1 mutations in hepatocellular carcinomas, and growth suppression in cancer cells by virus-mediated transfer of AXIN1. *Nat Genet.* **24(3),** 245-250 (2000).

Neufeld, K.L., Zhang, F., Cullen, B.R., et. al. APC-mediated downregulation of beta-catenin activity involves nuclear sequestration and nuclear export. *EMBO Reports.* **1(6),** 519-523 (2000).

Morin, P.J., Sparks, A.B., Korinek, V. Activation of beta-catenin-Tcf signaling in colon cancer by mutations in beta-catenin or APC. *Science.* **275(5307),** 1787-1790 (1997).

Kageshita, T., Hamby, C.V., Ishihara, T., et. al. Loss of beta-catenin expression associated with disease progression in malignant melanoma. *British Journal of Dermatology.* **145(2),** 210-216 (2001).

Demunter, A., Libbrecht, L., Degreef, H., et. al. Loss of membranous expression of beta-catenin is associated with tumor progression in cutaneous melanoma and rarely caused by exon 3 mutations. *Mod Pathol.* **15(4),** 454-461 (2002).

Kielhorn, E., Provost, E., Olsen, D., et. al. Tissue microarray-based analysis shows phospho-beta-catenin expression in malignant melanoma is associated with poor outcome. *Int J. Cancer.* **103(5),** 652-656 (2003).

Persad, S., Troussard, A.A., McPhee, T.R., et. al. Tumor Suppressor PTEN inhibits nuclear accumulation of beta-catenin and T cell/lymphoid enhancer factor 1–mediated Transcriptional Activation. *J Cell Biol.* **153(6),** 1161-1174 (2001).

Pap, M., and Cooper, G.M. Role of glycogen synthase kinase-3 in the phosphatidylinositol 3-Kinase/ Akt cell survival pathway. *The Journ of Biol Chem.* **273(32),** 19929-19932 (1998).

Ng, S.S., Mahmoudi, T., Danenberg, E., et. al. Phosphatidylinositol 3-kinase signaling does not activated the wnt cascade. *The Journ of Biol Chem.* **284(51),** 35308-35313 (2009).

Carracedo, A., and Pandolfi, P.P. The PTEN-PI3K pathway: of feedbacks and cross-talks. *Oncogene.* **27(41),** 5527-5541 (2008).

Katso, R., Okkenhaug, K., Ahmadi, K., et. al. Cellular function of phosphoinositide 3-kinases: implications for development, homeostasis, and cancer. *Annu Rev Cell Dev Biol.* **17,** 615–675 (2001).

Fresno Vara, JA., Casado, E., de Castro, J., et. al. PI3K/Akt signalling pathway and cancer. *Cancer Treatment Reviews.* **30(2),** 193-204 (2004).

Engelman, JA., Luo, J., and Cantley, LC. The evolution of phosphatidylinositol 3-kinases as regulators of growth and metabolism. *Nat Rev Genet.* **7(8)**, 606–619 (2006).

Zhao, L., and Vogt, PK. Class I P13K in oncogenic cellular transformation. *Oncogene.* **27(41),** 5486-96 (2008).

Hanahan, D., and Weinberg, R.A. The hallmarks of cancer. *Cell.* **100(1)**, 57-70 (2000).

Bader, AG., Kang, S., Zhao, L., et. al. Oncogenic PI3K deregulates transcription and translation. *Nat Rev Cancer.* **5(12),** 921–929 (2005).

Aziz, S.A., Davies, M., Pick, E., et. al. Phosphatidylinositol-3-Kinase as a therapeutic target in melanoma. *Clin Cancer Res.* **15(9),** 3029-3036 (2009).

Zhang, X.C., Piccini, A., Myers, M.P., et al. Functional analysis of the protein phosphatase activity of PTEN. *Biochemical Journal.* **444(3),** 457-464 (2012).

Stambolic, V., Suzuki, A., de la Pompa, JL., et. al. Negative regulation of PKB/Akt-dependent cell survival by the tumor suppressor PTEN. *Cell.* **95(1),** 29–39 (1998).

Maehama, T., Taylor, G.S., and Dixon, J.E. PTEN and myotubularin: novel phosphoinositide phosphatases. *Annu Rev Biochem.* **70,** 247-279 (2001).

Myers, M.P., and Tonk, N.K. PTEN: sometimes taking it off can be better than putting it on. *Am J Hum Genet.* **61(6)**, 1234-1238 (1997).

Ramaswamy, S., Nakamura, N., Vasquez, F., et. al. Regulation of G1 progression by the PTEN tumor suppressor protein is linked to inhibition of the phosphatidylinositol-3 kinase/Akt pathway. *Proc. Natl. Acad. Sci. USA.* **96(5),** 2110–2115 (1999).

Li, D.M., and Sun, H. TEP1, encoded by a candidate tumor suppressor locus, is a novel protein tyrosine phosphatase regulated by transforming growth factor beta. *Cancer Res.* **57(11),** 2124–2129 (1997).

Datta, SR., Dudek, H., Tao, X., et. al. Akt phosphorylation of BAD couples survival signals to the cell-intrinsic death machinery. *Cell* **91(2),** 231–241 (1997).

Sansal, I., and Sellers, W.R. The biology and clinical relevance of the PTEN tumor suppressor pathway. *J Clin Oncol.* **22(14)**, 2954–2963 (2004).

Guldberg, P., thor Straten, P., Birck. A., et. al. Disruption of the MMAC1/PTEN gene by deletion or mutation is a frequent event in malignant melanoma. *Cancer Res.* **57(17)**, 3660–3663 (2007).

Tsao, H., Zhang, X., Benoit, E., et. al. Identification of PTEN/MMAC1 alterations in uncultured melanomas and melanoma cell lines. *Oncogene.* **16(26)**, 3397–3402 (1998).

Wu, H., Goel, V., and Haluska, F.G. PTEN signaling pathways in melanoma. *Oncogene.* **22(2)**, 3113–3122 (2003).

Trotman, LC., Niki, M., Dotan, Z.A., et. al. PTEN dose dictates cancer progression in the prostate. *PLoS Biol.* **1(3)**, E59 (2003).

Chudnovsky, Y., Adams, AE., Robbins, PB., et. al. Use of human tissue to assess the oncogenic activity of melanoma-associated mutations. *Nat Genet.* **37(7),** 745–749 (2005).

Dhawan, P., Singh, A.B., Ellis, D.L., et. al. Constitutive activation of Akt/protein kinase B in melanoma leads to upregulation of nuclear factor-kappaB and tumor progression. *Cancer Res.* **62(24),** 7335–7342 (2002).

Sauroja, I., Smeds, J., Vlaykova, T., et. al. Analysis of G(1)/S checkpoint regulators in metastatic melanoma. *Genes Chromosom Cancer.* **28(4),** 404–414 (2000).

Sharma, M., Chuang, W.W., and Sun, Z. Phosphatidylinositol 3-kinase/Akt stimulates androgen pathway through GSK3beta and inhibition and nuclear beta-catenin accumulation. *Journ of Biol Chem.* **277(34),** 30935-30941 (2002).

Omholt, K., Platz, A., Ringborg, U., et. al. Cytoplasmic and nuclear accumulation of beta-catenin is rarely caused by *CTNNB1* exon 3 mutations in cutaneous malignant melanoma. *Int J Cancer.* **92(6),** 839-842 (2001).

Rimm, DL., Caca, K., Hu, G., et. al. Frequent nuclear/cytoplasmic localization of beta-catenin without exon 3 mutations in malignant melanoma. *Am J Pathol.* **154(2),** 325–329 (1999).

Chien, AJ., Moore, EC., Lonsdorf, AS., et. al. Activated Wnt/beta-catenin signaling in melanoma is associated with decreased proliferation in patient tumors and a murine melanoma model. *Proc Natl Acad Sci USA.* **106(4),** 1193–1198 (2009).

Bachmann, IM., Straume, O., Puntervoll, HE., et. al. Importance of P-cadherin, beta-catenin, and Wnt5a/frizzled for progression of melanocytic tumors and prognosis in cutaneous melanoma. *Clin Cancer Res.* **11(24),** 8606–8614 (2005).

Daugherty, R.L., and Gottardi, C.J. Phospho-regulation of Beta-catenin adhesion and signaling functions. *Physiology.* **22**, 303-309 (2007).

Gottardi, C.J., and Gumbiner, B.M. Distinct molecular forms of beta-catenin are targeted to adhesive or transcriptional complexes. *J Cell Biol.* **167(2)**, 339-346 (2004).

Salmena, L., Carracedo, A., and Pandolfi, PP. Tenets of PTEN tumor suppression. *Cell.* **133(3),** 403–414 (2008).

Wu, H., Goel, V., Haluska, F.G. PTEN signaling pathways in melanoma. *Oncogene.* **22(20)**, 3113-3122 (2003).

Stahl, J.M., Cheung, M., Sharma., A. Loss of PTEN promotes tumor development in malignant melanoma. *Cancer Research.* **63(11),** 2881-2890 (2003).

Larue, L., and Bellacosa, A. Epithelial-mesenchymal transition in development and cancer: role of phosphatidylinositol -3' kinase/AKT pathways. *Oncogene.* **24(50),** 7443-7454 (2005).

Suzuki, H., Masuda, N., Shimura, T., et. al. Nuclear beta-catenin expression at the invasive front and in the vessels predicts liver metastasis in colorectal carcinoma. *Anticancer Res.* **28(3B)**, 1821-1830, (2008).

Bowen, K.A., Doan, H.Q., Zhou, B.P. et. al. PTEN loss Induces Epithelial-Mesenchymal Transition in Human Colon Cancer Cells. *Anticancer Research.* **29(11)**, 4439-4450 (2009).

Huang, D., and Du, X. Crosstalk between tumor cells and microenvironment *via* Wnt pathway in colorectal cancer dissemination. *World J Gastroenterol.* **14(12)**, 1823-1827 (2008).

Lee, E., Salic, A., Kruger, R., et. al. The roles of APC and Axin derived from experimental and theoretical analysis of the Wnt pathway. *PLoS Biol.* E10 (2003).

Benchabane, H., Huges, EG., Takacs, CM., et. al. Adenomatous polyposis coli is present near the minimal level required for accurate graded responses to the wingless morphogen. *Development.* **135(5),** 963-971 (2008).

McManus, EJ., Sakamoto, K., Armit, L.J., et. al. Role that phosphorylation of GSK3 plays in insulin and Wnt signalling defined by knockin analysis. *EMBO J.* **24(8)**, 1571-1583 (2005).

Ng, S.S., Mahmoudi, T., Danenberg, E., et. al. Phosphatidylinositol 3-kinase signaling does not activate the wnt cascade. *J Biol Chem.* **284(51),** 25308-25313 (2009).

Doble, B.W., Patel, S., Kockeritz, L.K., et. al. Functional redundancy of GSK-3alpha and GSK-3beta in Wnt/beta-catenin signaling shown by using an allelic series of embryonic stem cell lines. *Dev Cell.* **12(6),** 957-971 (2007).

Zhang, W., Yang, J., Liu, Y., et. al. PR55a, a Regulatory Subunit of PP2A, Specifically Regulates PP2A-mediated beta-catenin dephosphorylation. *Journ of Biol Chem.* **284(34),** 22649-22656 (2009).

Westermarck, J., and Hahn, W.C. Multiple pathways regulated by the tumor suppressor PP2A in transformation. *Trends Mol Med.* **14(4)**, 152-160 (2008).

Guenin, S., Schwartz, L., Morvan, D., et. al. PP2A activity is controlled by methylation and regulates oncoprotein expression in melanoma cells: a mechanism which participates in growth inhibition induced by chloroethylnitrosourea treatment. *Int J Oncol.* **32(1),** 49-57 (2008).

Gharbi, S.I., Zvelebil, M.J., Shuttleworth, S.J., et. al. Exploring the specificity of the PI3K family inhibitor LY294002. *Biochem Journal.* **404(1)**, 15-21 (2007).

Shpetner, H., Joly, M., Hartley, D., et. al. Potential sites of PI-3 kinase function in endocytic pathway revealed by the PI-3 kinase inhibitor, wortmannin. *Journ of Cell Biol.* **132(4)**, 595-605 (1996).

Courtney, K.D., Corcoran, R.B., and Engelman, J.A. The PI3K pathway as drug target in human cancer. *Journal of Clinical Oncology.* **28(6),** 1075-1083 (2010).

Sablina, A.A., Hector, M., Colpart, N., et. al. Identification of PP2A complexes and pathways involved in cell transformation. *Cancer Res.* **70(24),** 10474-10484 (2010).

van Noort, M., Meeldijk, J., van der Zee, R., et. al. Wnt signaling controls the phosphorylation status of beta-catenin. *Journ of Biol Chem.* **277(20),** 17901-17906 (2002).

Giese, K., Kingsley, C., Kirshner, JR., et. al. Assembly and function of a TCF-alpha enhancer complex is dependent on LEF-1-induced DNA bending and multiple protein-protein interactions. *Genes Dev.* **9(8),** 995-1008 (1995).

Behrens, J., von Kries, J.P., Kuhl, M., et. al. Functional interaction of beta-catenin with the transcription factor LEF-1. *Nature.* **382(6592),** 638-42 (1996).

Clevers, H., and Grosschedl, R. Transcriptional control of lymphoid development: lessons from gene targeting. *Immunol. Today.* **17(7),** 335-343 (1996).

Molenaar, M., van de Wetering, M., Oosterwegel, J., et. al. XTcf-3 transcription factor mediates beta-catenin-induced axis formation in Xenopus embryos. *Cell.* **86(3),** 391–399 (1996).

van de Wetering, M., Cavallo, R., Dooijes, D., et. al. Armadillo coactivates transcription driven by the product of the Drosophila segment polarity gene dTCF. *Cell.* **88(6),** 789–799 (1997).

Wu, B., Crampton, S.P., and Hughes, C.C. Wnt Signaling induces matrix metalloproteinase expression and regulates T Cell transmigration. *Immunity.* **26(2),** 227-239 (2007).

Zi, X., Guo, Y., Anne, R., et. al. Expression of Frzb/secreted Frizzled-related protein 3 a secreted Wnt antagonist in human androgen-independent prostate cancer PC-3 cells suppresses tumor growth and cellular invasiveness. *Cancer Res.* **65(21)**, 9762-9770 (2005).

Dilek, F.H., Topak, N., Tokyol, C., et. al. B-Catenin and its relation to VEGF and cyclin D1 expression in pT3 rectosigmoid cancers. *Turk J Gastroenterol.* **21(4),** 365-71 (2010).

Zhang, Z., Gaspard, J.P., and Chung, D.C. Regulation of vascular endothelial growth factor by the Wnt and K-ras pathway in colonic neoplasia. *Cancer Res.* **61(16),** 6050-6054 (2001).

Appendices

Chemical	**Company**	**Cat #**
Tween 20	Fisher	BP337
Sodium Chloride	Fisher	BP358
Glycine	Fisher	BP381
Ultrapure Tris	Invitrogen	15504
Methanol	Fisher	A412P-4
Albumin from Bovine Serum	Sigma	A9647
Gelatin, from cold water fish skin	Sigma	G7041
Tricine: N-[Tris(hydroxymethyl)methyl]glycine	Sigma	T5816
Sodium dodecyl sulfate electrophoresis purity reagent	Bio-Rad	161-0302
Dual Luciferase Reporter Assay System	Promega	E1960
Power Sybr Green PCR Master Mix	Applied Biosystems	4367659
BD Matrigel Invasion Chamber	BD Biosciences	354480
Protease Inhibitor Cocktail	Sigma	P83480
Western Lightning Plus-ECL	Perkin Elmer	NEL105001EA
Superscript II Reverse Transcriptase	Invitrogen	18064-014
5X First-Strand Buffer (250 mM Tris-HCl, pH 8.3 at room temperature; 375 mM KCl; 15 mM MgCl2)	Invitrogen	
0.1 M DTT	Invitrogen	
Deoxyribonuclease I, Amplification Grade	Invitrogen	18068-015

10X DNase I Reaction Buffer	Invitrogen	Y02340
25 mM EDTA (pH 8.0)	Invitrogen	Y02353
Oligo(dT)12-18 Primer	Invitrogen	18418-012
dNTP Mix	Invitrogen	
Assay Plate 96 well flat bottom white polystyrene	CoStar	3912
MicroAmp Fast Optical 96 well reaction Plate	Applied Biosystems	4346906
Recombinant Human Dickkopf Homolog 1 (DKK1)	Gibco	PHC9214

Appendix A: Chemical List

Appendix B: Buffer Recipes

TBS-T Buffer

10 mL 20% Tween solution

10 mL 2M Tris (pH 7.6)

11.68g NaCl

Dissolve all in 2L of ddH_2O

Store at 4^oC

Transfer Buffer

Glycine 14.4g

Tris Base 3.03g

200mL methanol

Dissolve in total volume of 1L ddH_2O

Store at 4^oC

2M Tris

60.57g Tris

In 250mL volume ddH_2O

Adjust pH to 7.6

10% APS

0.1g Ammonium Persulfate

In 1mL ddH_2O

Store at 4^oC

Ripa Buffer

37.5ml of NaCl (1M Stock)

12.5ml Tris Base (1M Stock)

2.26ml NP-40

1.25g Na-Deoxycholate

0.250g SDS

197.74ml ddH2O

Blocking Buffer

Use 5% Fish Gelatin in TBS-T

Stock Acylamide/Bis (43.65%, 1.35%)

109.12g acrylamide

3.37g bis-acylamide

Volume up to 250 mL ddH_2O

Tricine Gel Buffer

3M Tris

0.3% SDS

Volume upto 500mL with ddH_2O

Adjust pH to 8.45

Inner Chamber 10X Buffer

121.25g Tris

180g Tricine

40g SDS

Volume up to 1L with ddH_2O

Adjust pH to 8.5

Outer Chamber 10X Buffer

240g Tris

Volume upto 1L with ddH_2O

Adjust pH to 8.5

LB Medium

10g bacto-tryptone

5g bacto-yeast extract

10g NaCl

Volume upto 1L with ddH2O

Adjust pH to 7.2

Autoclave medium

6X Loading Buffer

7ml 4X TRIS-Cl/SDS pH 6.8

3ml Glycerol

1g SDS

0.6ml Bromomercapto-ehanol

1.2mg Bromophenol blue

Volume upto 10ml with ddH2O

10X TBE

108g Tris Base

55g Boric Acid

7.5g EDTA

Volume upto 1L with ddH_2O

10%Tricine Gel

Separating Gel

Stock Acrylamide 3.09ml

Tricine Gel Buffer 4.50ml

dd H2O 6ml

10% APS 67.5ul

TEMED 6.75 ul

Stacking Gel

Stock Acrylamide 540ul

Tricine Gel buffer 1.50ml

ddH2O 4ml

10% APS 30 ul

TEMED 6ul

5% non-denaturing gel for EMSA

Acrylamide Solution (30:0.8) 2.78ml

10X TBE 1.67ml

100% glycerol 830ul

ddH2O 11.3ml

10% APS 125ul

TEMED 16.67ul

5X DNA Loading Buffer

2.5ml TBE Buffer

2.5ml Glycerol

Bromophenol Blue

Xylene cyanol

5ml ddH_2O